DROSOPHILA MYOSIN VI FUNCTION IN DORSAL CLOSURE

Ifeoma Daramfon Ezeigwe

2012

A thesis submitted to the University of Kent for the degree of

Doctor of Philosophy

In the Faculty of Science, Technology and Medical Studies, the Research School of Biosciences

Declaration

No part of this thesis has been submitted in support of an application for any degree or other qualification of the University of Kent or any other University or Institution of learning.

Signed: 

Date: 15-5-2012

Acknowledgements

I would like to thank my supervisor Dr Jim Bloor for his advice, guidance, patience and encouragement throughout this project. I would also like to thank Dr Lisha Ma for her generous guidance and help in the lab. I thank the fly members, Dr Pauline Phelan and Dr Marcus Allen for their encouragements and advices.

To the members of the Cancer Biology lab, thank you for the invaluable support you have shown. I would also like to thank Mr Ray Newsam and Mr Ian Brown for their help with microscopy.

To my sponsor the University of Kent thank you for providing funding for the project.

To New Life Church, thank you for being my Canterbury family. Always there for me through all the good and bad times. Again, thank you. I would also like to thank all my good friends (you know who you are). Thank you all. You are all stars.

Special thanks to Mr Ojemuekpen. Thank you for your understanding, support, encouragement and your wisdom. With you as companion, this trip has been a rewarding one. God bless you.

Finally, I would like to thank my two wonderful parents Mr Godfrey and Mrs Ekom Ezeigwe. It has been a challenging 3-4 years of my life. Thank you for all your unconditional love, undying support, wisdom, patience and guidance. Thank you for nurturing me through it all. To my sister and brother, thank you, thank you and again, thank you. You are all amazing.

Abstract

Myosin VI is a minus-end directed actin-based motor protein. In vertebrate cells, myosin VI is of importance in endocytic and exocytic-membrane trafficking pathways, and in regulating Golgi morphology. Myosin VI is also implicated in genetic diseases and is transcriptionally regulated upon DNA damage in a p53-dependent manner and shown to be over-expressed in cancer types.

In *Drosophila*, myosin VI encoded by the *jaguar* (*jar*) gene is implicated in a range of cellular processes including dorsal closure. Although understanding of its cellular function is developing, little is known about the mechanisms regulating myosin VI. *In vitro* studies on vertebrate myosin VI have demonstrated that it is phosphorylated within its motor domain by the serine/threonine kinase PAK and that alters its function in a similar manner to that which occurs in myosin I. More importantly, *jar* has a Pak phosphorylation site in the same location as the vertebrate myosin VI. Expression of either a dominant negative Jar or a dominant negative Pak causes if not exact, overlapping dorsal phenotypes in *Drosophila*. The aim of this study was to investigate a working model that Jar functions during dorsal closure are dependent on Pak-mediated phosphorylation.

During my thesis research a published report concluded that *jar* is required but not essential for *Drosophila* development as 40% null *jar* mutants survived. On the contrary, I report here that *jar* is of importance for development as RNAi-mediated knockdown of Jar protein level is lethal and is found to cause abnormal dorsal closure. Further delineation of jar^{322} mutant allele showed varied phenotypes including wing defects that implicates *jar* in Notch signalling and in integrin function and signalling. Importantly, I found that Jar is directly regulated by JNK transcriptional activation pathway and down-regulated by the RhoGTPase pathway.

Together this work emphasises the multifunctional nature of myosin VI. Further the work suggests that the pro-survival function of vertebrate myosin VI is conserved in *Drosophila*.

Abbreviations

aa	Amino acid
AMPARs	alpha-amino-3-hydroxy-5-methyl-4-isoxazole propionic acid-type glutamate receptors
Arm	Armadillo
Arp2/3	Actin Related Protein 2/3
AS	Amnioserosa
ATM	ataxia telangiectasia mutated
Bad	Bcl-2-associated death promoter
bp	base pair
BSA	bovine serum albumin
CBD	cargo-binding domain
CCP	clathrin-coated pit
CCV	clathrin-coated vesicle
CNS	Central nervous system
C-terminus	Carboxy-terminus
Dab2	Disabled homolog 2
DCLIP-190	*Drosophila*-Cytoplasmic linker proteins-190
DE-cadherin	*Drosophila*-E-cadherin
DN	dominant negative
DNA	Deoxyribonucleic Acid
dNTP	deoxynucleotide triphosphate
E-cadherin	Epithelial-cadherin
ECL	enhanced chemiluminescence
Ed	Echinoid
EDTA	Ethylenediaminetetraacetic Acid
EGTA	Ethylene glycol tetraacetic acid
F-actin	Filamentous actin
GFP	green fluorescent protein

GIPC	GAIP (Gαi3-interacting protein) interacting protein C terminus
GTPases	guanosine triphosphates
JNK	c-Jun N-terminal Kinase
LE	leading edge
LMTK2	lemur tyrosine kinase 2
MAPK	Mitogen-activated protein kinase
NMJ	neuromuscular junction
N-terminal	Amino-terminal
PAGE	polyacrylamide gel electrophoresis
PBS	Phosphate buffered saline
PCP	planar cell polarity
PCR	Polymerase chain reaction
PFA	paraformaldehyde
PIP_2	phosphatidylinositol 4,5-bisphosphate
PNS	Peripheral nervous system
RFP	red fluorescent protein
RNAi	Ribonucleic acid interference
RNAPII	RNA polymerase II
rpm	revolutions per minute
SB	squishing buffer
SDS	sodium dodecyl sulfate
T6BP	TRAF (tumour necrosis factor receptor-associated factor) 6-binding protein
TAE	tris acid EDTA
TEMED	N,N,N',N'-tetramethyl- ethane-1,2-diamine
V	voltage

List of Figures

List of Movies

The enclosed DVD contains movies of live imaging confocal microscopy. The movies are playable using Windows Media Player or equivalent. The genotypes of each embryo in the movies are shown below.

1.1 *w;SGMCA*

5.1 *GFPactin/jar-RNAi;69BGal4/+*

5.2 *GFP-α-tubulin/jar-RNAi;69BGal4/+*

5.3 *enGal4;SGMCA/jar-RNAi*

List of Tables

Table of Contents

Chapter 1. Introduction

1.1. Introduction

Myosin VI is of a growing interest amongst the myosin superfamily because in contrast to all characterised myosins, it is a minus-end directed motor. There are uncertainties about the structure and thus, the functions of myosin VI. The ongoing debate revolves around the oligomeric state of the protein. It is monomeric in its natural occurring state but is proposed to dimerise in response to physiological and environmental stimuli which is how myosin VI is understood to function in vesicle trafficking. Myosin VI is shown to be a multifunctional protein because of the structural features of its C-domain which shows it can associate with a variety of cargoes.

In this study, I used the process of dorsal closure which occurs during *Drosophila melanogaster* embryogenesis as the preferred model system. Dorsal closure is a multistep morphogenetic process reminiscent of embryonic wound healing, whereby different cell types are orchestrated to migrate in sync with each other and from opposing sides come to meet along the midline in closing a gap in the epithelium that was leftover from the previous development process. Worth noting, many of the different signalling events involved in dorsal closure are conserved between the fly and vertebrates.

Myosin VI is thought to play crucial roles in dorsal closure. Myosin VI is postulated to be involved in actin organisation and act in cooperation with adhesion molecules to stabilise and thus, maintain the integrity of the epithelial sheets. However, the importance of myosin VI for *Drosophila* development has been challenged as reports of loss-of-function *jar* alleles are in contrast to reported dorsal phenotypes observed in the driven expression of dominant negative *jar*.

This project addresses the uncertainties revolving around the importance of myosin VI for *Drosophila* development, specifically during dorsal closure in embryogenesis.

1.2. Myosin superfamily

1.2.1. General function

Myosins are of a large family of molecular motor proteins and are the only known type of actin-based motors (Berg *et al.*, 2001). They utilise energy from ATP hydrolysis to generate force for the movement along actin filaments. They perform a diverse set of cellular processes such as muscular contraction, cell movement, cytokinesis, vesicular transport, phagocytosis and signal transduction (Baker and Titus, 1998; Mermall *et al.*, 1998). They are generally grouped into 18 distinct classes of myosins based on sequence analysis of their ATP-hydrolyzing motor domains (Berg *et al.*, 2001; Hodge *et al.*, 2000). However, an updated report has annotated at least 35 classes of actin-based molecular motors (Odronitz and Kollmar, 2007). Although a few myosins are restricted to plants, members of the myosin superfamily are expressed in virtually all eukaryotic cells.

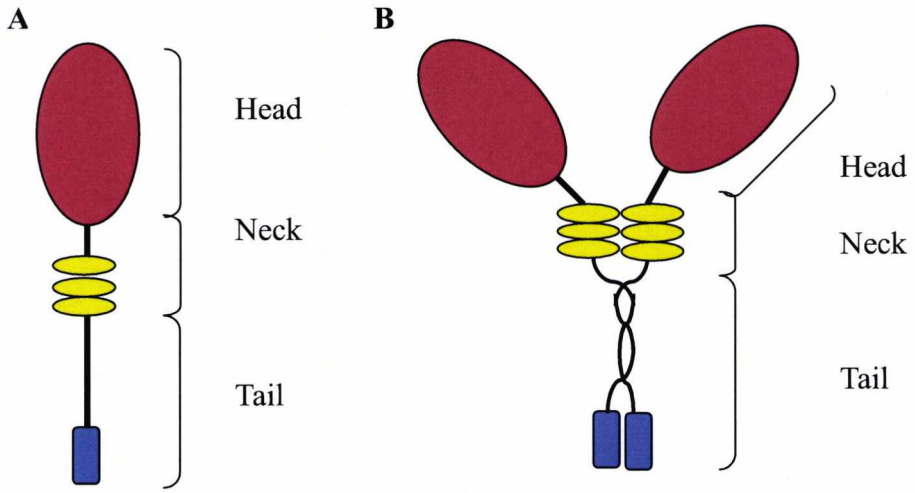

Figure 1.1. Schematic structure of myosin. A. Myosin monomer. B. Myosin dimer. The head contains the myosin ATPase and actin binding site. The neck consists between 1-6 IQ motifs for light chain and/or calmodulin binding. The tail varies considerably from one myosin to another for functions in a wide variety of cellular processes.

1.2.2. General structure

Myosins are composed of N-terminal head domain, a neck region and a variable tail. The head domain contains the actin binding site and the ATPase and its sequence is highly conserved in all myosins (Figure 1.1). The neck domain consists of one-six IQ motifs which bind light chains and/or calmodulin. The variable tail acts as a binding for cargos, as a dimerisation site in some myosins and, in the case of myosin II, is required for filament assembly (Seller, 2000).

1.3. Vertebrate Myosin VI

1.3.1. Structure

Myosin VI is a unique 140 kDa actin-based motor protein expressed in all vertebrates (Baker and Titus, 1997; Hasson and Mooseker, 1994). It is unique because it is the only myosin that moves towards the minus ends of actin filaments (Wells *et al.*, 1999).

Myosin VI, like other myosin superfamily members, is composed of an N-terminal head domain, followed by a single IQ motif, and a C-terminal tail domain (Figure 1. 2). Additionally, myosin VI has unique features that enables it perform as a minus-end directed protein. The head contains a small insert of 22 amino acid (aa) residues next to the ATPase site that is thought to be responsible for slowing down the rate of ATP and in so doing gives myosin VI high duty ratio properties; most of its ATPase cycle is spent strongly bound to actin (Naccache and Hasson, 2006; Altman *et al.*, 2004; De La Cruz *et al.*, 2001).

Furthermore, between the head and the neck domain sits a 53 aa residue insert that binds to calmodulin, despite it containing no known calmodulin binding motif (Bahloul *et al.*, 2004; Wells *et al.*, 1999). This 53 insert is also known as the 'reverse gear' and is responsible for the reverse directional motility of myosin VI (Bryant *et al.*, 2007; Park *et al.*, 2007; Ménétrey *et al.*, 2005; Wells *et al.*, 1999).

The neck domain consists of a single IQ motif with a calmodulin and light chain binding motifs. The tail domain contains a sequence that previously was predicted to form a coiled coil but forms a stable single alpha-helix and it precedes a cargo-binding region (Spink *et al.*, 2008; Knight *et al.*, 2005). In addition, myosin VI has alternative spliced exons that produce different myosin VI isoforms. There is a large insert that sits between the helical and the globular tail and a small insert found within the globular tail.

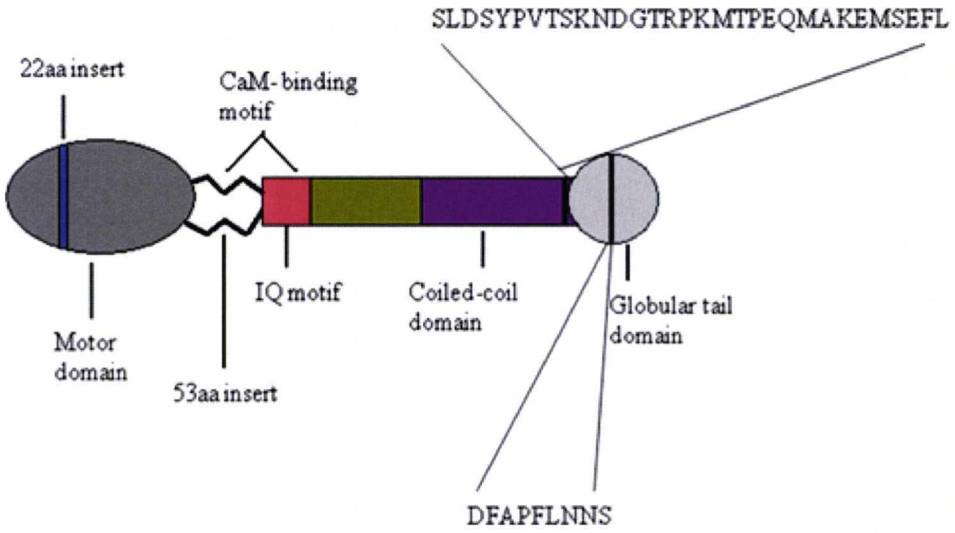

Figure 1.2. Schematic structure of myosin VI. The unusual features of myosin VI to highlight are the 22 residue insert, 53 insert, a region that forms the single alpha-helix (in place of the coiled-coil domain), alternative spliced exons: the 31aa sequence shown expressed in human intestine and 9aa sequence (completely conserved between rat and human) shown within the globular tail.

1.3.2. Function

So far, reports of myosin VI functions are based on the theory that it can function both as a dimeric and as a monomeric motor protein. Myosin VI in its dimer state moves processively with a 'hand over hand' (backward) mechanism (Okten *et al.*, 2004; Yildiz *et al.*, 2004) along actin tracks for translocation of cargos in similar manner operated by myosin V in membrane trafficking (Baker *et al.*, 2004). Myosin VI in its monomer state can function as a non-processive motor in like manner as

monomeric class I myosin (Buss *et al.*, 2004). Class I myosin functions as an anchor to maintain structural integrity of membranes (reviewed in, Kim and Flavell, 2008).

Localisation studies have shown myosin VI to localise to membrane ruffles, tips of filipodia, and lamellipodia, microvilli, stereocilia, nucleus, Golgi complex, cytosol, clathrin-coated and uncoated vesicles (Vreugde *et al.*, 2006; Aschenbrenner *et al.*, 2004; Warner *et al.*, 2003; Buss *et al.*, 2001a,b & 1998; Hasson *et al.*, 1997). Furthermore, myosin VI has been demonstrated to be of importance in cell migration, cytokinesis, RNAPII-dependent transcription of genes, exocytosis and clathrin-mediated endocytosis (Au *et al.*, 2007; Vreugde *et al.*, 2006; Sahlender *et al.*, 2005; Hasson, 2003; Buss *et al.*, 2001b & 1998). Below, I review cellular functions of myosin VI and the multitude of myosin VI cargo-binding proteins (summarised in Table 1.1).

1.3.2.1. Membrane trafficking

Membrane trafficking is a mandatory feature for all cells as it is a requirement for the uptake of recycled extracellular molecules such as nutrients, proteins, receptors, peptides and fluids.

Of the myosin superfamily identified, myosins I, II, V, VI and VII are involved in membrane trafficking. However, myosin VI is the first motor protein involved in clathrin-mediated endocytosis due to its ability to bind endocytic proteins such as, Dab2, PIP_2 and GIPC (Spudich *et al.*, 2007; Reed *et al.*, 2005). Furthermore, myosin VI may be involved in exocytic pathway (Au *et al.*, 2007; Warner *et al.*, 2003).

Functional studies have shown that the loss-of-function of myosin VI leads to defects in the endocytosis regulation of cystic fibrosis transmembrane conductance regulator (CFTR) in intestinal enterocytes (Ameen and Apodaca, 2007; Swiatecka-Urban *et al.*, 2004), reduction in internalisation of AMPARs in the hippocampal neurons (Osterweil *et al.*, 2005), reduced collagen secretion (Warner *et al.*, 2003) and impairment in clathrin-mediated uptake of transferrin, an iron-binding glycoprotein (Buss *et al.*, 2001b). The loss-of-function of myosin VI also alters the morphology of intracellular organelles such as the Golgi complex (Warner *et al.*,

2003), hippocampus (Osterweil *et al.*, 2005), intermicrovillar domain of the brush border in the kidney (Gotoh *et al.*, 2010) and the intestine (Collaco *et al.*, 2010; Ameen and Apodaca, 2007).

1.3.2.2. Clathrin-mediated endocytosis

Clathrin-mediated endocytosis is a sequence of events beginning at the plasma membrane (for an extensive review see, Doherty and McMahon, 2009). Typically, the basic steps of clathrin-mediated endocytosis are: (1) the binding of cargo to the cytosolic tail of its receptor at the plasma membrane, (2) clathrin adaptor proteins typified by AP-2 are recruited to the site to serve as a hub for protein-protein interactions. A pit begins to form around the cargo-receptor complexes and subsequently, clathrin assembles around the pit to form a clathrin-coated pit (CCP), (3) the plasma membrane invaginates to form a clathrin-coated vesicle (CCV), (4) dynamin, a membrane scission protein upon GTP hydrolysis mediates the fission of the CCV from the plasma membrane and into the interior of the cell, (5) the vesicle is stripped off the clathrin coat and is transported further in the cell where it fuses with its destination intracellular compartment.

Myosin VI is predominantly found in association with clathrin-coated pits/vesicles at microvillus domain in the intestinal and kidney proximal tubule brush borders (Biemesderfer *et al.*, 2002; Buss *et al.*, 2001a; Heintzelman *et al.*, 1994). Additionally, myosin VI also associates with clathrin-coated pits/vesicles at synapses in hipppocampal neurons (Osterweil *et al.*, 2005) and in non-polarised cells but to a lesser degree (Buss *et al.*, 2001a).

Lack of functional myosin VI is clearly noted to cause endocytosis and secretion defects but the function and the specified stages of myosin VI in vesicle transport are ill defined (Buss and Kendrick-Jones, 2008; Hasson, 2003; Buss *et al.*, 2001a).

Myosin VI may be involved in the early and late stages of endocytosis (illustrated in Figure 1.3). At the early stage of endocytosis, myosin VI has been shown to localise intensively at stages of coated pit formation and plasma membrane invagination.

These observations are consistent with reports that myosin VI can bind to Dab2 and PIP_2 at the apical surface and in turn, serve as a linker to CCV (Spudich *et al.*, 2007; Buss *et al.*, 2001a). Once the clathrin, clathrin adaptor proteins and other host of endocytic accessory proteins that signals through PIP_2 are assembled at the plasma membrane, myosin VI is thought to exert a pulling force on the assembled clathrin complexes towards the interior of the cell as the minus ends of actin filaments points inwardly (Cramer, 2000). Following the fission of the CCV from the plasma membrane and subsequently, the un-coating of the vesicle myosin VI transports the uncoated vesicle towards the early endosome through its binding with GIPC (Reed *et al.*, 2005; Aschenbrenner *et al.*, 2003).

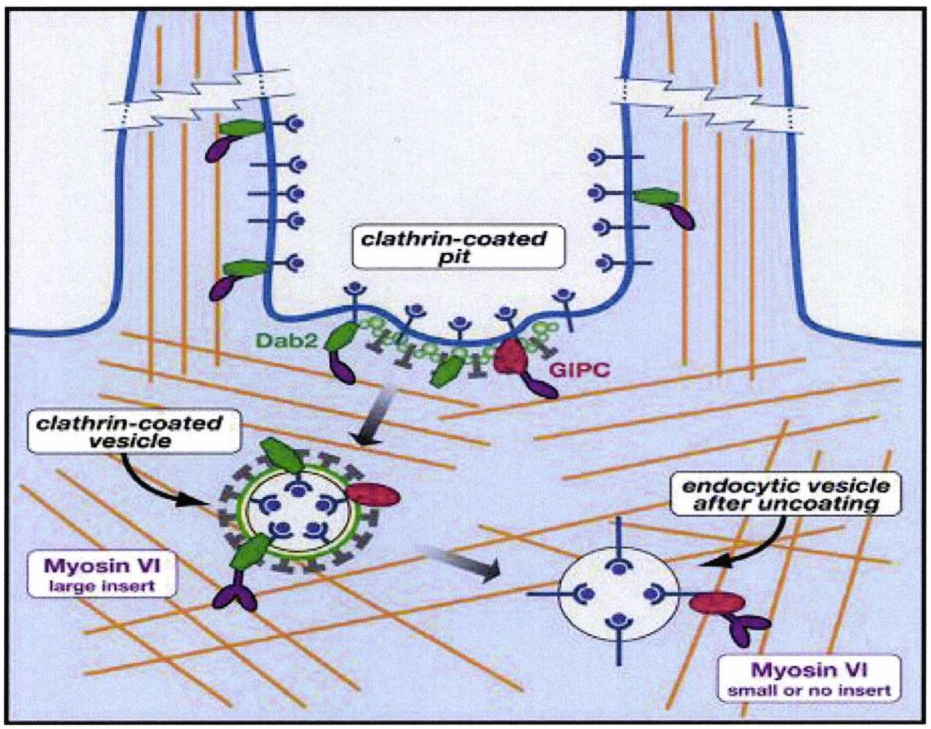

Figure 1.3. An overview of the sequential steps of myosin VI during clathrin-mediated endocytosis. Dab2 modulates the recruitment of the large insert myosin VI isoform to sites of CCV formation (Dance *et al.*, 2004). Subsequently, the CCV is pinched off the plasma membrane and the myosin VI isoform lacking the large insert translocates uncoated vesicles to the endosomal compartment through its binding to GIPC (Aschenbrenner *et al.*, 2003). (Adapted from Buss *et al.*, 2004).

1.3.2.3. Exocytosis

Myosin VI is seen at the trans-side of the Golgi network (Warner *et al.*, 2003; Buss *et al.*, 1998). The Golgi apparatus is stacks of membrane-bound structures classified into three networks, the *cis*, *medial* and *trans*-Golgi networks (Nakano and Luini, 2010). At the trans-Golgi network, the newly synthesised proteins from the endoplasmic reticulum are sorted and packaged for destination to different cellular compartments.

Myosin VI functional activity at the Golgi complex is mediated through its binding to optineurin, a protein also known to bind Rab8, a small GTPase involved in post-Golgi vesicular transport (Sahlender *et al.*, 2005). Myosin VI is involved in regulating intracellular membrane trafficking (Sahlender *et al.*, 2005). In Snell's waltzer, a myosin VI knock-out mice, the loss of myosin VI function resulted in 40% reduction of the Golgi network structure and moreover, a reduction in exocytosis and secretion (Sahlender *et al.*, 2005; Warner *et al.*, 2003). In further support, the expression of a full length myosin VI can rescue the fragmented Golgi network and the reduced secretion (Warner *et al.*, 2003).

Additionally, in polarised epithelial cells the no insert myosin VI isoform, in complex with optineurin and Rab8 proteins is specifically involved in basolateral sorting and transport of newly synthesise tyrosine motif containing cargos to basolateral surface with AP-IB (clathrin adaptor protein complexes) which acts as a mediator (Au *et al.*, 2007).

1.3.2.4. Cytokinesis

Cytokinesis is the last phase of mitosis during which the cytoplasm and plasma membrane of a single cell divides into two daughter cells (reviewed in Pollard, 2010). The process of cytokinesis is driven by contractile acto-myosin II.

Myosin VI is shown to colocalise with GIPC (endocytic adaptor protein) for its role in membrane trafficking during cytokinesis (Arden *et al.*, 2007). The inhibition of myosin VI function through small interfering RNA (siRNA)-mediated knockdown in

cultured cell lines (HeLa and MDCK) or by over-expression of dominant-negative myosin VI tail leads to cytokinesis defects, delay in chromosome assembly during metaphase and thus, slowing the progress of the mitotic cells.

Table 1.1. Summary of myosin VI binding partners

Binding partner	**Function**	**Reference**
DCLIP-190	A microtubule binding protein	Lanzt and Miller, 1998
DOC-2/DAB2	RAS signaling protein, tumor suppressor, endocytosis of LDLR	Inoue *et al.*, 2002 Morris *et al.*, 2002
GLUT1CBP/GIPC	GLUT1 transporter binding protein, Endocytosis & receptor trafficking via Golgi	Reed *et al.*, 2005
Optineurin	Secretory pathway via the Golgi	Sahlender *et al.*, 2005
T6BP	Functions in signal transduction, cell adhesion and secretion	Morriswood *et al.*, 2007
LMTK2	Serine/threonine kinase	Chibalina *et al.*, 2007
PtdIns(4,5)P_2	A polyphosphoinositide that acts as second messenger for endo and exocytosis	Spudich *et al.*, 2007
SAP97	Trafficking of AMPA receptors	Wu *et al.*, 2002

1.3.2.5. Other cellular functions

Mutations among the myosin superfamily are linked to several genetic diseases (reviewed in, Redowicz, 2002). Familial hypertrophic cardiomyopathy caused by mutations in beta cardiac myosin II. Defect in a myosin V gene causes abnormal pigmentation and early death in mouse and Griscelli disease in human. The Griscelli disease is characterised by hypopigmentation which is sometimes accompanied by immunodeficiency and neurological symptoms. Defects in myosins VII and myosin XV genes cause deafness disorder, Usher syndrome (type 1B) and DFNB3, respectively in humans. Additionally, defects in both genes cause similar deafness disorder in mouse.

Myosin VI expression in the sensory hair cells of the inner ear is of importance for auditory and vestibular function both in humans and mice (Self *et al.*, 1999; Avraham *et al.*, 1997; Hasson *et al.*, 1997). Myosin VI accumulates at the cuticular plate, an actin-dense area at the base of stereocilia. Functional loss such as a mutation in the myosin VI gene causes a recessive deafness disorder in mice because of fused stereocilia and consequent the lack of structural integrity. Subsequently the human homologue was found to cause two hereditary hearing defects, DFNA22 syndrome, a dominant inherited form and DFNB37 syndrome, a recessive inherited form, as well as an associated hypertrophic cardiomyopathy (Ahmed *et al.*, 2003; Melchionda *et al.*, 2001).

Furthermore, myosin VI is shown to be overexpressed in ovarian and prostate cancer cells (Dunn *et al.*, 2006; Yoshida *et al.*, 2004). The inhibition of myosin VI reduces cell spreading and migration of both ovarian and prostate cancer cells *in vitro* and ovarian tumour dissemination *in vivo*. Upon DNA damage and stress signal response myosin VI level has been shown to increase. Myosin VI is regulated by DNA damage in a p53-dependent manner (Jung *et al.*, 2006). In myosin VI knock-down cells activated ATM (ataxia telangiectasia mutated) that is known to phosphorylate, and in turn activate p53 was found reduced. This resulted in weakened p53 stabilisation. Thus, myosin VI knock-down cells are sensitised to DNA damage-induced apoptosis. Additionally, myosin VI is rapidly upregulated in response to stress levels which was observed in the hippocampus of male mice subjected to water-immersion restraint stress experiment (Tamaki *et al.*, 2007).

1.4. Regulation

The unusual feature and the wide-ranging biological activities of myosin VI require the understanding of its complex regulation mechanism. This subject has been under intense scrutiny. Notably, there are several mechanisms (outlined below) but nonetheless, regulation of myosin VI still remains a poorly understood subject.

1.4.1. Myosin VI isoforms

In the majority of vertebrates myosin VI is encoded by a single gene that possesses two alternatively spliced exons that produce four distinct protein isoforms (Buss *et al.*, 1998 & 2001b). There is an isoform containing a large insert that, depending on the species, is between 21-31aa that are inserted between the helical and the globular tail, an isoform with a small insert of 9aa in the globular tail, an isoform that contains both inserts and one that contains neither. The large insert is highly conserved between human, rat and chicken whereas the small insert shares complete similarity between rat and human (Buss *et al.*, 2001a). In few species namely, *Caenorhabditis elegans* (Baker and Titus, 1997) and *Morone saxatilis*, a striped bass fish (Breckler *et al.*, 2000) there is a second myosin VI gene.

These isoforms are expressed in a tissue-specific manner and are thought to be important in the differential localization of myosin VI (Au *et al.*, 2007; Spudich *et al.*, 2007; Buss *et al.*, 2001a,b). The large insert isoform is involved in the early stages of endocytosis (Biemesderfer *et al.*, 2002). It is predominant in polarised cells at sites of clathrin-mediated endocytosis (Buss *et al.*, 2001b) and is shown to target myosin VI to sites of CCV and CCP (Spudich *et al.*, 2007). The small insert isoform and isoform lacking insert are involved in the last stages of endocytosis where there are shown to translocate vesicles for fusion with the early endosomal compartment (Aschenbrenner *et al.*, 2003). These isoforms are found predominantly in non-polarised cells such as fibroblasts and HeLa cells (Puri, 2010 & 2009).

However, a report in the literature had argued that these isoforms cannot alone account for the targeting of myosin VI because all the different isoforms are able to target to the same endocytic vesicles (Dance *et al.*, 2004). In addition to the

isoforms, it was shown that myosin VI binding partners such as Dab2 can modulate the recruitment of myosin VI to sites of clathrin-mediated endocytosis.

1.4.2. Calcium regulation

Myosin VI has two calmodulin (CaM) binding sites. The first site is within the unique 53 residue insert that sits between the motor and neck domain (also called the lever arm). This insert is a 50 KDa subdomain proven in the literature to be responsible for the reverse directional motility of myosin VI (Bryant *et al.*, 2007; Park *et al.*, 2007; Sweeney *et al.*, 2007). The proximal part of this unique insert binds to CaM with four Ca^{2+} molecules on the condition that the distal part of the insert-bound CaM is engaged with calcium. This unique CaM-binding site does not exert a regulatory effect but rather is of structural CaM importance allowing repositioning of the myosin VI lever arm for reverse motility (Liao *et al.*, 2009; Homma *et al.*, 2001). Moreover, calcium does not readily dissociate from the insert-bound CaM in the constant changing calcium environment reinforcing the idea that the unique insert subdomain is of an integral part of myosin VI structure.

The second binding site is a conventional IQ motif. The IQ motif plays a regulatory role. In the absence of IQ-CaM bound calcium, gating between the two heads of a dimeric myosin VI motor is feasible. Head "gating" is a hand-over-hand walk mechanism along the actin filament by which one head is bound strongly to actin but leaves the second head free until the first head detaches from actin and this is repeated throughout the course of its ATPase cycle (Yildiz *et al.*, 2004). At high calcium concentration, the motility activity of myosin VI is altered by slowing the rate of ADP release and uncoupling of the two heads of dimeric myosin VI (Bahloul *et al.*, 2004; Morris *et al.*, 2003). The nature of this regulation effect is not known. However, in a report calcium is regarded as an "on/off" switch for myosin VI which is in contrast to other works (Yoshimura *et al.*, 2001). It was shown that at high calcium concentration myosin VI motility activity was inhibited.

Furthermore, the IQ motif associates weakly with CaM. It is thought that the weak binding possibly allows interchange for light chain binding though it is yet to be proven (Bahloul *et al.*, 2004).

1.4.3. Conformational change

Myosin VI is thought to function as a processive dimeric protein. However, extraction of myosin VI from tissues, as well as when expressed in baculovirus and NMR studies show that a full length myosin VI is a monomer in its native state (Yu *et al.*, 2009; Sakata et al., 2007; Lister *et al.*, 2004). Furthermore, the full length myosin VI is also said to be compact (Lister *et al.*, 2004) as a result of cargo-binding domain (CBD) being folded back onto the head domain (Spink *et al.*, 2008). Nonetheless, myosin VI has been shown to have similar large working step size 36nm as myosin V to effectively perform a "hand over hand" motion (Nishikawa *et al.*, 2002; Rock *et al.*, 2001).

Myosin VI has a two-part coiled coil region in its tail domain (Roberts *et al.*, 2004; Buss *et al.*, 1998). The first part of the helical region is composed of a helix-loop-helix structure to promote dimerisation of the molecule. Whereas, the second part consists of four basic and four acidic residues which cannot form a coiled coil structure, but which are well conserved among the vertebrate myosin VI sequences (Figure 1.4). The alternate bands of positively and negatively charged areas completely exposed to the aqueous environment results in the formation of a salt bridge helix structure is thought to aid in dimerisation (De La Cruz *et al.*, 2000; Buss *et al.*, 1998).

Furthermore, a report has shown myosin X to have similar pattern of alternating positive and negative charges to that found in myosin VI (Figure 1.4) (Knight *et al.*, 2005). However, it was demonstrated that the highly charged domain of myosin X does not dimerises even when present in high concentration. In contrast, using electron microscopy shows that at high concentration, two myosin VI monomers in close proximity and in the absence of the CBD can dimerise similarly to artificial dimeric myosin VI (Park *et al.*, 2006). Another report showed that a binding of cargo

to the CBD causes the release of myosin VI head domain and a consequent CBD dimerisation of myosin VI tail domain (Spink *et al.*, 2008). Consistent with this are reports that, myosin VI binding partners such as optineurin and Dab2 can initiate dimerisation of myosin VI (Phichith *et al.*, 2009; Yu *et al.*, 2009; Spudich *et al.*, 2007). Additionally, a fluorescence resonance energy transfer assay *in vivo* further supports the possibility of myosin VI dimers (Spudich *et al.*, 2007; Altman *et al.*, 2004).

Figure 1.4. Charge repeats in the predicted coiled-coil domain of myosins. The precise amino acid numbers are shown to the left. The shaded regions indicate similarity between *Drosophila* myosin VI coiled coil domain with that from vertebrate myosin VI and myosin X. Arg (R) and Lys (K) are positively charged residues *in yellow* whereas Glu (E) and Asp (D) in *dark yellow* are negatively charged residues. *Dro, Drosophila; Hs, Homo sapiens; Hu, Human; Ss, Sus scrofa.*

The highly charged domain in myosin X is reportedly a stable single alpha helix structure, a model also proposed for myosin VII, another controversial myosin (Knight *et al.*, 2005). Myosin VII and myosin X are both described to function as a transporter and as anchors (Yang *et al.*, 2006; Knight *et al.*, 2005). These myosins are postulated to employ a regulatory switch shifting from a nonprocessive monomer to a processive dimer motor protein. Thus, implying that myosin VI could possess a similar regulatory switch.

1.4.4. Phosphorylation

Phosphorylation is another likely regulatory mechanism for myosin VI cellular activities. There are three potential phosphorylation sites identified in myosin VI; one in the motor domain and two in the C-terminal domain.

The first phosphorylation site was identified as threonine 406 (T^{406}) in the cardiomyopathy loop at the actin binding site in the head domain (Buss *et al.*, 1998). This site obeys the TEDS (threonine (T), glutamic acid (E), aspartic acid (D), serine (S)) rule site as proposed by Bement and Mooseker, (1995) and moreover the site is replica to that found in the motor domains of class I myosins (Figure 1.5) (Brzeska *et al.*, 1997). The second and third sites are located in the tail domain and were designated as $T^{1089}INT^{1092}$ (Sahlender *et al.*, 2005).

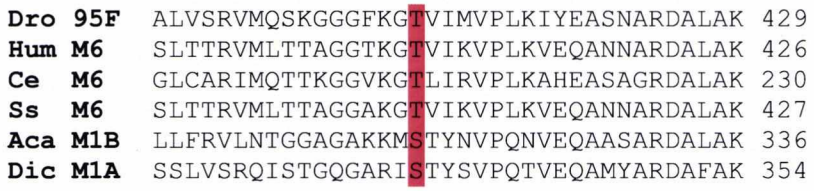

Figure 1.5. Comparison of phosphorylation (serine/ threonine kinase PAK) sites within the motor domain. The alignment of a phosphorylation site (red) between myosin VI and amoeboid myosin Is. All the above myosins have conserved serine/threonine residues at the site of phosphorylation. The precise amino acid numbers are shown to the right. *Dro, Drosophila; Hum, Human; Ce, Caenorhabditis elegans; Ss, Sus scrofa; Aca, Acanthamoeba; Dic, Dictyostelium.*

Preliminary evidence has shown that Pak1, a Cdc42/Rac activated kinase has the potential to phosphorylate the threonine residue located in the motor domain of myosin VI (Buss *et al.*, 1998). Pak1 belongs to the same kinase family that is responsible for the phosphorylation of motor domains of class I myosins. During actomyosin VI ATPase cycle, myosin VI strongly binds to actin due to its high affinity for ADP as opposed to ATP; ADP release is the rate limiting step in the myosin VI ATPase cycle. However, *in vitro* kinetic reports pertaining to the regulation of myosin VI by phosphorylation are contradictory. Yoshimura *et al.*, (2001), proposes that the phosphorylation of the myosin VI heavy chain by Pak3 which belongs to Group I Paks as Pak1, acts as an "on/off" switch for motility activity but not for actin-activated ATPase activity like in the case of class I myosin. *In vitro* actin-sliding activity of myosin VI showed that diminishing the phosphorylation effect on myosin VI significantly reduced the number of sliding actin filaments (Yoshimura *et al.*, 2001). However, actin-activated ATPase activity

remained the same for phosphorylated and dephosphorylated states of myosin VI. Phosphorylation of myosin I by MIHCKs (myosin I heavy chain kinases) has been shown to increase actin affinity and ATPase activity of myosin I (Fujita-Becker *et al.*, 2005).

In contrast, De la Cruz *et al.* (2001) demonstrated that the phosphorylation of myosin VI heavy chain only increases the rate of Pi release, hence increasing the duty cycle but leaving ADP release unaffected. Additionally, mutants generated to mimic phosphorylated ($T^{406}E$) and dephosphorylated ($T^{406}A$) states of myosin VI, display a similar ATPase activity. Overall, the phosphorylation of myosin VI has no effect on its motility activity. These findings are echoed by similar report that showed that phosphorylation of the T^{406} does not alter either the rate of actin filament sliding or the maximal actin-activated ATPase rate of myosin VI activity (Morris *et al.*, 2003). Nonetheless, the rate of phosphorylation induced actin-activated Pi (phosphate) is much higher in myosin I compared to myosin VI (Ostap *et al.*, 2002). Phosphorylation appears not to significantly affect myosin VI binding to actin but could possibly exert a subtle role in the cell by altering its functionality from a motor to a tether thereby reinforcing membrane tension (Naccache and Hasson, 2006; Buss *et al.*, 1998).

Additionally, another serine/threonine specific protein kinase, LMTK2 (lemur tyrosine kinase 2) has been identified as a myosin VI binding partner (Chibalina *et al.*, 2007). LMTK2 is a transmembrane protein that binds myosin VI at the same site as endocytic adaptor protein Dab2 in the C-terminal domain of myosin VI. However, LMTK2 is not shown to exert phosphorylation activity on binding to myosin VI.

Furthermore, the $T^{1089}INT^{1092}$ phosphorylation sites in myosin tail region are essential to regulate optineurin binding to myosin VI cargo-binding tail but otherwise no other known myosin VI binding partners are regulated in this fashion (Sahlender *et al.*, 2005).

1.5. *Drosophila* myosin VI (*jar*)

Myosin VI was originally discovered in *Drosophila melanogaster* as an F-actin binding protein (Kellerman and Miller, 1992). Myosin VI, also known as myosin 95F is encoded by the *jaguar* (*jar*) gene in *Drosophila* (Hicks *et al.*, 1999). Importantly, the BLAST program and alignment tool show that the full length of Jar is 52% identical to the human myosin VI (Figure 1.6). Thus, Jar will help understand the function of its vertebrate homologue.

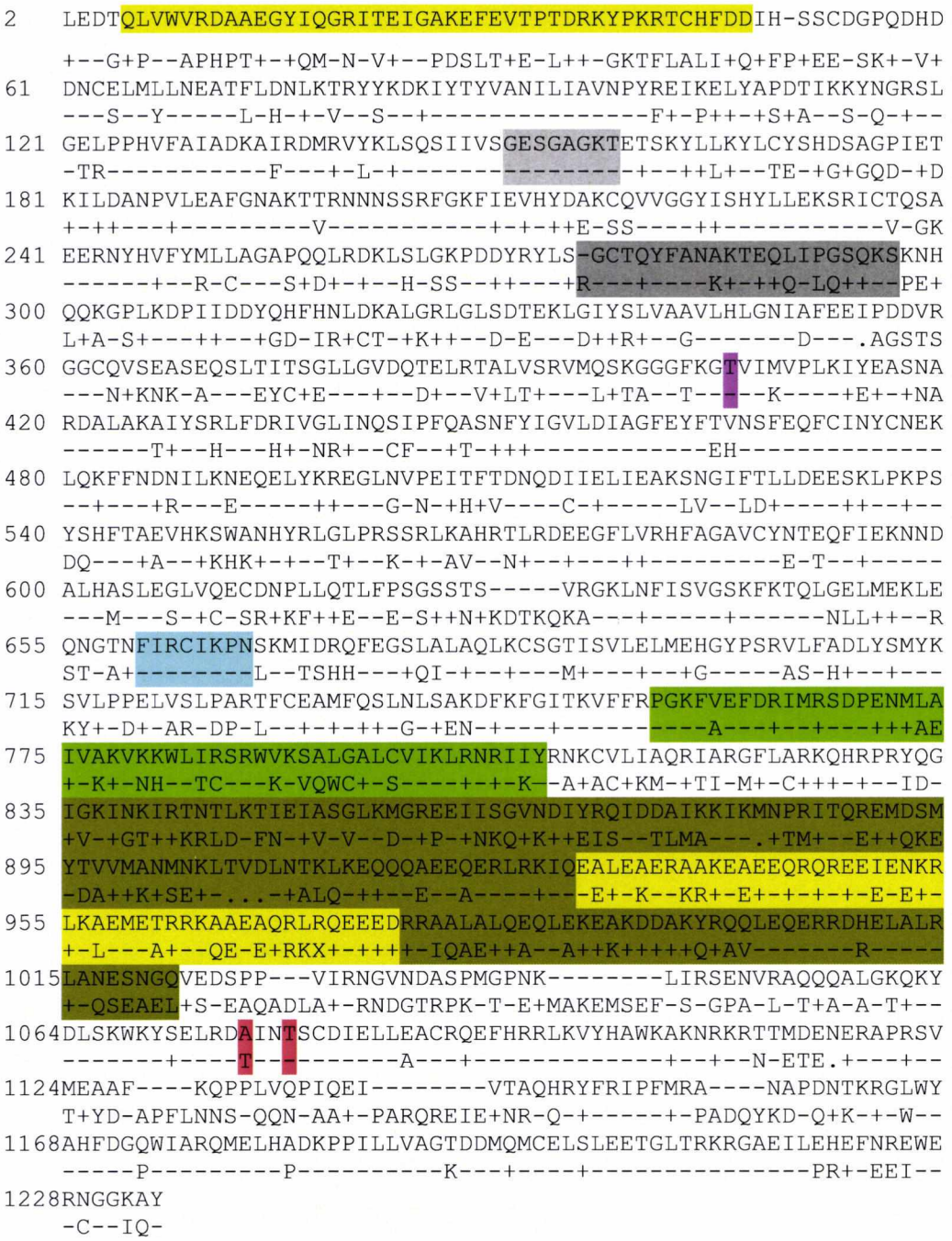

Figure 1.6. Amino acid sequence of *Drosophila* myosin VI. The full length representation of the domain organisation above showing the alignment of the *Drosophila* myosin VI sequence (top) with human myosin VI (bottom). The precise amino acid numbers are shown to the left of each line of *Drosophila* myosin VI sequence. A dash indicates identical amino acids while positives indicate degree of similarity and dots are gaps introduced during the alignment. Features highlighted are as follows (starting from the N-terminus): SH3-like fold (yellow), ATP binding site as proposed by Kellerman and Miller, 1992 (light grey), region responsible for slow ATPase activity (dark grey), phosphothreonine region (pink), Actin binding site (turquoise), C-terminus of the motor domain consisting the 53aa insert (green), region of the alpha-helix region (dark yellow) and within this region is the highly charged repeats (yellow), the $T^{1089}INT^{1092}$ phosphorylation sites (human) in the tail domain (red).

1.5.1. Structure

Structurally Jar shares many conserved residues with other class VI myosins such as the 22aa insert in the head domain and the 53aa insert responsible for the reverse motility (Figure 1.7). However, Jar features a N-terminal SH3 (Src homology 3)-like domain not noted in other class VI myosins. Generally, the function of SH3 domain is not well understood but is thought to bind to proteins rich in proline-containing sequences for mediating protein-protein interactions (Shawn, 2005). Notably, *Drosophila* contains the most proline-containing sequences in its proteome (Shawn, 2005).

Furthermore, *Drosophila* has one *jar* gene and similarly to other class VI myosin, Jar has distinct protein isoforms (Deng *et al.*, 1999). Importantly, the charge repeats RKRREEEE are also conserved in *Drosophila* though, less defined as compared to the vertebrates (Figure 1.4).

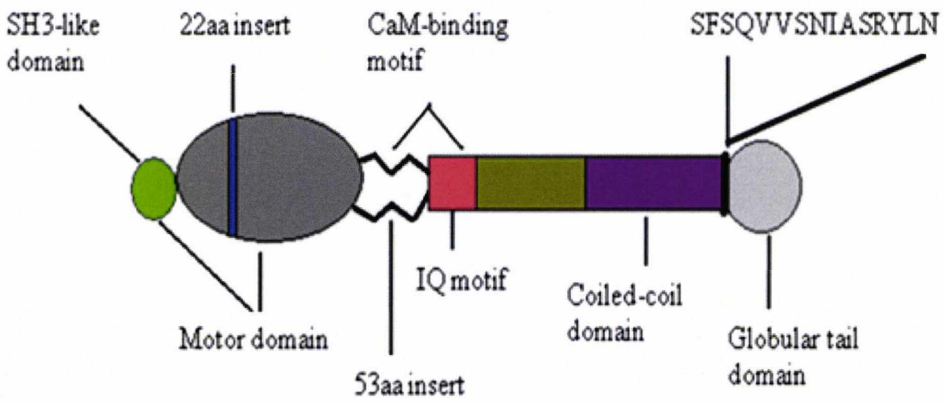

Figure 1.7. Schematic structure of *Drosophila* myosin VI. Starting from the head domain the highlights are: N-terminus with SH3-like fold (green), 22aa insert within motor domain (blue), 53aa insert consisting of CaM-binding motif (thick flexible hinges), and a large insert of 15aa alternatively spliced exon that will produce the different isoforms.

1.5.2. General function

Jar is of importance in variety of cellular processes such as actin dynamics during spermatid individualisation (Noguchi *et al.*, 2006; Hicks *et al.*, 1999), border cell migration during oogenesis (Geisbrecht and Montell, 2002; Deng *et al.*, 1999), membrane invaginations for syncytial blastoderm (Mermall and Miller, 1995), imaginal disc morphogenesis during metarmorphosis (Deng *et al.*, 1999), spindle orientation in the metaphase neuroblast (Petritsch *et al.*, 2003) and integrity of epithelial cell layers (Millo *et al.*, 2004). In these cellular events, Jar like other class VI myosin is involved in membrane anchor, migration and possibly, endocytosis.

1.5.2.1. Actin cytoskeleton regulation

Jar is envisaged as a structural cross-linker of actin filaments thus, creating tension and in-turn stabilising the cell's architecture (Noguchi *et al.*, 2006). Possibly, Jar could serve as an anchor for binding partners thereby acting as a linker to the actin cytoskeleton (Noguchi *et al.*, 2006). These concepts are clearly exemplified in several cellular processes such as the process of spermatid individualisation, oogenesis and dorsal closure.

Spermatid individualisation (Figure 1.8) involves the separation of the 64 syncytial spermatids into mature sperm by membrane remodelling of the actin-dense cone and the removal of excess cytoplasm and organelles (Hicks *et al.*, 1999). During the remodelling of the cone, active actin dynamics are observed along the length of each axoneme during which the excess cytoplasm and organelles are pushed out of the individualisation sperm tails. Jar is observed to accumulate at the front of the cones in region of dense actin network during migration. It is postulated that Jar is involved in the continuous supply of actin polymerisation regulatory proteins such as Arp2/3 (actin-related protein 2/3) complex and other actin-regulating proteins that are of importance in polymerisation and depolymerisation of actin filaments at the moving front cones (Rogat and Miller, 2002). Moreover, Jar is thought to influence the regulation process of the actin dynamics by acting in parallel pathways with

dynamin. Although in this case dynamin is thought to play a redundant role in actin dynamics.

In the depletion of functional Jar, actin complexes are lost at the front cones and consequently, disrupt the completion of the spermatid individualisation process (Noguchi *et al.*, 2006; Rogat and Miller, 2002; Hicks *et al.*, 1999). The resulting failure of cone progression is supposedly due to insufficient accumulation of actin which is required to remove the bulk of the cytoplasm and organelles. Notably, the accumulation of actin in the moving front cone overlaps with the concentrated sites of Jar (Noguchi *et al.*, 2006; Rogat and Miller, 2002). In further support, the initial cone formation is seen to progress as normal in *jar* mutants but there is a reduced density of actin filaments. This disrupts the movement of the actin cones down the length of the sperm axonemes.

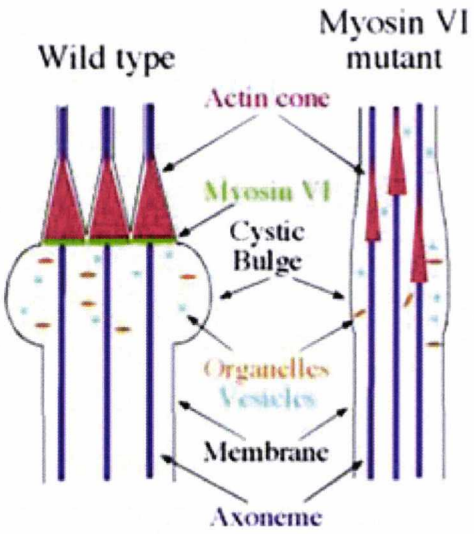

Figure 1.8. Function of Jar in spermatid individualisation. Shown above is a schematic diagram of spermatid individualisation in wild type and myosin VI mutant. In myosin VI mutant, insufficient actin accumulation in the cone fails to exclude cytoplasm and organelles and consequently, disrupts movement of cone down along the length of each axoneme (Adapted from Noguchi *et al.*, 2009).

Jar function to support cellular architecture is further exemplified in syncytial blastoderm stage embryos and during dorsal closure. The inhibition of Jar function

through microinjection of myosin VI antibodies results in defects in the formation of actin pseudocleavage furrow (membrane invagination) (Mermall and Miller, 1995). However, the defective pseudocleavage furrow was postulated to be caused by defects in the delivery of furrow components. It is on the basis that class myosin VI vertebrate is implicated to function in vesicle transport (Mermall and Miller, 1995). Alternatively, the defect could be as a result of sequestration of myosin VI-associated proteins as suggested by a report (Morrison and Miller, 2008). A similar role for Jar as an actin stabiliser or anchor is shown during dorsal closure. Expressing dominant-negative ΔATP-jar was shown to cause loss of actin cable at the leading edge (LE) cells and consequent loss of the integrity of the epithelial cell layers (Millo *et al.*, 2004).

1.5.2.2. Migratory cells

Cell locomotion is a complex multistep event that involves a retractable trailing edge, a forward force in the direction of movement generated by actin-based protrusions like the filopodia and lamellipodia and adhesion components to hold together adjacent cells to achieve a coherent migration (Le Clainche and Carlier, 2008; Vicente-Manzanares et al., 2005; DeMali and Burridge, 2003). Like its vertebrate class VI myosin, Jar is also of importance in cell migration.

Border cell migration during oogenesis, a model system reminiscent of cancer cell invasion is a classic example that demonstrates the function of Jar in cell migration (Geisbrecht and Montell, 2002). Jar is concentrated in the border cells that then migrate between the nurse cells. Jar is also found within actin-based protrusions that are extended in-between nurse cells. Cell adhesions molecules DE-cadherin and armadillo (*Drosophila* homologue of β-catenin) are also shown expressed in the border cells. DE-cadherin is a homophilic cell-cell adhesion molecule that connects to the cytoskeleton with direct binding to armadillo (Tepass *et al.*, 1996). DE-cadherin is of importance in the process of oogenesis (Niewiadomska *et al.*, 1999). The cell adhesion molecules have been found in complex with Jar demonstrated through co-immunoprecipitation assay (Geisbrecht and Montell, 2002).

The loss of functional Jar through the driven expression of antisense-Jar controlled by the GAL4/UAS system of Brand and Perrimon (1993) (Figure 1.9) resulted in severe failure of border cell migration and the reduction of the adhesion complexes. Furthermore, the overexpression of DE-cadherin can rescue the migration defects. Jar is suggested to function in stabilising DE-cadherin and armadillo in border cells. Thus, Jar is necessary to promote stable cell adhesion for correct migration (Lin *et al.*, 2007). Consistent with that, the expression of dominant-negative ΔATP-jar during dorsal stage embryos resulted in reduced levels and mislocalisation of cell surface DE-cadherin (Millo *et al.*, 2004).

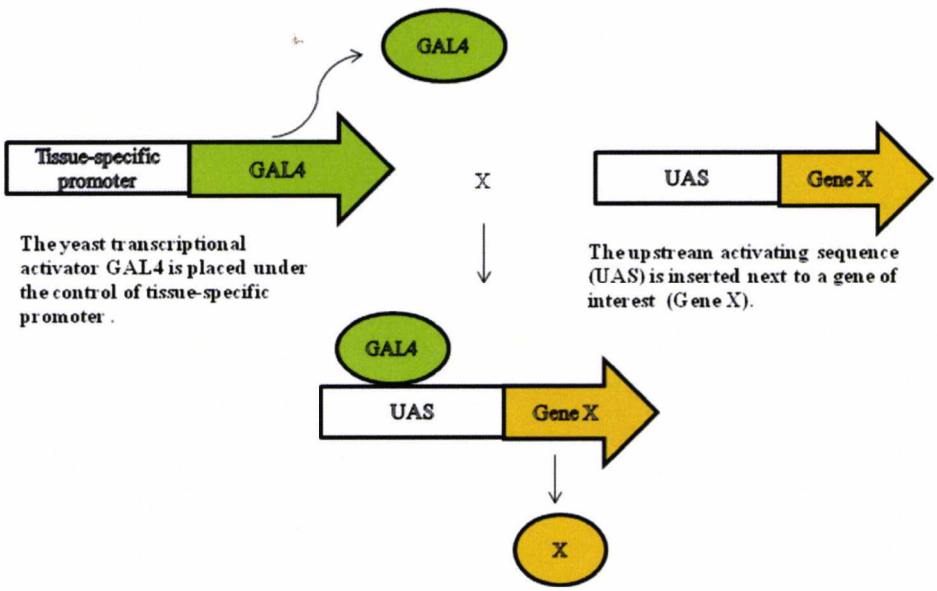

Figure 1.9. The GAL4/UAS expression system. Flies expressing the yeast transcription factor GAL4 in a tissue-specific manner are crossed to flies with a UAS element which controls the expression of the gene of interest (Gene X). In the offspring, GAL4 binds to the UAS and stimulate transcription of Gene X.

1.5.2.3. Dorsal closure

Dorsal closure is a process of complex orchestrated morphogenetic events during which epithelial sheets from opposing sides of the embryo are drawn up towards

each other and fuse along the dorsal midline covering the exposed extraembryonic tissue, the amnioserosa (AS) (Figure 1.10, movie 1.1). Dorsal closure is driven by two major forces generated from the LE cells and the amnioserosa cells in response to cues emanating from respective domains (Gorfinkiel *et al.*, 2009; Jacinto *et al.*, 2002a; Reed *et al.*, 2001; Stronach and Perrimon, 2001; Kiehart *et al.*, 2000, Glise and Noselli, 1997). Its key players are, c-Jun N-terminal Kinase (JNK) encoded by *basket* (*bsk*), TGFβ homologue *decapentaplegic* (*Dpp*) and the small GTP binding proteins of the Rho family (reviewed in, Martin and Parkhurst, 2004; Xia and Karin, 2004). Importantly, the JNK signalling pathway is the central player during the dorsal closure events. Moreover, these signalling cascades are evolutionarily conserved in cell migration, cytoskeletal rearrangement and epithelial morphogenesis in vertebrates and *Drosophila* (Figure 1.11).

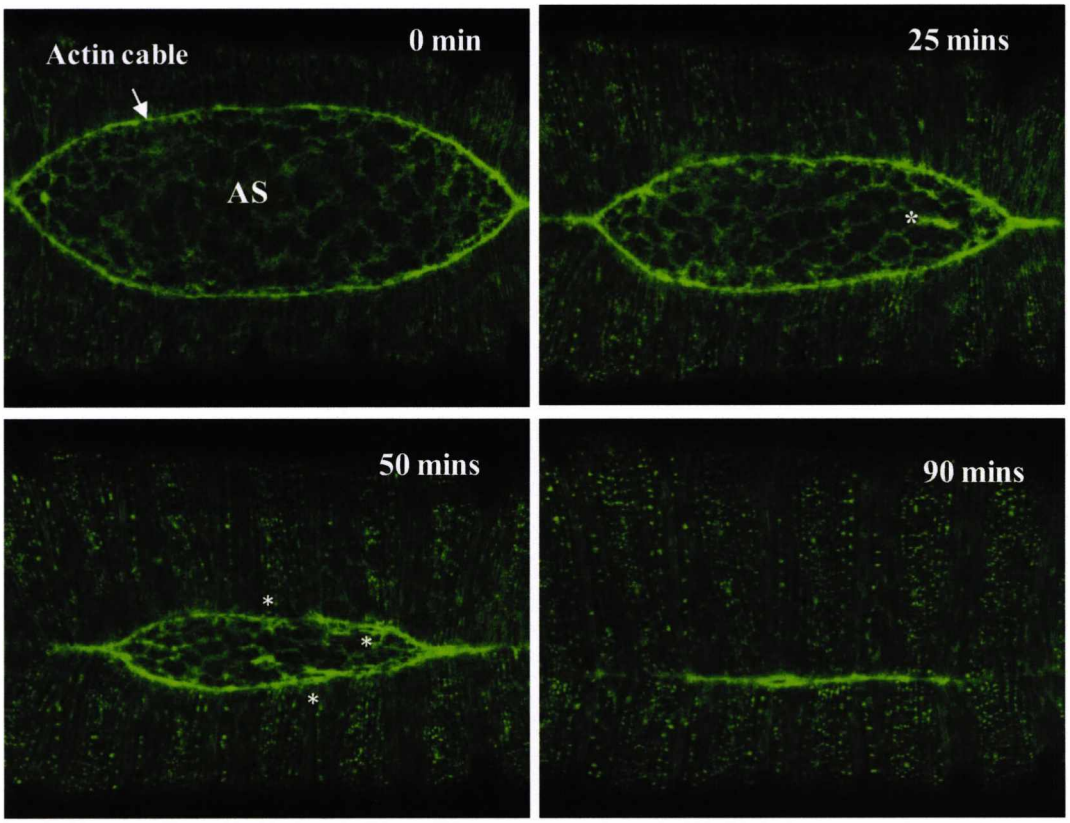

Figure 1.10. GFP-fused embryo demonstrating the process of dorsal closure morphogenesis. Above pictures are of still images from live movie with time (in minutes) numbered at the top of each images. At time 0 is an early stage 14 showing the circumference of the dorsal hole enriched with actomyosin cable (arrow). At this time the sweeping of the epithelial sheets has begun, brought about by the combined contraction of actomyosin cable and AS (within which are active protrusions). Into 25 mins of the process, the dorsal hole closes in as AS undergoes apoptosis (asterisk) and consequently, pulling in the opposing epithelial sheets towards each other. In 50 mins at stage 15, active membrane protrusions (asterisks) become obvious along the front row of cells required for sensing opposing sheets for correct cell-cell matching and fusion along the midline (90 mins).

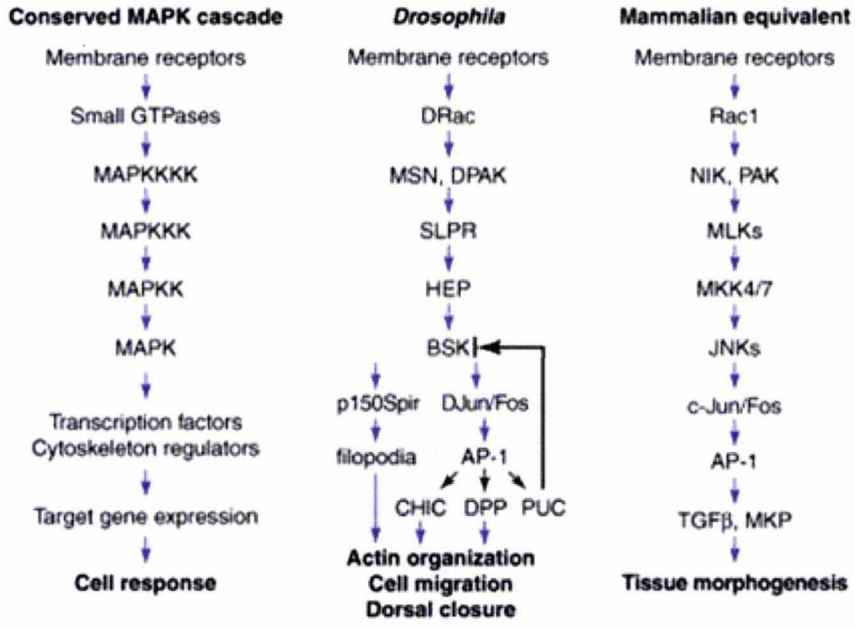

Figure 1.11. Evolutionarily conserved signalling cascade between *Drosophila* and vertebrate homologue. The diverse cellular activities are in part, influenced by JNK signalling. (Adapted from Xia and Karin, 2004).

At stage 12/13 of embryogenesis following the end of germ band retraction, dorsal closure is initiated. Jun Kinase signalling cascade is activated and the dorsal-most epidermal (also designated leading edge, LE) cells that lie over the outer most rows of AS cells begin to elongate along the dorsoventral axis of the embryo. Subsequently, Dpp causes the cells of the dorsal epidermis to elongate which is pulled up by the also elongated and stretched lateral epidermis cells sweeping over the dorsal hole.

Purse string also referred to as actomyosin cable is a combination of actin and non-muscle myosin II, forms at the very leading edge of the LE cells (Franke *et al.*, 2005; Jacinto *et al.*, 2002b; Wood *et al.*, 2002; Young *et al.*, 1993). The LE cells also accumulate components of the focal complexes (Franke *et al.*, 2005; Jacinto *et al.*, 2002b; Wood *et al.*, 2002; Harden *et al.*, 1996; Young *et al.*, 1993).

The contractible actin cable runs throughout the circumference of the dorsal hole driving the sweeping of the epithelial sheets over the active apoptotic AS cells whilst ensuring that the synchronised movement of the LE cells are constant, maintaining the taut, defined row of cells (Rodriguez-Diaz *et al.*, 2008). The key players of the

actin cytoskeleton at the LE cells is of the Rho-family small GTPases specifically Rac1, Cdc42 and Rho1, acting upstream of JNK. The Rho small GTPase family establish and maintain the organisation of the "purse string" (Bloor and Kiehart, 2002; Jacinto *et al.*, 2002a; Martin and Wood, 2002; Harden *et al.*, 1999; Ricos *et al.*, 1999).

The rows of cells are held together at junctions by cadherins. Cell-cell adhesion at the adherens junctions is mediated by DE-cadherin (Tepass *et al.*, 1996). Armadillo (*Drosophila* homologue of β-catenin) links DE-cadherin to α-catenin, and in turn, the tight regulated cadherin-catenin complexes are connected to the actin cytoskeleton. Zygotic loss of DE-cadherin results in segmental mismatches, loss of ventral epidermis and weakened actin cable (Gorfinkiel and Arias, 2007). Furthermore, the complete loss of DE-cadherin causes severe dorsal defect.

Whilst the contractility of the purse string and the elongation of the dorsal epidermis are ongoing, the amnioserosa cells are also contracting. Apical cell junctions in the amnioserosa are enriched with cortical actin network and they generate the driving forces required for the contraction of amnioserosa and the consequent cell shape changes (Rodriguez-Diaz *et al.*, 2008). The cells of the amnioserosa actively change shape whilst undergoing apoptosis promoting the advancement of the lateral epidermal cells (Gorfinkiel *et al.*, 2009; Jacinto *et al.*, 2002b; Kiehart *et al.*, 2000).

In the final phase of dorsal closure, on nearing the dorsal midline, actin-membrane protrusions, filopodia and lamelliopodia, reach out from opposing leading edges to matching segments and consequently, mediate adhesion for seamless zipping and by stage 15 of embryogenesis, the process of dorsal closure is completed (Bloor and Kiehart, 2002; Jacinto *et al.*, 2000).

Overall, both purse string and the amnioserosa contribute force for dorsal closure, but can provide enough singly to drive dorsal closure to completion (Layton *et al.*, 2009; Rodriguez-Diaz *et al.*, 2008; Kiehart *et al.*, 2000). Although acting alone slows dorsal closure.

Importantly, myosins have been shown to play important roles in the process of dorsal closure. Myosin II generates the driving force and subsequently, results in the contraction of the LE cells (Franke *et al.*, 2005). Sisyphus, *Drosophila* myosin XV

homologue is found within LE cells and their protrusions. It was demonstrated to be of importance for correct cell-cell matching for the subsequent zipping of the opposing epithelial sheets during the last phase of dorsal closure (Liu *et al.*, 2008).

Jar is involved in actin organisation and in cell-cell adhesion in epithelial cells (Lin *et al.*, 2007; Milo *et al.*, 2004). Additionally, Jar was shown to interact genetically with echinoid (Ed), an immunoglobulin domain containing adhesion molecule known to couple with DE-cadherin to mediate adhesion at adherens junctions (Lin *et al.*, 2007; Wei *et al.*, 2005). During dorsal closure Jar is expressed at the apical side of the LE cells and in the amnioserosa and the lateral epidermis that flanks the amnioserosa cells (Figure 1.12).

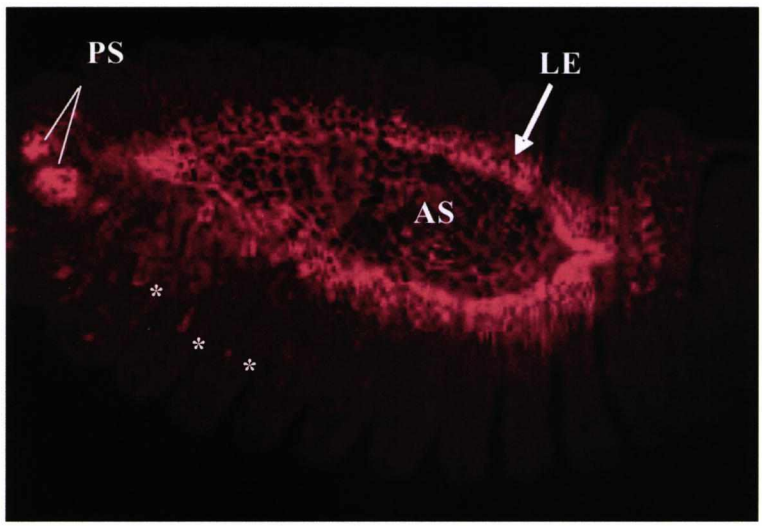

Figure 1.12. Dorsolateral view of late stage 14 embryo showing ubiquitous expression of Jar protein. Jar protein expression can be seen along the LE cells, little expression in the amnioserosa (AS) cells, posterior spiracles (PS) and muscle attachment in the epithelial sheets (asterisks).

1.5.2.4. Genetics

The importance of Jar for *Drosophila* development has been a subject of controversy. Mutagenesis such as a P-element induced mutations, has allowed one to unravel and identify the many functions of Jar. A P-element is a transposon and it encodes a transposase for its mobility within the fly genome. P-element mutagenesis

is primarily through P-element insertions into genes and imprecise excision of P-elements near genes (Ryder and Russell, 2003). The excision of the P-element can be determined following molecular analysis of the locus.

A partial loss-of-function of Jar in jar^{mmw14} and jar^{1} mutants (Figure 1. 13C) prevents Jar protein expression in the testes causing male sterility due to failure of spermatid individualisation but otherwise, does not affect the viability of the fly (Hicks *et al.*, 1999).

Homozygous null mutant, jar^{322} generated by imprecise excision of the P-element in the first intron of jar^{1} mutant allele has all the amino acid coding sequences in the Jar gene deleted and at least, the first exon of the neighbouring gene, CG5706 which encodes a phenylalanine tRNA ligase (Figure 1.13B) (Petritsch *et al.*, 2003). Maternal *jar* mRNA and Jar protein are shown expressed in late embryogenesis and thereafter, Jar protein is reduced in zygotic jar^{322} homozygous embryos. The zygotic jar^{322} mutants die as first or early second instar larval stage.

Jar deletion mutants, $jar^{R39}$and jar^{R235}cause loss of Jar protein expression in late embryos but Jar mRNA transcripts are reported to persist until larval stage though at a lower level in comparison to wild-type (Millo *et al.*, 2004). Consequently, $jar^{R39}$and jar^{R235} mutants die during embryogenesis and with occasional dorsal defects but large percentage of mutants die in the first instar larvae stage. Both jar^{R39} and jar^{R235} mutants were created by imprecise excision of P-element from the 5` UTR, upstream to Jar first exon (Figure 1.13D, E). The phenotypic defects of jar^{R39} and jar^{R235} mutants are probably due to neighbouring genes that were affected during the remobilisation of the P-element.

The excised P-elements in both jar^{R39} and jar^{R235} were reinserted in genes downstream of Jar and these genes have molecular function (Millo *et al.*, 2004, flybase.org). In mutant jar^{R39} the P-element reinserted itself within CG5991 gene. According to flybase the CG5991 gene is of a protein-coding-gene with a molecular function in phospholipid metabolism. Reportedly, it is one of the many genes involved in the suppression of *Drosophila* larval neuromuscular synapse overgrowth induced by dominant-negative expression of $UAS\text{-}NSF2^{E/Q}$ (Laviolette *et al.*, 2005). NSF (N-Ethylmaleimide sensitive factor) an ATPase molecule is shown to be of

importance in vesicle trafficking in neuromuscular junction (NMJ). Interestingly, null NSF2 alleles die during first instar larval stage.

Upstream from Jar gene from which the P*[GawB]*-element was excised from, is an Organic cation transporter 2 (ORCT2) gene. The ORCT2 gene, *calderon* (*cald*) encodes an organic cation transporter of the major facilitator superfamily that aides in the uptake of organic metabolites (Herranz *et al.*, 2006). It is a downstream effector of the insulin receptor (InR) pathway required for growth and proliferation of larval tissues in *Drosophila*. Loss of the *cald* gene results in the characteristic U-shape phenotype of embryos unable to retract the germ band. Interestingly, similar U-shape phenotype is portrayed by the trans-heterozygous mutant embryos jar^{R39}/jar^{R235} (Millo *et al.*, 2004).

In contrast, the striped expression of dominant negative ΔATP-jar construct is embryonic lethal and exhibiting severe dorsal defects such as loss of contractile purse string and loss of adhesive properties due to reduced/mislocalised cell surface DE-cadherin (Millo *et al.*, 2004). However, Morrison and Miller (2008) conclusively demonstrated that Jar is not critical for the viability of the fly because 40% of mutants lacking maternal and zygotic Jar protein can survive to adulthood. Nonetheless, this project sets to resolve the pressing issue.

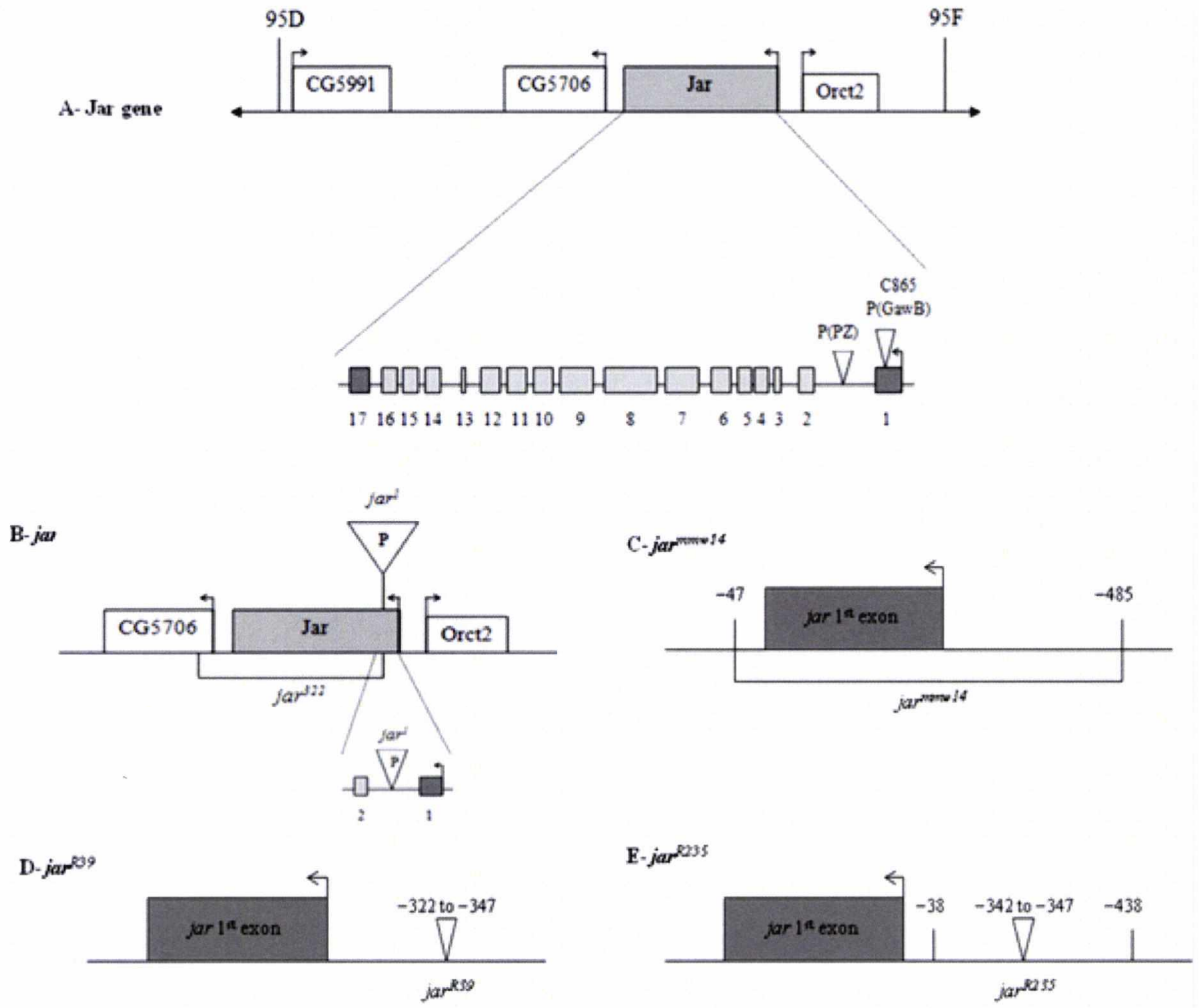

Figure 1.13. Jar genomic structure and *jar* mutated genes. (A) Schematic depicts a portion of the right arm of the third chromosome, showing Jar gene and its neighbouring genes. The unfilled arrows indicating the transcription start site and direction. Diagram below illustrates the exons and non-coding exons (dark grey) of Jar gene and relative positions of P-element insertions. P insert line, *C865* contains a single *P[GawB]* element inserted 5′ of Jar first exon and *P(Z)* is inserted within the first intron (Hicks *et al.*, 1999). The imprecise excision of *P[GawB]* element line generated Jar alleles, jar^{322}, jar^{mmw14}, jar^{R39} and jar^{R235}while *P(Z)* element insertion generated jar^{1} mutation. (B) jar^{322} mutation was created by imprecise excision of the *P(Z)* element inserted within the first exon of jar^{1}(as illustrated by the diagram below) (Petritsch *et al.*, 2003). The imprecise excision of the insertion removed the whole of Jar coding gene (exons 3-17) and the first exon of CG5706. (C) The mutation jar^{mmw14} resulted from the deletion of the whole first exon of Jar plus 485 bp flanking the 5′ and 47 bp flanking the 3′ end of Jar first exon (Millo *et al.*, 2004). (D) Mutated jar^{R39} resulted from the deletion of 340-347 bp upstream to Jar first exon while sequence 322 to 341 bp is duplicated (E) jar^{R235} mutation was as a result of sequence from 342 to 347 bp upstream to Jar first exon changed to GTTTTC. 438 bp upstream to Jar first exon, the nucleotide A was deleted while 38 bp upstream to the first exon of Jar the nucleotide G was replaced with an A. Modified from Morrison and Miller (2008) and Millo et al. (2004).

1.6. Pak

1.6.1. Vertebrate Paks

The p21-Activated kinases (Paks) belong to a family of Cdc42/Rac regulated serine/threonine protein kinases (Brzeska *et al.*, 1997). Cdc42 and Rac are the direct upstream signalling molecules of Paks. In vertebrates, six Pak isoforms (Pak 1-6) are subdivided into two groups (Jaffer and Chernoff, 2002). Group I Paks comprise of Paks 1, 2 and 3 whereas Group II Paks are of 4, 5 and 6. All Paks share highly conserved catalytic domain at the C-terminus but vary at the N-terminal domain.

The Group I Paks share a conserved Cdc42/Rac-interactive binding (CRIB) domain also termed p21-binding domain (PBD) that overlaps the autoinhibitory domain (AID), another shared domain. They are activated upon binding of GTP-bound forms of Rac and Cdc42. The autoinhibitory domain functions by inhibiting Pak kinase activity in the absence of activated GTP-bound Cdc42 or Rac.

Conversely, the Group II Paks possess the CRIB domain but lack the conserved AID. They do not require activated form of the Rho GTPases for their kinase activity (Pandey *et al.*, 2002), but their interaction with the Cdc42/Rac is essential for differential targeting of the Pak proteins to cellular compartments (Abo *et al.*, 1998).

Paks are evidently important for maintaining and remodelling cytoskeletal architecture (reviewed in, Szczepanowska, 2009). The role of Paks in cytoskeletal rearrangement is supported by the findings that several of the Pak-interacting proteins are cytoskeletal regulators (Figure 1.14). Furthermore, Paks especially that of the Group I are extensively demonstrated to be of importance in regulating cell migration, gene transcription through MAPK signalling cascades, cell-cycle, cell transformation, microtubule dynamics, hormone signalling and apoptosis (reviewed in, Wells and Jones, 2010; Szczepanowska, 2009; Arias-Romero and Chernoff, 2008; Zhao and Manser, 2005). In addition, Paks are shown to be overexpressed in numerous types of cancer cells and moreover, promote cancer cell invasion. Conversely, Paks are also implicated in cell survival pathways (Wells and Jones, 2010; Schürmann *et al.*, 2000). Thus, Paks can homeostatically maintain balance between cell survival through the phosphorylation and inactivation of proapoptotic

protein, Bad amongst many survival signals and cell death through proteolytic activation of Pak2 (Wells and Jones, 2010; Molli *et al.*, 2009; Schürmann *et al.*, 2000).

The various physiological effects of Paks are triggered through its phosphorylating target proteins. Myosins are among substrates such as LIMK (LIM domain kinase), filamin A, cortactin, to name a few that are of target of Paks (reviewed in, Szczepanowska, 2009). Myosin light-chain kinase (MLCK) is one of regulatory mechanisms for class II myosin. Paks are shown to phosphorylate the serine residues on MLCK and thus, inhibiting its activity on phosphorylating MLC for actin-activated ATPase activity of myosin II. As earlier stated, class I and VI myosins are also regulated by Pak proteins for functional and motility activities though, that of myosin VI regulated in such manner is yet to clarified *in vivo* (Buss *et al.*, 1998; Brzeska *et al.*, 1997).

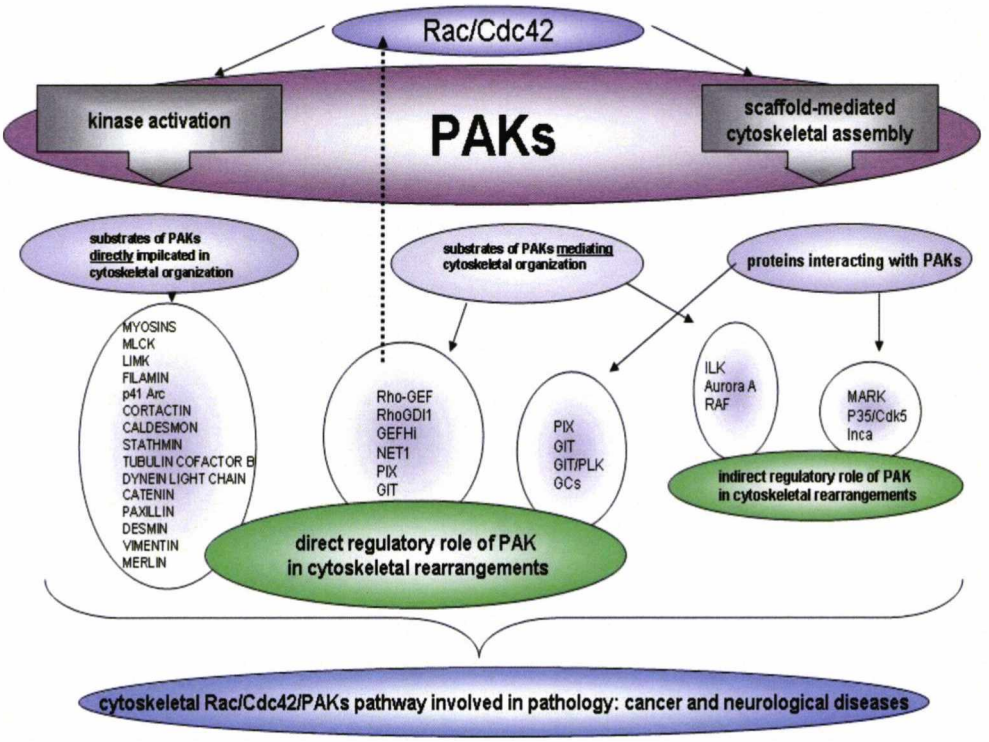

Figure 1.14. An overview of Rac/Cdc42/Pak pathway involved in the establishment of cytoskeletal reorganisation directly and indirectly through various substrates and binding partners. (Adapted from Szczepanowska, 2009).

1.6.2. *Drosophila* Paks

Similarly to vertebrate Paks, *Drosophila* has two subgroups of Paks, each representative of the two groups of human Paks (Conder *et al.*, 2004). *Drosophil*a Group I Pak consist of two Pak proteins, DmPak and DmPak3 whereas *Drosophila* Group II Pak is of one protein Pak encoded by *Mushroom bodies tiny*, *mbt* (DmPak2). Additionally, the autoinhibitory domain is also conserved in *Drosophila* Group I Paks and not in DmPak2.

Group I DmPaks are importance for actin reorganisation in the LE cells during dorsal closure (Conder *et al.*, 2004), polarised organisation of the actin cytoskeleton and in maintaining apical-basal polarity of border cells during oogenesis (Conder *et al.*, 2007), axon guidance in growth cones of photoreceptor (R) cells (Mentzel and Raabe, 2005; Hing *et al.*, 1999), in septate junction (analogue to vertebrate tight junctions function) formation (Bahri *et al.*, 2010) and in muscle morphogenesis and myotube guidance during embryogenesis (Bahri *et al.*, 2009).

On the other hand, DmPak2 is predominantly found at adherens junctions where it is demonstrated to phosphorylate Armadillo on serine residues, Ser^{561} and Ser^{688} which are both conserved in vertebrate β-catenin (Ser^{552} and Ser^{675}) to help regulate and maintain the integrity of DE-cadherin mediated cell-cell contacts (Menzel *et al.*, 2008 & 2007). Furthermore, DmPak2 could be involved in cell neuronal survival as is its vertebrate homologue (reviewed in, Wells and Jones, 2010).

During dorsal closure dPak (DmPak) is shown recruited to the LE cells but weakly in the AS cells (Bahri *et al.*, 2010; Conder *et al.*, 2004; Harden *et al.*, 1996). Disrupting the function of Pak by expressing dominant-negative dPak-AID causes dorsal defects (Conder *et al.*, 2004).

1.7. Project aims

1.7.1. Summary

In vertebrates, myosin VI is implicated in diverse cellular processes and several binding partners are responsible for the differential targeting and/or recruitment of myosin VI. However the precise functions and the regulatory mechanism(s) of myosin VI in these cellular processes remain under extensive research because it is the only class of myosin so far identified to walk along actin cable in the opposite direction to other characterised myosin superfamily members.

Seemingly, the functions of myosin VI are conserved between vertebrates and invertebrates. *Drosophila* myosin VI is demonstrated to function in membrane remodeling, actin organisation, maintenance of rigidity in migrating epithelial sheets, cohesion between cell-cell contacts.

Furthermore, myosin VI is found to be a monomer throughout the course of *Drosophila* development (Noguchi *et al.*, 2009). Consistent with this, myosin VI monomers were found to rescue the defective spermatid individualization more effectively as opposed to artificial myosin VI dimers during an add-back experiment assay (Noguchi *et al.*, 2009). That said, myosin VI may possibly, undergo dimerisation for roles such as the transportation of cargoes in certain cell types and in response to physiological and environmental cues.

1.7.2. Hypothesis

Phosphorylation of vertebrate myosin VI in the motor domain by Group I Paks has been demonstrated *in vitro*. Expressing either a dominant negative Jar or a dominant negative Pak construct causes highly overlapping dorsal closure phenotypes. Importantly, *Drosophila* myosin VI has a Pak phosphorylation site within its motor domain homologous to that of the other myosin VI-containing species (Figure 1.5).

This study tests the hypothesis that *Drosophila* myosin VI is dependent on Pak-mediated phosphorylation for its function in dorsal closure.

Chapter 2. Materials and Methods

2.1. Materials

All reagents were supplied by Sigma, Fisher Scientific, Melford laboratories or BDH laboratories unless otherwise stated.

2.1.1. General stock solutions

All solutions were made with autoclaved deionised water (dH_2O).

10X PBS pH 7.4 (1 L)

NaCl	1.3 M
Na_2HPO_6	70 mM
$NaH_2PO_42H_2O$	30 mM

A litre volume was made up with dH_2O. 10X stock solution was diluted 1X for working solution.

PT (50 ml Falcon tube)

1X PBS	40 ml
Triton-X	0.3%

PBS was added to make the final volume.

PBT (50 ml Falcon tube)

1X PBS	30 ml
Triton-X	0.3%
BSA	0.5%

Volume was made up with PBS and stored at 4°C.

0.5 M EDTA pH 8.0 (500 ml)

93.06 g of EDTA disodium salt was dissolved in 350 ml of dH_2O and pH adjusted to 8 with the addition of NAOH pellets. Final volume of 500 ml was made up with dH_2O.

0.5 M EGTA pH 8.0 (500 ml)

19.02 g of EGTA was dissolved in 100 ml of dH_2O and pH adjusted to 8 with the addition of NAOH pellets. Final volume of 500 ml was made up with dH_2O.

2.1.2. Western blot buffers

Lysis Buffer

Triton X-100	1%
Tris-HCl pH 7.4	0.05 M
NaCl	0.15 M
complete Protease inhibitor cocktail (Roche)	0.005%

2X SDS sample buffer

Tris-HCl pH 6.8	1 M
SDS	4%
Bromophenol blue	0.2%
Glycerol	20%
Dithiothreitol (DTT)	1 M

7 % Resolving gel

Acrylamide / Bis solution 29:1	7%
Tris-HCl pH 8.8, 2 M	5.6 µl
SDS	0.1%
N,N,N,N'-Tetra-methyl-ethylenediamine (TEMED)	15 µl
10 % Ammonium persulfate	450 µl

3.75 % stacking gel

Acrylamide / Bis solution 29:1	3.75%
Tris-HCl pH 6.8	0.1 M
SDS	0.1%

10X Running buffer pH 8.3

Tris-HCl	0.25 M
Glycine	1.92 M
SDS	10 %

Transfer buffer pH 8.3 (1 L)

10x running buffer	100 ml
Methanol	100 ml

Ponceau S staining solution

Ponceau S	0.2%
Acetic acid	3%

Sample wash for immunodetection (1 L):

Added 0.1% Tween-20 and 100 ml of 10 X PBS stock solution to 900 ml dH_2O.

Blocking Buffer

Marvel (milk powder)	3%
BSA in PBS	1%

2.1.3. DNA extraction and Gel electrophoresis

Squishing buffer

Tris-HCl pH 8.2	10 mM
EDTA	1 mM
NaCl	25 mM
Proteinase K 20 mg/ml (Ambion)	200 ug/ml

10X TAE (1 L)

Tris base	48.8 g
Glacial acetic acid	11.4 ml
0.5M EDTA	20 ml

A litre volume was made up with dH_2O. 100 ml of 10X stock solution was added to 900 ml of dH_2O to make 1X working solution.

PCR Nucleotide Mix (Promega)

An equal volume of each dNTPs (dCTP, dATP, dGTP, and dTTP) from stock solution of 100 mM was added to dH_2O in a 1.5 ml eppendorf tube to give a final concentration of 10 mM. Stored at -20°C.

0.8% Agarose gel (50 ml)

Agarose	0.4 g
1XTAE	50 ml
SYBR® (Invitrogen)	4 µl

Agarose was weighed out and added to 50 ml of 1X TAE buffer in a conical flask. This was heated in a microwave until the agarose had melted. SYBR DNA gel stain was added to the mixture. This was left to cool and poured into gel plate containing a comb to make wells. Prior to sample loading, the gel was immersed in 1XTAE in a gel tank (Labnet Gel XL Ultra) and ran at 50 volts for 40-45 minutes.

2.1.4. Fly media

Media was dispensed using an automatic dispenser into vials (7-8 ml) creating 2 cm depth or bottles (20-25 ml) a depth of 3 cm. When mixture was set, the media was kept at 18°C.

Standard cornmeal medium (1 litre)

Component	
Agar	8.5 g
Cornmeal	75 g
Yeast	31.5 g
Dextrose	93 g
Sodium potassium Tartrate	8.6 g
Calcium Chloride	0.7 g
$_{p}$-Hydrobenzoic Acid Methyl Ester (Nipagin)	2.5 g
Ethanol	9.3 ml

Embryo laying plates

Component	Volume
Apple juice	500 ml
Agar	9 g
Glacial acetic acid	6 ml
Ethanol	6 ml

This recipe is enough to make 40 apple juice plates. 9 grams of agar was weighed out and added to 250 ml of apple juice. Agar is heated in microwave until melted. 6 ml of acetic acid and 6 ml of ethanol was added to the mixture. The reminder of the apple juice (250 ml) was added to cool down the mixture. The apple agar mixture was poured into petri dishes, left to set and stored at 4°C.

Yeast paste: yeast granules are added to water in a falcon tube. This was mixed with spatula to a smooth consistency. Stored at 4°C.

2.1.5. Preparation for live confocal imaging

Embryo glue: Strips of double-sided tape were transferred to a glass scintillation vial containing heptane. This was mixed for 1 hour or more on a rotation until the right strength of glue was achieved. The strips were removed and glue that was too strong was diluted with heptane.

Halocarbon oil: Added equal volumes of Halocarbon oil 27 and 700 (Sigma-Aldrich).

2.1.6. Antibodies

The primary antibodies and (dilutions) were used are as follows: mouse monoclonal anti-myosin VI antibodies (1:20), rat DCAD2 (1:125), rabbit anti-non-muscle myosin II (1:500). Secondary antibodies were used for 2 hours at room temperature at a 1:500 dilution, were conjugated to Alexa Fluor® (Molecular probes), goat and rabbit FITC, goat and mouse TRITC, or Cy5 fluorescent dye. Rhodamine-conjugated phalloidin (Sigma) was used to visualise F-actin filaments.

2.1.7. *Drosophila* Stocks

Drosophila stocks were obtained from the Bloomington *Drosophila* Stock Centre (Indiana University, Bloomington, IN) unless otherwise stated. The following fly strains were gifts: *w;SGMCA* and *w;sqhGal4* (Dan Kiehart, Duke University) and *UAS-PakAID* (Nick Harden, Simon Fraser University). The following recombinant and stock were created in-house: $jar^{322}pak^{11}$/ *TM3, KrGFP* and jar^{322}/*TM3, KrGFP*. UAS lines were expressed using the GAL4 system of Brand and Perrimon (1993) (Figure 1.9). The RNAi transgenic lines were obtained from the Vienna Drosophila RNAi Centre (VDRC): *jar RNAi* (VDRC 37534), *pak RNAi* (VDRC 12553), *ed RNAi* (VDRC 3087) and *synectin RNAi* (VDRC 31522).

***Drosophila* stocks**

Stocks	**Bloomington Stock No.**
w^{1118}	3605
w; UAS-DRhoA^{N19}	7372
kar ry pnr^{VX6}*/TM3,Sb Tb*	Kyoto 101673
bsk^{1} *cn bw sp/CyO*	3088
y; ed^{KG093686}*/CYO; ry*	15182
w; jar^{2095}*/TM3,Sb Ser*	7246
jar^{322}*/TM3, Sb UbxlacZ*	8776
pak^{6}*/TM3, Sb*	8809
pak^{11}*/TM3, Sb*	8810
tkv^{7} *cn bw sp/ CyO*	3242
yw; UAS-tkv^{QD}*/TM3, Sb Ser*	36536
w; SGMCA, $Egfr^{f6}$*/CyO,KrGal4 UAS-GFP*	Tubingen stock
w; His2Av-mRFP(III.1)	23650
w; UAS-hep^{ACT}*/CyO*	9306
UAS-GFP-actin,w^{1118}	7309
w;UAS—GFP- αTubulin84B	32075
w; UAS-GMA	31775
Df(3R)crb87-5	2363
w; L Pin/Cyo, KrGal4 UAS-GFP	5194
y w; Dgl/TM3, KrGal4 UAS-GFP	5195

GAL4 drivers and their expression pattern

Gal4 driver lines	**Expression pattern** (http://flybase.org)	**Stock No.**
w; wg^{Sp-1} /CyO;dppGal4/TM6, Tb	Expressed in posterior spiracles and cells of the dorsal ectoderm from stage 12 of embryogenesis	1553
yw; pnrGal4/TM3, Ser UAS-y	Restricted to the promixmal-most part of the notum in the wing disc during 3rd instar larval stage. Dorsal band along the length of the adult body: thorax, head, abdomen and cuticle	3039
w; 109-69/CyO	Expressed in stage 8 follicle cells, in the embryonic dorsal epidermis, parts of the peripheral nervous system, wing imaginal disc and brain	7026
w; enGal4	Expression from stage 11 of embryogenesis, in larval tissues and imaginal disc but restricted to the posterior compartment	6356
w; 69BGal4	Expression in embryonic epiderm (stages 9-17) and imaginal discs (larval stage)	1774
w; sqhGal4	Ubiquitous expression throughout *Drosophila* development	See text
w; c381Gal4	Expression in amnioserosa and in stage 14 PNS of embryos	3734

2.2. Methods

2.2.1. *Drosophila* stock maintenance

General stocks were raised at 18°C on a standard cornmeal medium contained in vials or bottles supplemented with fresh yeast granules. At 18°C, a fly's life span is doubled compared to 25°C, an optimum rearing condition for flies. Flies are

transferred into new vials every 4 weeks. The vials were sealed with cotton wool bungs at the top whilst allowing air to circulate. Old stock vials were maintained as backup stocks in the case the new stocks fail to generate. w^{1118} was used as a wild-type control strain and mutations were maintained over standard balancers with GFP markers.

2.2.2. Anesthetising flies using CO_2

Fly sorting and crossing were done at a fly station. The fly station consisted of a dissection microscope, a porous pad, a CO_2 gas canister and a light source. Prior to fly sorting or genetic crossing, a nozzle connected to the CO_2 gas canister was used to circulate CO_2 briefly into the vial or bottle containing the flies. The flies were transferred and kept immobilise on the porous pad through which CO_2 circulates. Prolonged exposure to carbon dioxide is avoided at the fly station as it can cause headaches/ dizzy spells to humans.

2.2.3. Sexing flies

Generally, females are larger than males. Males have a darker and rounder abdomen and in addition have extra hairs (sex combs) on their front pair of legs.

2.2.4. Collecting virgins

Females mate when they are 10-12 hours old after eclosion. Thus, virgin females were collected in the window frame between 8-10 hours. Virgin females are paler in colour and have greenish spot on the underside of the abdomen. Collections were stored in vials until enough were collected for crossing.

2.2.5. *Drosophila* crosses

Typically, for genetic crosses it was 5 virgin females to 3 males (preferably three days old) in vials whereas in cages or bottles, it was 20-30 virgin females to 10-15

males. All experimental crosses were raised at 25°C, optimum temperature for *Drosophila melanogaster* and the GAL4 expression system.

2.2.6. Sample collection and Antibody staining protocol

2.2.6.1. Embryos

Parents were provided with a ventilated fly cage attached to apple juice plate supplied with yeast paste and allowed to lay eggs for several days. Plates were regularly changed to prevent overcrowding. Prior to collection, a clearing plate was provided for 1-2 hours and this allows embryos retained by the females released onto the plate. A collection plate was provided and eggs were laid for 1-3 hours. The collection plate is retrieved, and left to age appropriately. After an appropriate development stage was obtained, the embryos were carefully dislodged into a collection basket using a paintbrush and washed with deionised water. Embryos were dechorionated in 50% sodium hypochlorite (Acros organics) in water for 2 minutes and washed with deionised water. The embryos were transferred to a glass scintillation vial containing two phase 1:1 mixture of 4% paraformaldehyde (pfa) in PBS and heptane. The mixture was given a brief shake and fixed for 20 minutes on a rotator. The fixation mixture was then allowed to separate and the bottom aqueous was aspirated off using a 150 mm glass Pasteur pipette. The fixative was replaced with Pasteur pipette full of methanol and vigorously shaken for 10 seconds to devitellinise the embryos. The mixture was again allowed to separate creating an upper heptane layer and the devitellinise embryos sank to the bottom. The heptane layer was aspirated off and embryos rinsed with 2X Pasteur pipette full of methanol. The embryos were transferred to a 1.5 ml eppendorf tube and were given a final rinse with methanol. The embryos are used immediately for antibody staining or stored at -20°C in methanol.

Embryos were rehydrated in methanol and rinsed with PT. Embryos were then blocked in PBT for I hour at room temperature. Followed by incubation with

primary antibody in PBT for I hour at room temperature or overnight at 4°C. The incubation was done on a rotator. Embryos were thereafter washed with 4X with PBT for 10 minutes and incubated with secondary fluorescent-conjugated antibody in PBT for 2 hours at room temperature on a rotator. Embryos were then washed with 4X with PT for 10 minutes and rinsed once with 30% glycerol. The solution was then replaced with 50% glycerol and was stored at -20°C or mounted on a glass slide and with cover slip for viewing using a confocal microscope.

2.2.6.2. Imaginal disc

Parents were placed in a bottle containing standard cornmeal medium supplied with fresh sprinkle of yeast granules and left to lay eggs for 3-5 days before parents were discarded. The bottle was left to sit at 25°C and larvae were collected using forceps into a 1.5 ml eppendorf tube and rinsed in PBS.

For imaginal disc dissection, larvae were transferred from the eppendorf tube to a depression glass side with 1-2 drops of PBS on stage of a dissecting microscope. Using two pairs of fine forceps and holding the larva at the anterior end (near mouth hooks) with one pair of forceps, the other was used in inverting the head section. Thus, larva body was seen inside out and fat body was easily pulled away and discarded. The imaginal discs were left intact to the body wall. These were collected into eppendorf tubes containing PBS placed and put on ice until sufficient larvae were dissected. Dissected larvae were transferred into fix solution containing 4% pfa in PBS and fixed for 40 minutes at room temperature on a rotator. The dissected larvae were washed twice with PT which was drawn off and replaced with PBT. The dissected larvae could then be stored for several days at 4°C.

For antibody staining, the dissected larvae were blocked in PBT for 1 hour at room temperature. The dissected larvae were then incubated in primary antibody in PBT overnight at 4°C on a rotator and washed 4X with PBT for 15 minutes on a rotator. Dissected larvae were then incubated with secondary fluorescent-conjugated antibody in PBT for 2 hours at room temperature with gentle shaking on a rotator. The dissected larvae were then washed 4X with PT for 15 minutes, and washed once

with 30% glycerol. The dissected larvae were then mounted in 50% glycerol that was stored at 4°C. For control, antibody staining procedure was followed as described with the exception that the primary antibody step was omitted.

2.2.6.3. Antibody double labelling

Samples were collected and fixed as described above, with the exception of the primary antibody incubation step. Samples were incubated with the first primary antibody and washed 4X with PBT for 15 minutes before the second incubation with the second primary antibody (raised in different animal to the first). Samples were then washed 4X with PBT for 15 minutes. Both secondary florescent-conjugated antibodies were added to the same tube containing the samples and incubated for 2 hours at room temperature on a rotator. Samples were then washed 4X with PBT for 15 minutes and rinsed once with 30% glycerol before mounting in 50% glycerol.

2.2.6.4. Rhodamine phalloidin staining

For F-actin detection, antibody staining protocol was followed as normal, with the exception of the fixation time which was for a maximum of 5 minutes. And also methanol step was replaced with 80% ethanol. Rhodamine phalloidin staining was done in tubes wrapped with foil to exclude light. Sample was blocked in PBT for 1 hour at room temperature on a rotator. Prior to staining, rhodamine phalloidin suspended in methanol in a 1.5 ml eppendorf tube was wrapped in foil and placed in a 50°C oven for 10 minutes. The top of the tube was left open so that methanol could evaporate. Phalloidin was resuspended in PBT and was transferred to tube containing the sample. The sample was incubated for 1 hour at room temperature on a rotator. Because rhodamine phalloidin is fluorescent-conjugated, secondary antibody incubation step was omitted. Sample was washed 4X with PT for 15 minutes and rinsed once with 30% glycerol before mounting in 50% glycerol.

2.2.7. Calculation of lethality percentages

General calculation:

$$\frac{\text{Number observed}}{\text{Number of expected genotypic ratio}} \times 100$$

2.2.8. Cuticle preparation

Embryos were collected on apple juice agar plates and aged for 46 hours at 25°C. Unhatched fertilised embryos were hand dechorionated on a double-sided tape affixed to a glass slide and transferred to an apple agar slab where they were appropriately oriented with the dorsal region facing upward. The eggs were mounted in 30 µl of acetic acid:Hoyers (1:1) on a glass slide. A cover slip was placed over the glass slide slowly to avoid bubbles and the slide was incubated at 65°C for 24 hours to allow embryonic tissues to clear and cuticles to flatten. The slides were processed to visualise cuticle pattern on a Leica DMR fluorescence microscope. Images captured with a Leica DC500 camera and processed using a Leica IM50 program.

2.3. Generation of mutants

2.3.1. Generating *jar*^{322}*/TM3, KrGFP* stock

Males of *jar*^{322}*/TM3, Sb* were out-crossed to virgin females of *y w; Dgl/TM3, KrGal4 UAS-GFP* balancer. From the F1 crossing progenies recognised by their Stubble (Sb) marker were generated and kept as stock.

2.3.2. Maternal and zygotic *jar*^{322}*/Df(3R)crb87-5, His2-RFP* construct

To generate zygotic *jar* mutant, *jar*^{322}*/TM3, KrGFP* females were crossed to *Df(3R)crb87-5;His2-RFP/TM3, KrGFP* males. For maternal *jar* mutant, the resulting F1 virgin females were back-crossed to *jar*^{322}*/TM3, KrGFP* males and maintained in an egg collection cage with fresh apple juice agar plates for several days at 25°C. Worth noting, test cross was performed for positive identification of the His2-RFP. Salivary glands of the *Df(3R)crb87-5,His2-RFP/TM3, KrGFP* stocks and the original stock, His2-RFP were dissected from larvae and examined under confocal microscope at 20X objective lens. RFP was observed to stain intensely in the nuclei of the salivary glands. However, it was evident that it was impossible to differentiate *jar*^{322}*/jar*^{322} embryos from *jar*^{322}*/Df(3R)crb87-5* embryos because of the maternal contribution of the RFP. Therefore, the cross scheme was reverted back to the cross scheme previously done by Morrison and Miller (2008) (2.3.3).

2.3.3. Maternal and zygotic *jar*^{322}*/Df(3R)crb87-5* mutant

Females of genotype *jar*^{322}*/TM3, KrGFP* were crossed to *Df(3R)crb87-5, TM3 Ser* males in generating zygotic *jar* mutant. The resulting F1 virgin females were back-crossed to *jar*^{322}*/TM3, KrGFP* males to generate maternal and zygotic *jar* null.

2.3.4. Generating *jar*^{322}*pak*^{11} double mutant stocks

Virgin females of balanced *pak*^{11}*/TM3, Sb* were out-crossed to males of *jar*^{322}*/TM3* in a vial and kept for 3-4 days before parents were discarded. The resulting F1 heterozygous virgin females were collected and sorted for the absence of the Stubble (Sb) marker. These were crossed to males of genotype *y w; Dgl/TM3, KrGal4 UAS-GFP (KrGFP)* balancer- noted as held-out wing. At this stage the resulting F2 males could either be *pak*^{11}, *jar*^{322} or *jar*^{322}*pak*^{11} recombinant. Therefore, 50 males from the F2 cross were collected and placed singly in vials (50 vials in total) with 2-3 virgin females of *KrGFP* balancer. The high number was to increase the chance of

recombinant. 11 lines (out of the total 50 lines) tested positive for recombinant during the backcross test (see 2.5.2). To keep stocks of $jar^{322}pak^{11}$ double mutant, virgin females of $jar^{322}pak^{11}$/*TM3, KrGFP* from each of the 11 lines were crossed to males in their respective vials.

2.4. Genetic crosses

2.4.1. Lethality score of *jar* and *pak* loss-of-function mutants

In an experiment to score percentage of lethality of *jar* mutants and *pak* mutants, balanced virgin females of jar^{322}/*TM3, Sb* and pak^{11}/*TM3, Sb* mutants were out-crossed to w^{1118} males. The resulting heterozygous mutant males from each cross were then back-crossed to virgin females of the original stocks, jar^{322}/*TM3, Sb* and pak^{11}/*TM3, Sb* mutants. The resulting embryos were manually collected and placed on fresh apple juice agar plates that were gridded on the underside for easy scoring. The plates were kept for more than 36 hours at 25°C. Unhatched eggs were counted and the fertilised ones were further assessed by cuticle preparation (see 2.2.8). The exact cross scheme and procedure were applied for the score of percentage lethality of $jar^{322}pak^{11}$ double mutants.

2.4.2. Genetic analysis of *jar* and *pak* in wing morphogenesis

To test for genetic interaction between *jar* and *pak* in wing morphogenesis, females of *enGal4* driver line were crossed to males of jar^{322}/*TM3, Sb*. The resulting F1 males were crossed to *UAS-pak RNAi* females and were allowed to lay eggs. The eggs were left to hatch and 160 larvae were randomly picked using forceps and transferred to vials, with 10 larvae in each vial. The larvae in the vials were left to eclose and adult wings were examined for enhancement of the Pak-associated crumpled wing phenotype.

2.4.3. Lethal phase analysis of *jar*^{322}*/Df(3R)S87-5* mutants

Virgin females of *jar*^{322}*/Df(3R)crb87-5* crossed to *jar*^{322}*/TM3, KrGFP* males were caged with fresh apple juice agar plates and maintained for several days at 25°C. Fresh apple plates were provided and test flies were allowed to lay eggs for 3-4 hours. Thereafter, 1000 embryos were collected at random using a dissecting microscope and were set on fresh apple plates. These plates were kept for 36 hours for larval hatching and for further 12 hours more to score embryonic lethality. After hatching, 170 non-fluorescent first instar larvae were separated from the fluorescent larvae using a Leica MZFLIII dissecting microscope with GFP band filter and were transferred to fresh apple plates supplied with yeast paste. The larvae were monitored daily for carcasses and provided with fresh collection of apple plates with yeast paste as they underwent larval stage transition. Larvae were identified by size or by anterior spiracle morphology if uncertain, and were transferred to vials containing the standard cornmeal medium. The larvae were followed through to eclosion. The adults were monitored for 2 weeks for observable defects. Worth noting, a pilot study was performed and, I found that the results were reproducible.

2.4.4. Determining that the lethal effect of Jar RNAi is Gal4 line dependent

Virgin females of *UAS-jar RNAi* were crossed to males of *jar*^{322}*/TM3, Sb* in a vial. The resulting F1 males indentified by wild-type bristles were crossed to *enGal4* virgin females in a fly cage. They were left to lay eggs for several days before collection plate was provided. 200 embryos were randomly selected and transferred to fresh apple juice plate. This was left for 28 hours to allow enough larvae to hatch. 150 first/second instar larvae were counted and transferred to vials (10 larvae in each vial) containing the standard cornmeal medium. The vials were left for nearly 2 weeks, long enough to allow time for any delay development. The number of pupae cases was counted and this accounted for larval lethality. Empty pupae cases were counted and this was in agreement with the number of eclosed adults.

2.4.5. Analysis of RNAi-mediated Jar knock down on actin and microtubule cytoskeletons

Males of the genotypes *UAS-GFPactin/+;69BGal4/+* and *α-TubulinGFP/+; 69BGal4/+* were mated to virgin females of the *UAS-jar RNAi* for analysis of actin and microtubule, respectively. Progenies of the crosses were screened under the Leica MZFLIII dissecting microscope with a GFP band filter for the selection of GFP-positive embryos. Cytoskeletal organisations of the GFP-expressing embryos were examined using the confocal microscope.

2.4.6. Dorsal closure analysis of *jar^{322}/Df(3R)S87-5* embryos

Virgin females of genotype *w;SGMCA* were crossed to males of *Df(3R)crb87-5*. The resuling F1 males of the genotype, *w;SGMCA;Df(3R)crb87-5/+* were crossed to *jar^{322}/TM3, Sb* virgin females. Following on from the F2 cross, half of the progenies would test positive for SGMCA (identified by GFP) and are *Df(3R)crb87-5/jar^{322}* mutants. Therefore, a total of 22 embryos were monitored every 20 minutes during the live analysis of dorsal closure using the confocal microscope.

2.4.7. Analysis of the amnioserosa cells in Jar knock down embryos

Virgin females of *w;SGMCA* were crossed to males of *w; L Pin/Cyo, KrGal4 UAS-GFP*. The resulting F1 males of the genotype *w;SGMCA;Cyo, KrGFP/+* were crossed to *w; c381-Gal4* virgin females. Virgin females resulting from the F2 cross were crossed to *UAS-jar RNAi* males. Because half of the embryos are positive for SGMCA (GFP-positive) and co-expressing *UAS-jarRNAi* and *c381-Gal4* (AS driver), a number of embryos were randomly monitored. A total of 15 embryos were monitored every 30 minutes for their behavioural pattern of AS cells during the live analysis of dorsal closure using the confocal microscope.

2.5. Test cross

2.5.1. Fertility test

Individual males and females of the test genotypes were placed with 2-3 virgin females and a single male of w^{1118}, respectively in vials. After 3 days parents were discarded and vials were kept for several days and examined.

2.5.2. Backcross test

To clarify the $jar^{322}pak^{11}$ double mutant, the same 50 single males that were crossed to females of the KrGFP balancer in making the recombinant stock (2.3.4) were taken out after 3 days from the vials and crossed to virgin females of pak^{11}/*TM3, Sb* original stock in 50 separate numbered vials. After three days the males were again taken out and out-crossed to virgin females of jar^{322}/*TM3, Sb* in 50 separate numbered vials. After three days, the parents were discarded. The emerged adults that scored positive for wild-type bristles in parallel vials of the respective crosses to pak^{11}/*TM3, Sb* and jar^{322}/*TM3, Sb* imdicated positive for $jar^{322}pak^{11}$ recombinant.

2.5.3. Positive identification of *jar^{322}/TM3, KrGFP* stocks

jar^{322}/*TM3, KrGFP* stocks can easily be identified by visual observation of the dichaete-like wing or by GFP examination using a Leica MZFLIII dissecting microscope with a GFP band filter.

2.6. Genomic PCR

2.6.1. Single-fly DNA preparation for PCR

Single-fly DNA preparation for PCR was preformed according to Gloor *et al.* (1993). Individual carcass was collected into a 0.5 ml tube and mashed for 10secs using a yellow pipette tip containing 50 µl of squishing buffer (SB). The remaining SB was released into the tube and the mixture was incubated for 30 minutes at room temperature. To inactivate Proteinase K, mixture was then heated to 95°C in a heat block for 5 minutes. The fly remnants were spun down for 10 seconds using a bench centrifuge. The supernatant was drawn off and transferred to a clean 0.5 ml tube, leaving behind the remnants. The mixture was then stored at -20°C.

2.6.2. PCR

PCR protocol was done according to instructor's manual (Promega). A single 50 µl PCR was performed on DNA extracted from the individual carcass of $jar^{322}/Df(3R)S87\text{-}5$ mutants and for comparison I used w^{1118} fly. A trial was first done on the standard w^{1118} fly to obtain the correct band size of 513 bp and optimum yield in amplification. For multiple PCR, a mastermix was prepared and excluding the template DNA. Mastermix was prepared as a volume of a single reaction multiplied 110% of the volume of the samples needed. The extra volume allow for losses during pipetting. Template DNA was added respectively to each labelled 0.5 ml thin-walled PCR tubes with the mastermix solution. For negative control, template DNA was omitted and the volume made up with dH_2O. Negative control was to check for contamination. An Eppendorf Mastercycler® personal with 105°C heated lid was used to perform the PCR amplification. PCR machine was programmed for 30 cycles. After DNA amplification, the samples and a 1 Kb marker ladder (Promega) were loaded directly onto a 0.8% agarose gel. The gel was run at 50 volts until the DNA has separated. Gel was placed on a UV light box and a

photograph was captured with a Kodak camera, using a Kodak Gel Logic 100 Bio-Rad bioimaging system.

2.6.2.1. Primer for *jar*^{322}/*Df(3R)crb87-5* carcass

For a working solution for PCR, 5 µM stock solutions of forward and reverse primers were prepared from their original stock solution of 100 pmol/µl (MWG-Biotech). Working solutions were stored at -20°C.

Primer	Sequences 5' → 3'
Forward	AACCGCAAGCGCACCACCATGGATG
Reverse	GGGCCGGCTGCAGCAATGCAGAAAC

50 µl PCR components

Component	Volume
5X Green Go Tag	10 µl
$MgCl_2$(25 mM)	4 µl
dNTPs	1 µl
Primer 1	2 µl
Primer 2	2 µl
GoTag® DNA polymerase	0.25 µl
Template DNA	0.5 µl
dH_2O	30.25 µl

Thermal cycling conditions

Step	Temperature	Time
Initial denaturation	95°C	5 minutes
Denaturation	95°C	1 minute
Annealing	68°C	30 seconds
Extension	72°C	1 minute
Final extension	72°C	5 minutes
Soak	4°C	Indefinite

2.7. Fluorescence microscopy

2.7.1. Fixed samples

Embryos: The end tip of a yellow pipette was cut off with a sharp razor blade to enable the uptake of embryos. 30 µl of mounting media containing fluorescent-fixed embryos were taken up from storage using a Gilson pipette with the yellow pipette tip. The embryos were then mounted on a glass slide. Cover slip placed gently on the glass slide and a drop of immersion oil on the cover slip. The images were captured using the Leica TCS SP2 confocal system with the Leica Confocal Software.

Imaginal disc: After antibody staining of the dissected larvae, they were transferred to a depression slide and imaginal discs were removed from the larvae body wall with fine forceps using the dissection microscope. The imaginal discs were transferred to a glass slide with 30 µl of mounting media and then carefully covered with a cover slip. The slide was examined under the confocal microscope. The slides could also be stored at 4°C if examination was postponed.

Adult wings: Wings were clipped from adults using fine forceps and placed on a glass slide with 30 µl of 50% glycerol. This was left at room temperature in a dark

storage for 24 hours for glycerol to solidify. Images processed and were captured using a Leica MZFLIII dissecting microscope.

2.7.2. Time-laspse movie

Stages 12-13 of embryos were hand dechorionated on a double-sided tape, stuck to a glass slide and transferred to an agar slab where they were appropriately oriented using a forcep. The well of the live imaging chamber was coated with a drop of the halocarbon oil and vacuum grease smeared around the edge of the well where the end of a coverslip will sit. A coverslip was coated with embryo glue using a glass pipette. Once dried, the embryos were mounted on the coverslip with their dorsal side glued to the coverslip and coated with halocarbon oil. The coverslip was inverted over the well of the live imaging chamber.

Imaging of the embryos was done using the Leica TCS SP2 confocal system with a 40X oil immersion lens or 63X oil immersion lens. Images were acquired every 5 minutes. Stacks of images were projected using the maximum projection feature with the Leica Confocal Software.

2.8. Western blot

Drosophila extracts for western blotting were collected from embryos that were laid overnight, first, second and third instar larvae, and pupae. RNAi-jar knock down and w^{1118} (control) were simultaneously staged.

2.8.1. Lysis

Samples were collected into a 1.5 ml eppendorf tube and rinsed twice with ice cold 2 mM of EGTA in PBS. The samples were then homogenised in lysis buffer (LB) in 5-10 strokes using a tight-fitting glass rod. Worth noting, volume of lysis buffer should

be enough to submerge the sample. As a rule of thumb, for example, 20 embryos equated to 40 µl of LB. The homogenised sample was centrifuged at 14000 rpm for 10 minutes. The supernatant was transferred to a clean 1.5 ml eppendorf tube. To quantitate the protein concentration of the homogenate was determined by Bradford assay (Bradford, 1976) using BSA (Bio-Rad, UK) as the standard.

2.8.2. The standard Bradford assay

Bradford protein assay protocol was followed through the Bradford reagent (Sigma, UK) instruction booklet. In brief, Bovine Serum Albumin (BSA) was set as the standard protein. Serial dilutions of 2 mg/ml BSA in PBS was prepared to fall within the linear concentration range of 0.1-1.4 mg/ml. The unknown samples were also serially diluted in PBS to fall within the linear range of the standard assay. 5 µl of the blank (PBS), BSA standard and the unknown samples were aliquot into a 96-well plate in triplicates. And added to each samples was 250 µl of the Bradford reagent. The sample was mixed on a shaker for 1 minute and left to incubate at room temperature for 10 minutes. Absorbance was read at 595 nm in a MRX Dynatech plate reader (Dynatech Laboratories, Inc., USA). The standard curve of absorbance versus microgram BSA standard was plotted using Microsoft excel and concentration of the unknown samples was then calculated. The volume of each sample was adjusted taking into account the protein concentration and mix with equal volume of 2X SDS sample buffer. Samples were placed in a heat block at 100°C for 5 minutes and stored at -20°C indefinitely.

2.8.3. Electrophoresis and blotting

Gel apparatus were cleaned with acetone and assembled according to instruction manual (Mighty Small II gel units from Amersham Biosciences). For making SDS-PAGE stack gel, 7% resolving gel was poured into the plate stack but leaving enough room for the stacking gel. Then a layer of saturated iso-butanol was poured carefully at the top to allow flat surface. The gel was then left to set completely before the addition of 3.75% stacking gel and the insertion of a comb to make wells.

The gels were placed in a tank containing 1X running buffer. Prior to loading, samples were heated at 100°C for 5 minutes. Using a syringe, 30 µl of test samples were loaded and volume of control was adjusted according to the amount of protein in the test samples. 5 µl of dual colour molecular weight marker (Bio-Rad, UK) was also loaded. Electrophoresis was initially carried out at 60 volts through the stacking gel and then increased to 120 volts through the resolving gel until the dye front reached the bottom of the gel.

The stacking gel was separated from the resolving gel. Two pieces of filter paper (Whatman, UK) and one piece of nitrocellulose membrane (Amersham Biosciences, UK) were cut out according to the gel size and soaked in transfer buffer. The gel, filter paper and nitrocellulose were sandwiched accordingly and placed in the transfer tank (Bio-Rad, UK) filled with transfer buffer. Protein transfer onto nitrocellulose was done overnight at 100 mA at room temperature.

2.8.4. Immunodetection

Protein transfer efficacy from the gel to the blot was confirmed by staining with Ponceau S. The blot was then rinsed 3X with PBS. The blot was then blocked in blocking buffer for 1 hour and probed with 3C7 monoclonal antibody at 1:20 dilution in blocking buffer for 2 hours with gentle agitation at room temperature. The blot was rinsed 5X with 0.1% Tween-20 in PBS for 5 minutes. The blot was then probed with horseradish peroxidise-conjugated secondary antibody (Sigma-Aldrich) for 1 hour at room temperature and rinsed 5X with 0.1% Tween-20 in PBS for 5 minutes. Proteins were detected using enhanced chemiluminescent (ECL) detection system (Amersham). The blot was exposed to X-ray film (Amersham) and the film was developed using a compact x4 hyperprocessor (Xograph imaging systems, UK).

Chapter 3. Genetic analysis of interaction between Jar and Pak

3.1. Introduction

Phosphorylation of the head domain of vertebrate myosin VI is thought to regulate protein function (Buss *et al.*, 1998). Group 1 Pak's are known to be able to phosphorylate this site (Yoshimura *et al.*, 2001; Buss *et al.*, 1998). As both the head domain phosphorylation site in myosin VI and group 1 Pak is conserved between vertebrate and *Drosophila* (Figure 3.1) it is reasonable to hypothesise that the function of Jar might be regulated in the same way. This hypothesis is supported by phenotypic data from studies in which dominant negative Pak and Jar are expressed in the developing *Drosophila* embryo; expression of either dominant negative produces very similar phenotypes including loss of the actomyosin purse-string during dorsal closure. Here we look for genetic evidence to support a functional link between Pak and Jar.

A

Motor domain

```
                                  405
                                   |
Hum M6    SLTTRVMLTTAGGTKGTVIKVPLKVEQANNARDALAK 426
Dro 95F   ALVSRVMQSKGGGFKGTVIMVPLKIYEASNARDALAK 429
```

B

Tail domain

```
                              1089 1092
                               |    |
Hum M6      DLSKWKYAELRDTINTSCDIELLAACRE 1104
S.scrofa    DLSKWKYAELRDTINTSCDIELLAACRE 1081
C.elegans   DVGGCSFAYLRDTINTSMDINLLKACEE 1086
Dro 95F     DLSKWKYSELRDAINTSCDIELLEACRQ 1094
```

Figure 3.1. Comparisons of phosphorylation sites in both motor and head domains between vertebrates and *Drosophila* myosin VI. Panel A, shows the alignment of conserved threonine residue (shaded red) located upstream of the highly conserved DALAK sequence in the motor domain. Panel B, shows alignment of potential phosphorylation sites in the tail domain. The threonine residue of T^{1089} is not conserved between the vertebrates and *Drosophila* (shaded yellow) but T^{1092} is conserved (shaded red). The precise amino acid numbers are shown to the right. *Dro, Drosophila; Hum, Human; Ce, Caenorhabditis elegans; Ss, Sus scrofa.*

3.2. Results

3.2.1. Genetic analysis between Jar and Pak

One prediction of the hypothesis that Pak regulates Jar function is that loss-of-function mutations of Pak and Jar may enhance each other phenotypically. To test this I first had to determine the lethal score and phenotypes associated with individual mutants during embryogenesis. Two different *jar* mutants and two *pak* mutants were employed and scored for lethality (Table 3.1). Of all the mutants

assessed, jar^{322} mutant and pak^{11} mutant exhibited substantial lethality and were further employed in testing our hypothesis.

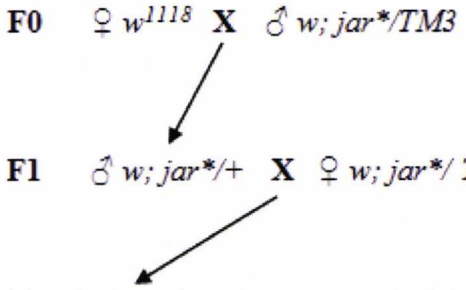

F2	Viability	Probability (%)
+;*jar/ jar****	**lethal**	**25**
+;*jar**/+	viable	25
+:*jar**/TM3	viable	25
+;TM3/+	viable	25

Figure 3.2. A review of a cross showing the probability of *jar* homozygous and *pak* homozygous mutants. A genetic cross between males of w^{1118} (indicated by the symbol ♂) and *jar*/TM3* females (♀) was carried out as outlined in the figure. *jar* is interchangeable with Pak and the supercript (*) denotes an individual mutant allele of the gene. The genetic cross of $jar^{322}pak^{11}$ double mutant was essentially the same. Based on the F1 mating, 25% of the F2 progeny will be homozygous for the mutant.

Table 3.1. Summary of the embryonic lethality score of *jar* mutants and *pak* mutants

Mutant alleles	Total progeny	Lethality (%)
jar^{2095}	195	2
jar^{322}	187	9
pak^{11}	171	14
pak^{6}	188	4

Note: jar^{322} mutant and pak^{11} mutant exhibited higher embryonic lethality in their respective gene alleles. Lethality calculated as to the 25% expected homozygous of the cross scheme (Figure 3.2, see 2.2.7 for calculation).

As earlier stated in Chapter 1, the jar^{322} has all of its amino acid coding sequences removed and also the first exon of the CG5706 gene (Petritsch *et al.*, 2003). On the other hand, $dpak^{11}$ encodes a truncated protein of Pak but otherwise, Pak is non-functional (Hing *et al.*, 1999). I report that the percentage embryonic lethality of jar^{322} and pak^{11} are 9% and 14% respectively, as oppose to the expected 25% rate (for calculation method, see 2.2.7). Furthermore, I found no dorsal defect by cuticle preparation (2.2.8) of the dead embryos which is consistent with previous reports. However, what was noted was that few first instar larvae of jar^{322} mutant displayed delayed development which is in accordance with report (Petritsch *et al.*, 2003).

In order to test for genetic interaction between jar^{322} and pak^{11}, a double mutant line was generated (see 2.3.4). Lethality analysis of the $jar^{322}pak^{11}$ double mutant was performed. I found no phenotypic enhancement, in fact there appears to be a mild suppression of the embryonic lethality.

After 2 hours of egg lay, 608 embryos were manually collected and kept for more than 36 hours at 25°C. Recombinant $jar^{322}pak^{11}$ displayed 3.3% embryonic lethality as to 25% and no observable dorsal defect by cuticle preparation which was expected as opposed to the individual *jar* and *pak* mutants gave similar result. However, the low embryonic lethality was of a surprise as compared to the lethality score of *jar* and *pak* loss-of-function mutants. Additionally, a back-cross test was done in order to verify the recombinant $jar^{322}pak^{11}$ mutant (detailed in 2.5.2).

3.2.3. Heterozygosity for *jar* does not enhance a Pak-associated wing phenotype

During the back-cross test, crumpled wings were noted. This is consistent with known findings of homozygous *pak* mutant escapers reported to have similar wing phenotype (Hing *et al.*, 1999). Thus, the crumpled wing phenotype is specific to loss-of-function of Pak and more importantly, noted in RNAi-mediated knock down of Pak protein levels (Figure 3.3). Furthermore, Jar has also been reported to be of importance in wing development and as a result of functional loss of Jar, adults were seen with unexpanded wings (Deng *et al.*, 1999).

During the back-cross test, crumpled wings were only observed when $jar^{322}pak^{11}$ mutant was crossed to pak^{11} mutant but not to jar^{322} mutant. In expressing UAS-pak-RNAi enGal4-driven in jar^{322} heterozygous background, I found no enhancement of the crumpled wing phenotype.

160 larvae of genotype enGal4/+;jar^{322}/+ x UAS-pak-RNAi (see 2.4.2 for detailed cross) were left to eclose. From the cross, a quarter of the adults (37 out of the 149) are expected to express Pak-RNAi enGal4-driven in the posterior compartment of the wing and thus, have the crumpled wing phenotype (Table 3.2). Of the 160 larvae, 2 were dead pupae and 9 larvae were unaccounted for (either lost or dead) and the remainder 149 larvae eclosed. I found that 36 (out of the 149) had the Pak-associated crumpled wing phenotype and the remainder adults had wild-type wing appearance. This clearly indicates that there is no interaction between *jar* and *pak* during wing morphogenesis.

Table 3.2. Driven expression of Pak-RNAi enGal4-driven in jar^{322} heterozygous background

Genotype	**Probability (%)**	**Expected of the 149 (%)**
pak-RNAi;enGal4; jar^{322}***/+****	25	37
+;enGal4;jar^{322}*/+*	25	37
pak-RNAi;+;+	25	37
+;+	25	37

Note: Genotype outcome from the cross *enGal4/+*jar^{322}*/+* x *UAS-pak RNAi* and the probability that 25% of the population are expected to express Pak-RNAi enGal4-driven in the posterior compartment of the wing blade (*).

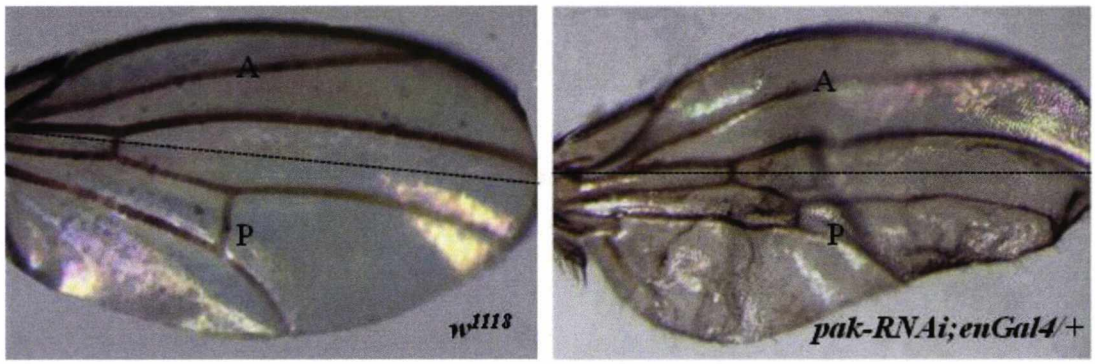

Figure 3.3. Knock-down of dPak protein levels produces crumpled wing phenotype. Dashed line demarcates anterior (A) and posterior (P) margins. The driven expression of *UAS-pak-RNAi* under the control of *enGal4* driver generates crumpled wing in the posterior compartment of the wing blade. Note: w^{1118} wing is shown here as wild-type control.

3.3. Discussion

Group I Paks supposedly have the potential to phosphorylate T^{406} in the head domain of myosin VI as was demonstrated in vitro. Pak homologues MIHCK/Ste20 in unicellular eukaryotes are known to phosphorylate class I myosin in a homologous position to myosin VI phosphorylation site. Phosphorylation of myosin I is important for its acto-myosin ATPase activity and functional motility (Attanapola *et al.*, 2009; Fujita-Becker *et al.*, 2005; Novak and Titus, 1998; Brzeska and Korn, 1996). More so, the phosphorylation of the class I myosin modulates recruitment and functions of motor activity at active endocytosis sites (Attanapola *et al.*, 2009; Yamashita and May, 1998). Independent studies have shown that loss-of-function of Jar and Pak resulted in overlapping phenotypic characteristics such as the loss of actin cable and dorsal holes (Conder *et al.*, 2004; Millo *et al.*, 2004). Therefore, we explored the possibilities that Jar is dependent on Pak-mediated phosphorylation for its cellular function.

From previous report what is known already is that mutant jar^{322} survives embryogenesis but, dies as first/early second instar (Petritsch *et al.*, 2003). Similarly, zygotic *dpak* mutants were also known to survive embryogenesis (Hing *et al.*, 1999). Notably, the insignificant embryonic lethality for *jar* and *pak* loss-of-function mutants is consistent with reports here. Furthermore, similar results were also noted for $jar^{322}pak^{11}$double mutant. Although, Jar and Pak are documented to be of

importance for dorsal closure, it has been suggested that in the absence of zygotic transcription, there is enough maternal contribution for these mutants to survive embryogenesis. Consistent with this, expressing either dominant negative Jar or dominant negative Pak is shown to cause dorsal defects (Conder *et al.*, 2004; Millo *et al.*, 2004).

Furthermore, Millo *et al.*, (2004) postulated that *jar* mutants survive embryogenesis because of maternal store of myosin VI RNA transcripts but otherwise, is undetectable prior to dorsal closure. However, this proposal was challenged by reports of Morrison and Miller (2008) that conclusively demonstrated that maternal Jar plays no part in their survival. In the case of *dpak* mutants, Pak3 transcripts are reportedly present during dorsal closure and could potentially rescue the loss of dPak function (Conder *et al.*, 2004). Congruent to that thought, only embryos that were depleted of both maternal and zygotic *dpak* were reported to display mild dorsal defects as compared to the severity of the driven expression of dominant negative dPak-AID (Conder *et al.*, 2004; Hing *et al.*, 1999).

Possibly, Jar interaction with Pak is redundant during dorsal closure. Therefore, an alternative approach was employed to establish the relationship between Jar and Pak in wing morphogenesis. The removal of one copy of Jar was shown to suppress planar cell polarity (PCP) defect which resulted from the overexpression of *Drosophila* GIPC (dGIPC) in the wing (Djiane and Mlodzik, 2010). Thus, implies that Jar is involved in wing development. However, the driven expression of Pak RNAi in *jar* heterozygous background had no enhancement of the crumpled wing phenotype. Intriguingly, a report proposed that the crumpled wing phenotype is because of Pak interaction with a G protein-coupled receptor kinase-interacting (GIT1-like proteins) (Bahri *et al.*, 2009). Importantly, *dgit* mutants displayed similar crumpled wing phenotype.

Jar isoforms are differentially expressed in tissues and at various developmental stages throughout the life cycle of *Drosophila* (Lantz and Miller, 1998; Kellerman and Miller, 1992). This clearly implies that Jar expression is most likely differentially regulated. Although, cellular localisation study has shown that Jar is highly expressed during embryogenesis, Jar could have a redundant role during dorsal closure (Millo and Bownes, 2007; Millo *et al.*, 2004). Possibly, dPak is not

the responsible kinase. Moreover, there are several Pak-like kinases identified in *Drosophila* genome and any one of them could potentially phosphorylate Jar (Morrison *et al.*, 2000).

Furthermore, a well known characterized myosin VI binding partner, GIPC was proven to bind to both dephosphorylation and phosphorylation state of myosin VI (Naccache and Hasson, 2006). Thus, implies that myosin VI can function in either unphosphorylated or phosphorylated state. More so, that Buss and Kendrick-Jones (2008) have summarised several mechanisms (see 1.4) by which myosin VI could potentially be regulated.

Overall, the genetic evidence presented here concludes that there is no detectable synergism between Jar and Pak in our preferred model systems.

Chapter 4. Positioning Jar in the regulatory hierarchy of dorsal closure

4.1. Introduction

The intricate nature of dorsal closure relies on the interplay of large variety of signalling networks necessary for cell migration, cell shape change and cytoskeletal reorganisation to produce the final well defined 3D body plan. Typical signalling pathways that are of importance for dorsal closure are of the JNK encoded by *basket* (*bsk*), *Decapentaplegic* (*Dpp*) a member of the transforming growth factor-β (TGF-β) family and the Wingless (Wnt) pathways (Jacinto *et al.*, 2002a; Reed *et al.*, 2001; Stronach and Perrimon, 2001; Glise and Noselli, 1997). The JNK and Wingless pathways act together to define the LE cells during dorsal closure.

Prior to the onset of dorsal closure, JNK activity is downregulated in the AS and upregulated in the LE cells and consequently, phosphorylate and activates the adaptor protein 1 (AP-1) transcription factor comprised of DJun and DFos (Reed *et al.*, 2001; Stronach and Perrimon, 2001). Additionally, *puckered* (*puc*) encoding a JNK phosphatase also a JNK target gene is induce to act in a feedback loop for negative regulation of the JNK activity. Furthermore, both DJun and DFos act cooperatively to induce the transcription of *dpp* in the same LE cells (Glise and Noselli, 1997). Subsequently, Dpp binds to a heterodimer membrane receptor, Punt and Tkv encoding type-II and type-I TGF-β receptors, respectively (O'Connor *et al.*, 2006). The activation of the TGF-β receptor causes the phosphorylation of SMAD family of transcription factors, Mad and Medea that translocate to the nucleus to transduce the signalling response of the Dpp (O'Connor *et al.*, 2006; Markus Affolter, 2001). The transduced activity of the Dpp causes the elongation of the dorsal epidermis. Furthermore, components that regulate the cytoskeletal architecture such as the Rho small GTPase family is also of importance for dorsal closure (Woolner *et al.*, 2005; Bloor and Kiehart, 2002; Jacinto *et al.*, 2002b; Harden *et al.*, 1999; Ricos *et al.*, 1999).

However, no experimental works have been conducted to question the status of Jar in the dorsal hierarchy and possibly, molecular linkers responsible for the recruitment and/or differential targeting of Jar. Here, the underlying issue was addressed by examining the expression profile pattern of Jar protein in loss-of-function dorsal

closure mutants as well as in embryos expressing constitutive active or dominant negative forms of key signalling components.

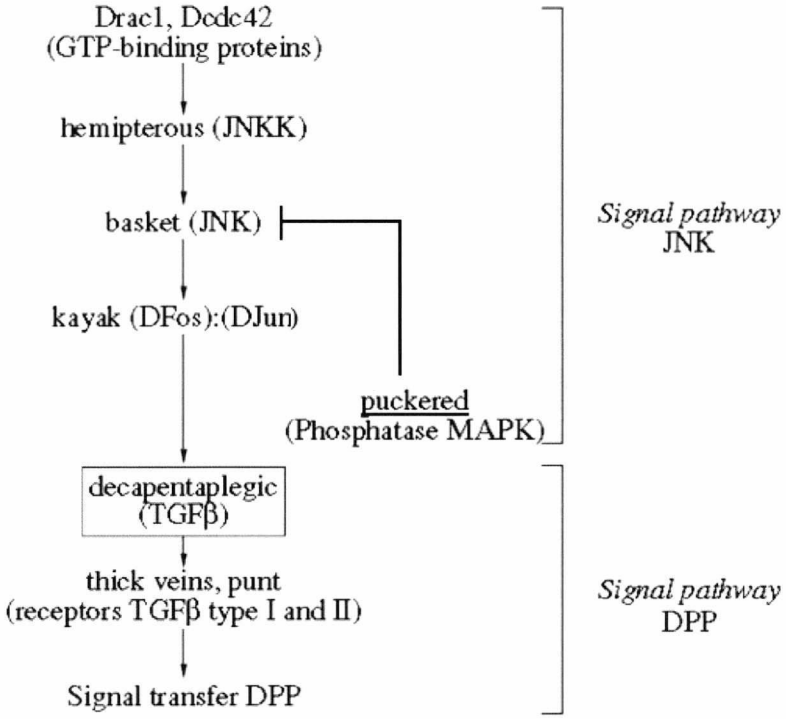

Figure 4.1. The scheme of signalling pathways JNK and DPP in the leading edge during the dorsal closure. Image adapted from Simonova and Burdina (2009).

4.2. Results

4.2.1. Jar expression is unaffected in loss-of-function dorsal closure mutants

Firstly, the pattern of Jar protein expression was examined in null zygotic loss-of-function dorsal closure, specifically, null pnr^{VX6}, bsk^{1}, shg^{1}, $Egfr^{f6}$, and tkv^{7} mutants and in expressing dominant negative dPak-AID in embryos.

There were no findings that functional losses of dorsal components have an effect in the expression pattern of Jar protein (Figure 4.2). Possibly, maternal inputs in these zygotic mutants may be enough to drive the expression of Jar protein.

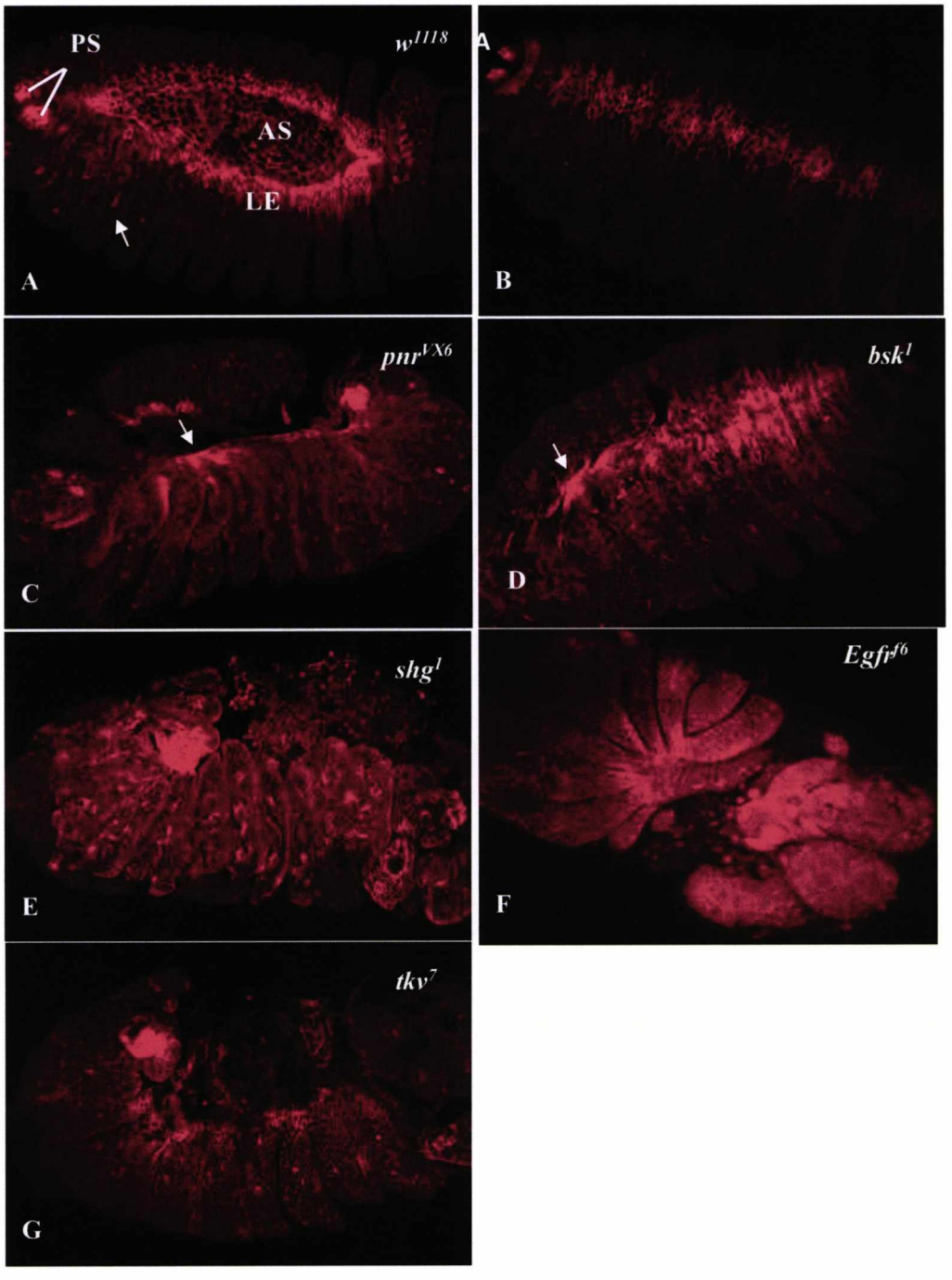
PS
w^{1118}
AS
LE
A
A
B
pnr^{VX6}
C
bsk^{1}
D
shg^{1}
E
$Egfr^{f6}$
F
tkv^{7}
G

Figure 4.2. The effect of Jar expression in embryos with functional loss of key dorsal components.

(A-B) w^{1118} embryos. (A) Dorsolateral view of stage 14 embryo showing Jar expression around the entire length of the LE cells. There is little expression in the AS cells, PS (posterior spiracle) and the muscle attachment (arrow). (B) Dorsal view of stage 15 embryo having completed dorsal closure. Jar expression is shown along the entire length of the dorsal midline.

(C) The null pnr^{VX6} mutant allele showing exposed gut contents and bunching of epidermis (arrow) which is coincident characteristic of mutant embryos of the TGF-β pathway (Ricos *et al.*, 1999). Jar protein expression is shown along the less defined LE cells and at nodes of epidermal bunching.

(D) Dorsolateral view of stage 15 bsk^{1} mutant embryo. The mutant embryo had successfully completed dorsal closure but exhibited failure of fusion and severe segment misalignment (arrow) at the dorsal midline which consequently, resulting to bunching of the epidermis. Nonetheless, Jar staining is clearly seen scattered along the defective midline.

(E) *Shotgun* (*shg*) mutant embryo. *Drosophila* E-cadherin is encoded by *shotgun* (Tepass *et al.*, 1996). DE-cadherin is a major mediator of cell-cell adhesion. Thus *shg* mutants are known not to secrete head and ventral cuticle, exhibit loss of integrity in ventral epidermis. Jar protein expression in the shg^{1} mutant, appears to be widespread in puncta and not restricted to the dorsal epidermis.

(F) Dorsal view of an $Egfr^{f6}$ mutant embryo showing failed germband retraction and bunching of the ventral ectodermal stripes characteristic of functional loss of Egfr signalling (Zhang *et al.*, 1999). Nonetheless Jar expression is apparent.

(G) Lateral view of a tkv^{7} mutant embryo. Tkv^{7} is a recessive lethal allele as a result of point mutation in the conserved glutamate residue contained in the kinase and consequently, there is loss of expression of Dpp targets (Affolter *et al.*, 1994). The above mutant embryo displays the classic bunching of epidermis typically seen in embryos mutant for TGF-β pathway genes. Jar protein expression appears reduced and could reflect an input from maternal *tkv*.

Expressing dominant negative *UAS-dpak-AID* causes head defects and dorsal holes (Conder *et al.*, 2004). The driven expression of dPak-AID affects the functions of Group I Paks because AID is known to inhibit Pak kinase activity. However, normal expression pattern of the Jar protein is seen along the LE cells and dorsal midline in dPak-AID en-Gal4-driven embryos (Figure 4.3). Interestingly, on close examination of the embryo Jar is seen distributed in punctate dots along the LE, not before reported.

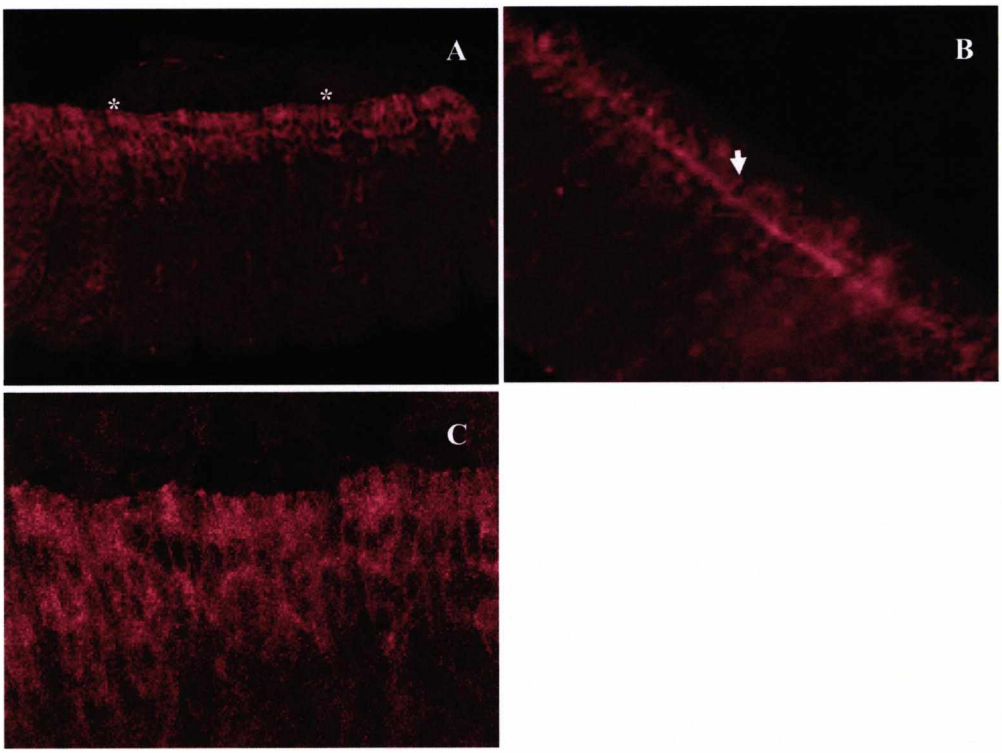

Figure 4.3. Expression pattern of Jar in *UAS-dpak-AID* driven controlled by *enGal4*. (A) Ventral view of stage 14 embryo showing ubiquitous expression of Jar along the LE cells. (B) Dorsal view of stage 15 embryo showing dorsal pucker but otherwise Jar protein expression remains unaffected. (C) Magnified view of the LE cells (asterisks in A) portraying punctate dots of Jar at what appears to be the cell-cell junctions.

4.2.2. Activation of the JNK Kinase Hemipterous is sufficient to direct Jar expression in the dorsal epidermis

In the earlier section I found that the dorsal expression of Jar protein was unaffected in zygotic or null mutants that are of importance for dorsal closure. This I reason could reflect maternal contribution in the mutants enough to drive the expression of Jar protein. Activating the JNKK pathway, is the key signal necessary to drive epithelial morphogenesis. Moreover, embryos lacking the components of the JNKK signalling are known to result in failure of dorsal closure (Stronach and Perrimon, 2002). Therefore, I question if in activating the JNKK pathway Jar is driven in the dorsal epidermis.

Here, an activated form of DJNKK (Hep^{act}) was ectopically expressed in the posterior compartment of each epidermal segment in embryos using the en-Gal4

driver line. Intriguingly, Jar is shown ectopically upregulated in embryos expressing-constitutively active form of Hep (Figure 4.4). To investigate further, I next assessed Jar expression response to one of many downstream effectors of the JNKK signalling by expressing a constitutively active form of Thickvein (Tkv^{QD}) a type 1 receptor for Dpp. Tkv^{QD} was ectopically expressed under the control of the same epidermal en-Gal4 driver line. However, normal expression of puncta distribution of Jar protein is observed along the LE (Figure 4.4C). This clearly indicates that Jar expression in the dorsal epidermis is not affected by the reduced Dpp signalling (Figure 4.2G) or downstream signalling components. Thus, Jar protein expression is not in response to Dpp signalling pathway.

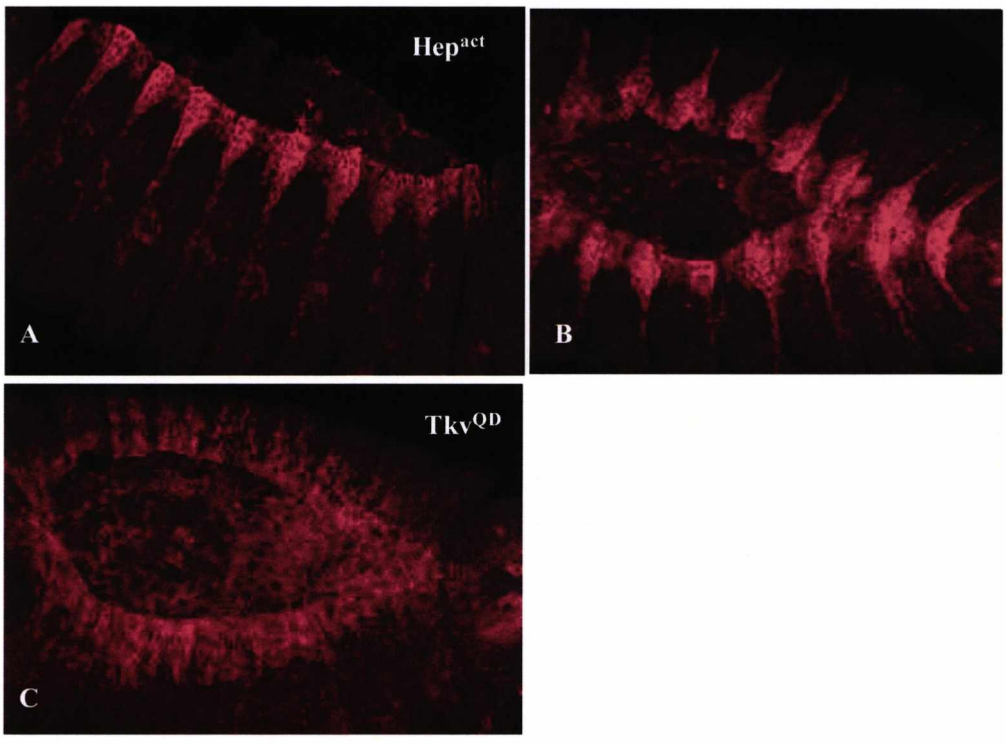

Figure 4.4. Mixed response of Jar expression in the ectopic activated forms of Hep^{act} and Tkv^{QD} controlled by enGal4 driver line. Embryos expressing constitutive active forms of (A-B) Hep and (C) Tkv. Ventral (A) and dorsolateral (B) views of embryos showing ectopic expression of Jar proteins in stripes of each epidermal segment in response to JNKK signalling. (C) Dorsal view of stage 14 embryo expressing activate form of Tkv showing punctate stain of Jar protein along the LE cells.

4.2.3. Ectopic expression of dominant negative DRhoA drives expression of Jar

RhoA (referred to as Rho1 in flybase) is demonstrated to be essential in regulating localisation of nonmuscle myosin II at the LE during dorsal closure (Bloor and Kiehart, 2002). The expression of dominant negative *RhoA*^{N19} by epidermal *prd*- and *en*-Gal4 driver lines resulted in loss of nonmuscle myosin II from the LE and gave a cytoplasmic staining in dorsal staged embryos. Therefore, I assessed whether dorsal expression of Jar will result to similar fate of mislocalisation as myosin II upon expressing the dominant negative RhoA.

Dominant negative RhoA^{N19} x enGal4 embryos were staged at dorsal closure and stained for Jar protein. It has already been established that in expressing dominant negative RhoA nonmuscle myosin II loses its ability to concentrate at the LE. However, in addition to previous work I noted that myosin II stain is expressed along the entire body plan of the embryos (Figure 4.5). On the other hand, Jar is ectopically expressed and in some instances Jar expression is seen away from the LE. I reasoned that Jar protein expression seen in cells lateral to the LE is because of cell rearrangement, a characteristic feature induced when expressing *RhoA*^{N19} (Bloor and Kiehart, 2002). Surprisingly, on closer examination of the embryos Jar protein expression is seen within apoptotic cells.

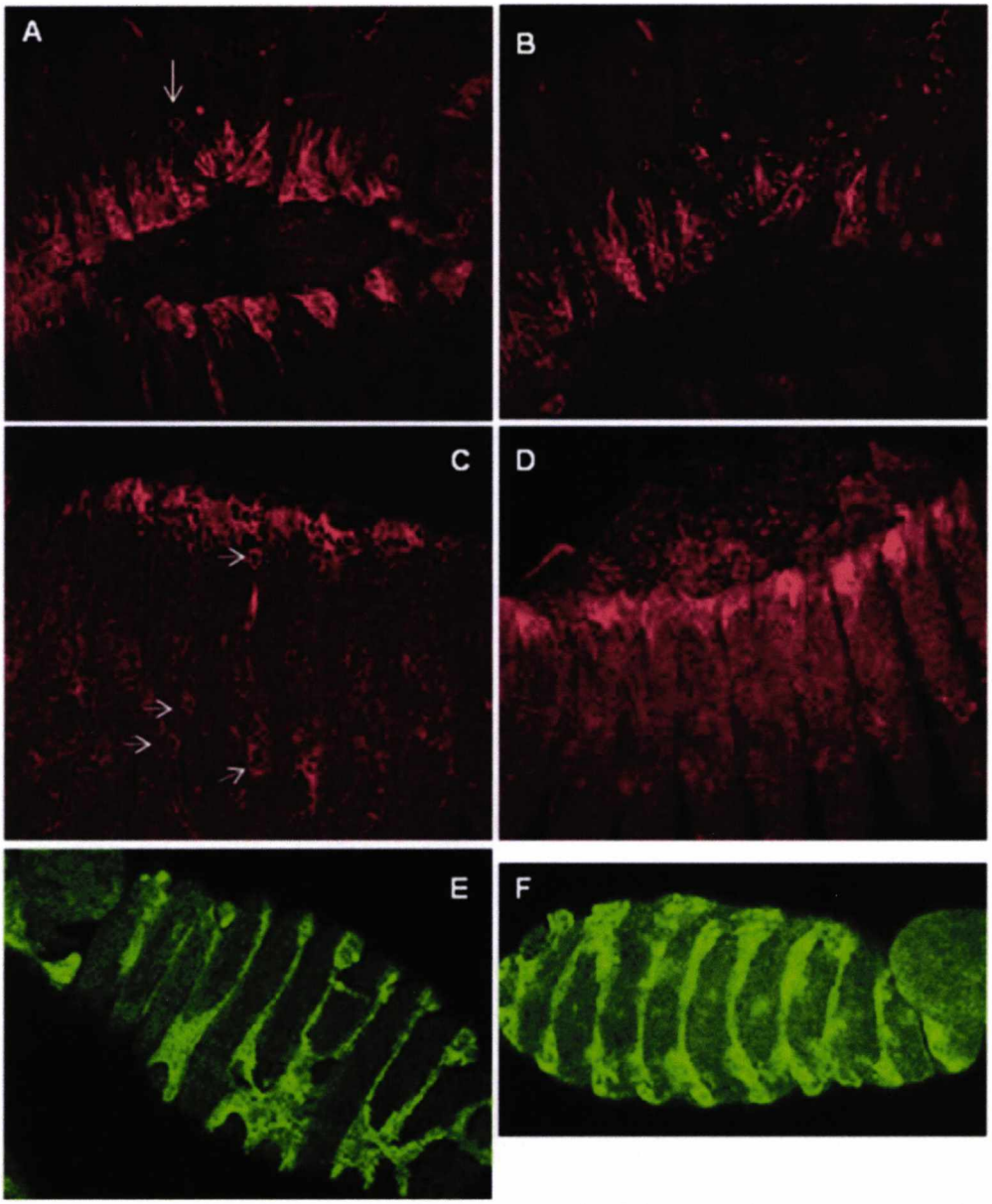

Figure 4.5. The effect of Jar protein expression in functional loss of RhoA. (A) Dorsolateral view of embryo showing stripe expression of Jar protein and punctate ring of Jar protein in apoptotic cell (arrow). (B) Same embryo as (A) but image magnified and contrast reduced to make clear of Jar expression within apoptotic cell. (C) Ventral view of an embryo and the apparent staining of Jar protein detected within apoptotic cells of the ventral epidermis (exemplified by the arrows). (D) Dorsoventral view of an embryo showing ectopic expression of Jar protein in epidermal stripes. Dorsal (E) and ventral (F) views of late embryos showing expression of nonmuscle myosin II protein detected around the entire body plan of the embryos.

4.3. Discussion

Cellular localisation and expression profile studies have established that Jar is expressed in epidermal cells prior and during the process of dorsal closure. However, on the basis of signalling pathways that defines the morphogenetic events of dorsal closure it is especially intriguing to identify a precondition for the expression of Jar protein in the dorsal epidermis. Therefore, in the initial step towards a better understanding of function of Jar in dorsal closure, expression pattern of Jar protein was examined in loss-of-function mutations of the components of the JNK transcriptional activation pathway. To investigate further, constitutively active form of JNKK and Tkv were ectopically expressed and epidermal expression of Jar was examined. Collectively, results here have shown that Jar expression is driven in the dorsal epidermis in direct response to the JNK signalling pathway.

The JNK pathway is required for activation of the Dpp pathway in LE cells which subsequently signals to the rest of the dorsal epidermis, directing their cell shape change (Figure 4.1). The results presented here, indicates that the JNK signalling pathway directs the expression of Jar in the dorsal epidermis but not the Dpp signalling. Pnr encodes a zinc-finger transcription factor of the GATA family. In early stage of embryogenesis *pnr* is activated by *dpp* but after stage 10, *dpp* pathway is activated by *pnr* signalling independent of JNK signalling pathway in the epidermal cells during dorsal closure (Herranz and Morata, 2001; Affolter *et al.*, 1994). In null pnr^{VX6} mutants dorsal dpp stripe is absence and thus, suggested to be the cause of the dorsal defects rather than the lack of Pnr activity during dorsal closure. Notably, in the null pnr^{VX6} mutants Jar expression is still observed especially, in cells of several segments pulled into points of focus (Figure 4.2C). I reason that Jar expression would be under the control of *pnr* as it defines the dorsal epidermal domain in which Jar is expressed. Therefore, the Jar protein expression in null pnr^{VX6} mutants could reflect a contribution from maternal *pnr* but that for full expression zygotic *pnr* is needed. More importantly, the lack of functional Pnr does not alter the activity of the JNK signalling pathway (Herranz and Morata, 2001).

In *tkv* mutants, Dpp signalling is lost and in expressing activated form of Tkv (Tkv^{QD}) the embryo is provided with constitutive Dpp signalling (Affolter *et al.*, 1994). However, in both loss and gain-of-function of Dpp signalling Jar protein

expression remains unaltered. Notably, in zygotic *bsk*^{1} mutants maternal contribution is shown to initiate the process of dorsal closure but however, fails before the completion of the process which reflects the input of zygotic *bsk* activity (Riesgo-Escovar *et al.*, 1996). Therefore, there is the possibility that the maternal *bsk* gave enough signalling input for the correct localisation of Jar in the LE cells.

In the earlier chapter, I showed that there is no genetic interaction between Jar and Pak. In support of the result, dorsal expression of Jar protein is evident in expressing dominant negative dPak-AID construct (Figure 4.3). Furthermore, Jar protein was in puncta along the LE cells, very similar to expression pattern in expressing activated form of Tkv. It is highly unlikely that dPak-AID and Tkv constructs generated the punctate dots because the constructs were expressed using the epidermal *en*-GAL4 driver line, expressed only in the posterior compartment of each epidermal segment. The punctate dots of Jar distributed along the LE coincide with reports that Jar participates in mediating cell-cell adhesion during dorsal closure (Lin *et al.*, 2007). In *shg* mutant, Jar protein expression is widespread in puncta. Furthermore, expressing dominant negative ΔATP-jar construct causes reduced/mislocalised DE-cadherin during dorsal closure (Millo *et al.*, 2004). More importantly, the expression of dPak-AID does not affect the JNK signalling cascade (Conder *et al.*, 2004).

Bearing all the above considerations in mind, it becomes tempting to suggest that the normal Jar expression in the loss and gain-of-function mutants is in part, at least, due to the active JNK activity in these mutants. Congruent to that thought, the expression of the activated form of DJNKK (Hep^{act}) produced ectopic expression of Jar in the dorsal epidermis. However, most of the target genes of the JNK signalling pathway when disrupted are almost always are embryonic lethal. Therefore, the most intriguing question is the biological significance of Jar during dorsal closure and more so, because its abolishment does not affect embryogenesis.

In the expression of the RhoA^{N19} construct apoptotic cells were observed at the LE and the ventral epidermis, which is accordance with previous work (Bloor and Kiehart, 2002). In addition, dominant negative RhoA^{N19} construct disrupts cell surface expression of DE-cadherin protein and activates the JNK transcriptional activation pathway. E-cadherin provides a molecular link between loss of cell polarity and tumour malignancy (Igaki *et al.*, 2006). The loss of polarity is shown to

prompt activation of proapoptotic role of JNK signalling pathway. Co-expression of p53 and the $RhoA^{N19}$ was shown to reduce the induced apoptosis. Consistent with the precedent reports, it has been shown that the activation of the JNK pathway by Rho1 is independent of GTP binding (Neisch *et al.*, 2010). Moreover, expression of wild-type Rho1 has been demonstrated to induce apoptosis in imaginal epithelia and is through the JNK pathway (Neisch *et al.*, 2010; Vidal *et al.*, 2006). Rho1 induction of apoptosis is achieved through a promotion of a complex consisting of upstream components of the JNK pathway such as the Slipper (Slpr), POSH, Tak1 and Hep at the cell cortex (Neisch *et al.*, 2010).

One of the many processes of the JNK signalling transduction is the induction of apoptosis and promoting cell survival (Davis, 2000). More so, constitutively active JNK kinase kinase (Slpr) or JNK pathway has been reported to induce apoptosis both in vertebrates and invertebrates (Adachi-Yamada and O'Connor, 2002; Fuchs *et al.*, 1998; Johnson *et al.*, 1996). Suppressor gene *DmP53*, *Drosophila* homolog activation is mediated by the activity of the JNK pathway (Martin *et al.*, 2009). Typically, pro-apoptotic genes *reaper* (*rpr*), *head involution* (*hid*) and *grim*, *sickle* and *jafrac2* are transcriptionally upregulated to suppress the activity of the DIAP1 (*Drosophila* Inhibitor of Apoptosis Protein I) which prevents the proteolytic activation of caspases, cysteine proteases that result in the destruction of cells (illustrated in Figure 4.6). The proapoptoic genes are expressed both during normal development and in response to apoptosis (Reviewed in, Martin *et al.*, 2009; Stronach, 2005).

Interestingly, vertebrate myosin VI is found to be regulated by DNA damage in a p53-dependent manner and function in the p53-dependent prosurvival pathway (Jung *et al.*, 2006). Moreover, p53 is shown to bind directly to the promoter of the myosin VI gene and transcriptionally regulates expression of the myosin VI gene. Cells depleted of myosin VI showed reduction in the activation of ATM, a protein kinase responsible for the phosphorylation and consequent activation of p53 (Jung *et al.*, 2006). Mutations in dATM, *Drosophila* homologue and knockdown of myosin VI are both shown to increase cell's sensitivity to apoptosis (Jung *et al.*, 2006; Song *et al.*, 2004). In support of the data presented here and of previous report, I propose that Jar has a pro-apoptotic and anti-apoptotic functions mediated by the activation of the JNK pathway but in a cell-type manner (Cho and Chen, 2010). Moreover, the AP-1

transcription factors (Jun/Fos) are capable of modulating gene expression (Davis, 2000).

Cellular localisation study during the course of *Drosophila* development has identified Jar protein in the cytoplasm and in the cell membrane (Millo and Bownes, 2007). In the event of p53-dependent apoptosis, a pool of myosin VI is shown to migrate from endocytic vesicles, membrane ruffles and the cytosol to the Golgi complex, perinuclear membrane and the nucleus (Jung *et al.*, 2006). Interestingly, p53 is also shown to follow similar relocalisation route as myosin VI upon DNA damage or in certain cellular conditions (O'Brate and Giannakakou, 2003). These cellular compartments to which both proteins relocalise to are clustered with both pro-apoptotic and anti-apoptotic proteins (Eferl and Wagner, 2003). Consistent with this, only membrane-associated Rho1 can induce apoptosis by the activation of Slpr and downstream components of the JNK pathway at the cell cortex (Neisch *et al.*, 2010).

Therefore, I propose a model (Figure 4.6) on the basis of the information from previous work and the preliminary results presented here. Membrane-associated Rho1 (independent on GTP-binding) forms a complex with Slpr and consequently, activates downstream components of the JNKK pathway. The core JNK pathway is activated and subsequent phosphorylation of the AP-1 transcriptional factors could modulate Jar expression. The increase in the levels of Jar expression promote stabilisation and activation of Dmp53 through dATM activation. Consequently, Dmp53 protein increases and transcriptional regulates intracellular relocalisation of Jar and possibly to Slpr-containing complex at the cell cortex. Additionally, transcriptional target of p53 are also upregulated and consequently, apoptosis is induced. Depending on cell-type and developmental cues, Jar may have proapoptotic and anti-apoptotic properties as has been demonstrated for the AP-1 transcription factors (Eferl and Wagner, 2003; Krilleke *et al.*, 2003; Jochum *et al.*, 2001). Thus, Jar may be involved in maintaining homeostatic balance.

Overall, based on previous work and this study I conclude on the remark that Jar functions as a homeostatic apoptotic protein. Nonetheless, the proposed model merits further investigation at elucidating the molecular role of Jar in the JNK signalling pathway.

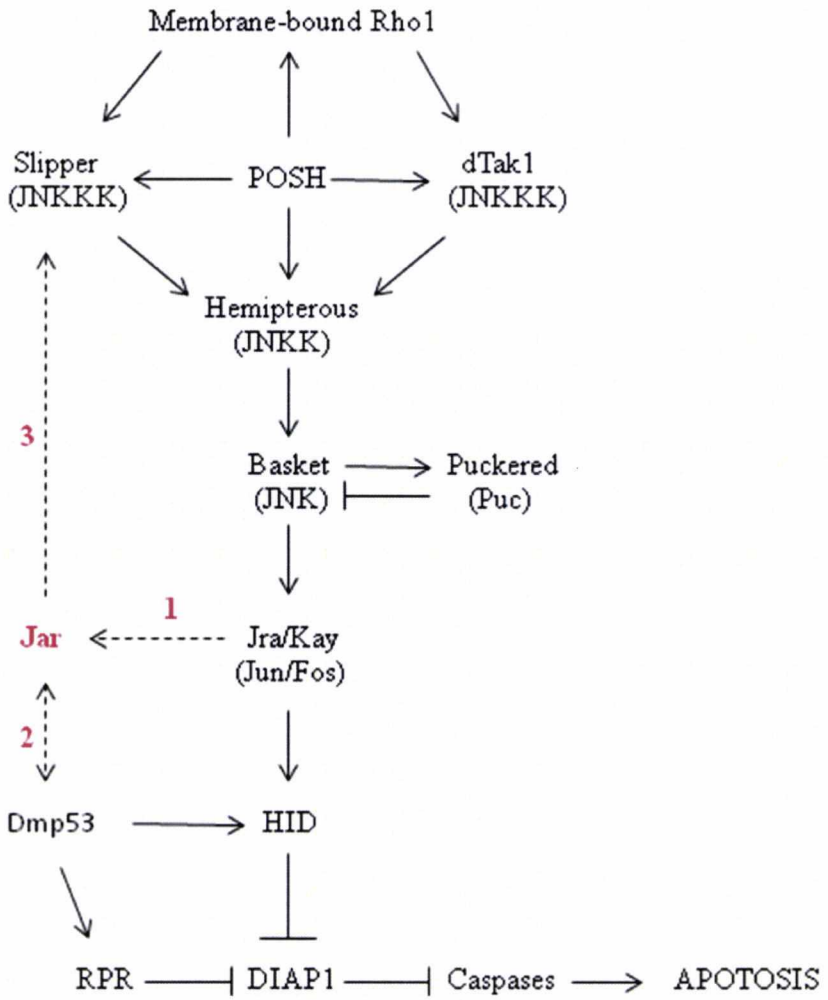

Figure 4.6. Proposed model of Jar function in active JNK signalling pathway. Shown above is a representation of how Jar expression could be induced during apoptosis and possibly, during normal development. The numbers represent the order of route for Jar expression and thus, function. In order as follows (1) upon activation of the JNKK signal cascade, the AP-1 factors (Jun/Fos) activate and modulate Jar expression in the dorsal epidermis (2) Dmp53 expression increases and trancriptionally regulates Jar. Jar in turn, stabilises and thus, activates DmP53 through dATM activation as reported for vertebrate myosin VI (Jung *et al.*, 2006). Consequently, proapoptotic genes Hid and Rpr are upregulated causing inhibition of DIAP1 and hence apoptosis (3) Jar undergoes relocalisation as demonstrated for vertebrate myosin VI (Jung *et al.*, 2006) and probably, to Slpr-containing complex at the cell cortex in similar manner as reported for Rho1 (Neisch *et al.*, 2010). Model adapted from Neisch *et al.* (2010) and McNamee and Brodsky (2009).

Chapter 5. RNAi-mediated knock down of Jar inhibits dorsal closure

5.1. Introduction

In this chapter, I set to further my understanding on the function of Jar protein in dorsal closure because reports of dorsal phenotypes of *jar* mutants are in contrast to expressing dominant negative ΔATP-jar construct in embryos. For this purpose, I undertook an alternative approach using RNA-mediated gene interference (RNAi) and the inducible GAL4/UAS system to knock-down protein Jar levels in specific tissues.

RNAi has increasingly become an effective tool in silencing a gene of interest in biological systems. It operates by specifically destroying the mRNA of a given gene hence eliminating production of the protein. A Jar RNAi transgene was obtained from the Vienna Drosophila RNAi Centre (VDRC). The RNAi in combination with the powerful tool of GAL4/UAS targeted expression system is effective in a tissue-specific manner and more so, at any development times of *Drosophila* life span (Dietzl *et al.*, 2007). In this tissue-specific manner one can possibly expand on the growing repertoire of functions of Jar. Furthermore, information from the VDRC website (http://www.vdrc.at) indicates that their *UAS-jar RNAi* transgene line should target all of the known isoforms of Jar.

Here, I demonstrate that the expression of *UAS-jar RNAi* by the GAL4 targeted expression system inhibits dorsal closure and is lethal. The effectiveness of the RNAi-mediated knock-down approach was clarified by immunofluorescence and western blot analyses, which revealed significant reduction of Jar protein levels at the various stages of *Drosophila* development.

5.2. Results

5.2.1. RNAi-mediated approach effectively knocks down Jar protein levels in embryos

Immunofluorescence and western analyses examined the levels of Jar protein knock down. For immunofluorescence analysis, the embryos were expressing UAS-Jar RNAi driven either ubiquitously in the epidermis using *69B*-Gal4 or in segmental stripes by *en*-Gal4. In either case of expressing UAS-Jar RNAi, there is no embryonic lethality (see 6.2.6). UAS-Jar RNAi 69BGal4-driven embryos show that Jar protein expression is undetectable during germ-band retraction and the result carries through to dorsal closure (Figure 5.1C, D). Alternatively, this result could just represent a failed antibody staining. However, UAS-Jar RNAi enGal4-driven embryos show knockdown in stripes commiserate with the expression pattern of enGal4 (Figure 5.1B). The immunofluorescence analysis of the RNAi-mediated Jar knock down is compared to temporal and spatial distribution of Jar protein in dorsal stage embryos (Figure 5.1A).

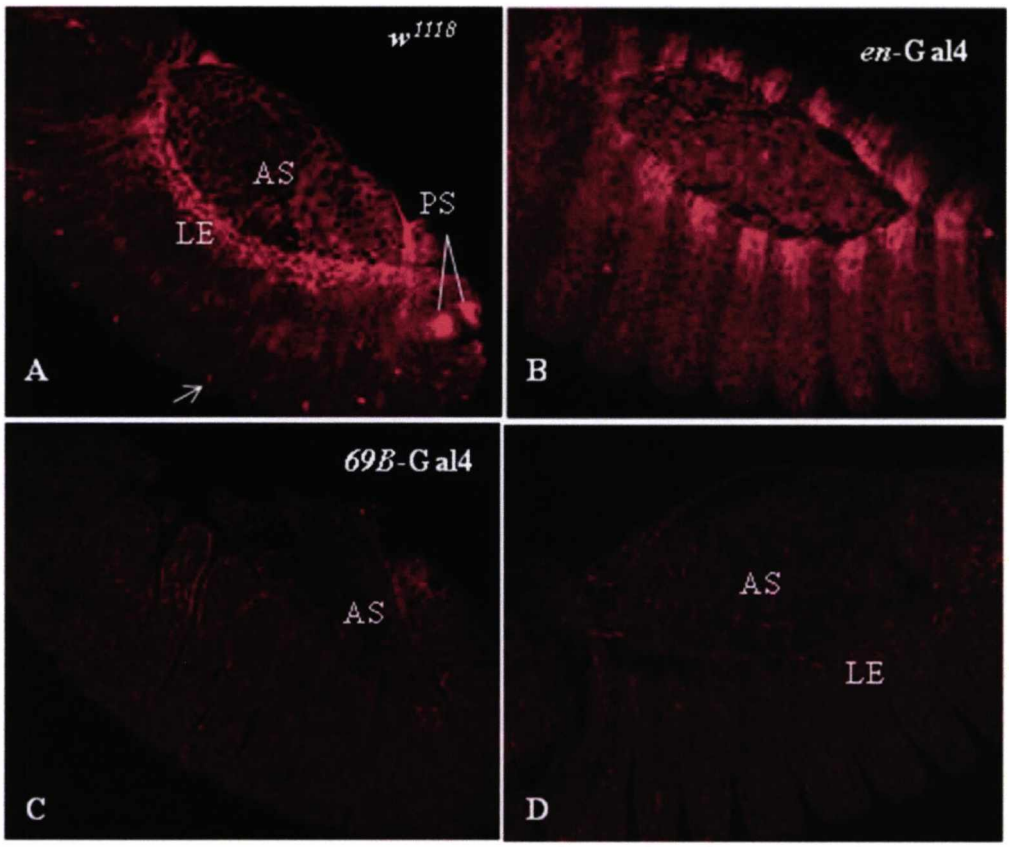

Figure 5.1. The driven expression of *jar-RNAi* controlled by *69B* and *en*-Gal4 drivers significantly reduces Jar protein levels in embryos. (A) w^{1118} embryo, (B) Jar-RNAi enGal4-driven embryo and (C-D) Jar-RNAi 69BGal4-driven embryos. (A) Dorsolateral view of stage 13/14 embryo showing ubiquitous expression of Jar protein expression along the LE cells, in amnioserosa (AS) cells, posterior spiracles (PS) and muscle attachments (exemplified by the arrow) across the ventral side of the epithelial sheet. (B) Dorsolateral view of stage 14 Jar-RNAi enGal4-driven embryo showing missing expression of Jar protein from the posterior compartment of the epidermal stripes. (C) Stage 12 of germ band retraction embryo shows missing Jar protein expression in the ectodermal germ band epithelium and in the compressed AS cells. (D) Stage 13 embryo shows undetectable expression of Jar protein at both the LE and AS cells.

The effectiveness of the RNAi-mediated Jar knock down was further verified through western blot method (Figure 5.2). Moreover, the western blot method was used to determine the extent of the Jar knock down protein levels in larval and pupal tissues expressing the Jar RNAi construct, which were unobtainable with the immunofluorescence analysis. For this purpose of testing lysates were obtained from crossing UAS-jar-RNAi x 69BGal4, a ubiquitous epidermal driver line. Embryos for the western analysis were that of overnight embryos collection. For comparison

lysates from the progeny of a cross between w^{1118} and the *69B*-Gal4 driver line were used. However, because of limited amount of the availability and the high usage of Jar antibody required for western blot analysis, the procedure was only done once.

In the control lane, the western blot data shows Jar protein in triplicate bands during embryonic and pupal stages, doublet band during third larval stage but no band during first instar phase. This clearly indicates that Jar protein expression is tightly regulated. More so, the bands correspond to Jar isoforms (Millo *et al.*, 2004; Deng *et al.*, 1999). In the UAS-Jar RNAi 69BGal4-driven lane, no band is detected during the embryonic stage. This data corresponds well with the immunofluorescence analysis. However, doublet bands are detected during the larval stage just as in the control lane. In the knock down pupae lane there is a clear reduction of the upper band and even more dramatic knock down of the two lower bands which are clearly undetected in the 10 minutes exposure.

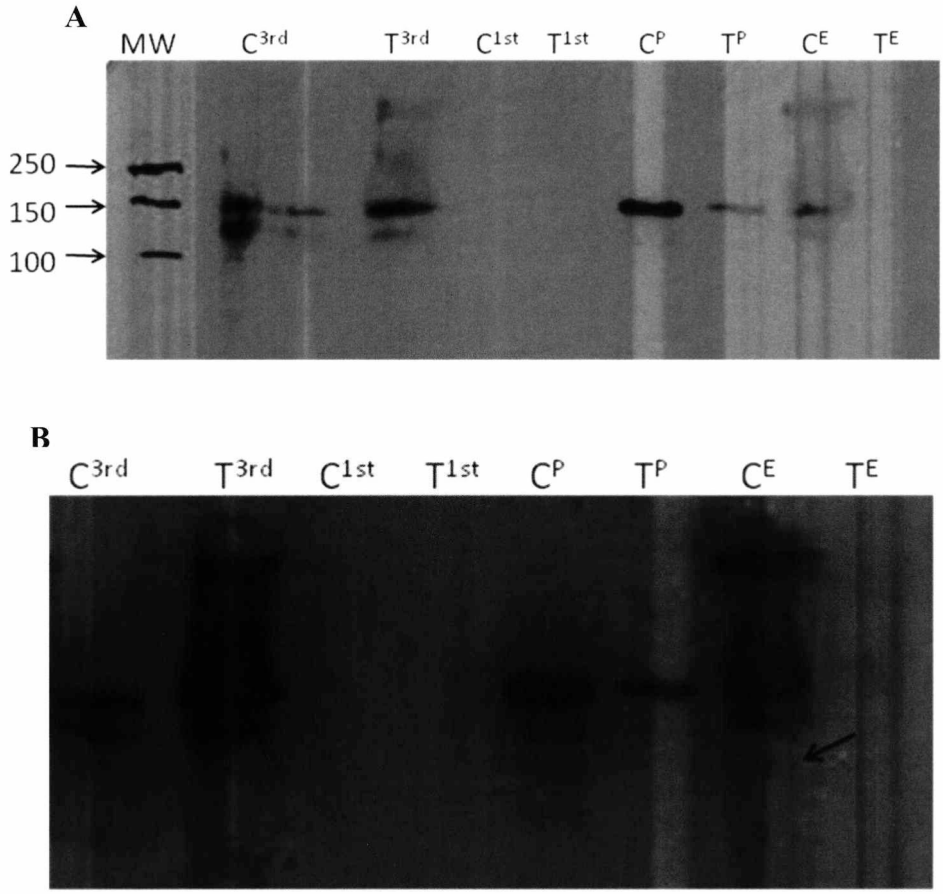

Figure 5.2. Western blot analysis of tissues expressing UAS-jar-RNAi 69BGal4-driven in the course of *Drosophila* development. (A) 1 minute exposure (B) 10 minutes exposure of X-ray films. C: control. T: test sample. 3rd: third instar. 1st: first instar. P: pupae. E: embryo. Compared to controls starting from the third instar phase no change is seen, no bands expressed both in the control and knock-down lane of the first instar, reduction of top band in the knock-down pupae lane and even more dramatic reduction of the two lower bands, and no detectable bands in the knock-down embryonic lane. (B) Clear indication of the Jar isoforms bearing the estimated molecular weights of 145, 140, and 120 kDa. Arrow in control embryonic lane points to a faded third band. Lane 1: marked molecular weights (MW, kD) in A.

5.2.2. enGal4 driven *jar-RNAi* slows dorsal closure

As there are conflicting reports of Jar function in dorsal closure and, indeed I have shown that although Jar expression is regulated by the JNK pathway, knockdown of zygotic Jar is not embryonic lethal I decided to examine the possibility that any defect in dorsal closure brought about by Jar knockdown is subtle. Worth noting, the loss of contractility in the purse string or amnioserosa through laser micro-ablation does not prevent dorsal closure, so subtle defects may not prevent the process completing (Kiehart *et al.*, 2000).

Confocal live analysis of UAS-Jar RNAi x enGal4;SGMCA (SGMCA, GFP fused to the *Drosophila* Moesin actin-binding domain) was examined. The live analysis reveals abnormality at the LE (Figure 5.3). Dorsal closure started as normal but on nearing the end, the LE cells show signs of irregularity. As the opposing epithelial sheets slowly advance towards the midline, during the zippering phase of stage 14/15 of embryogenesis, the LE cells are irregular. The LE cells are not moving in a synchronised manner with one another. Nonetheless, dorsal closure proceeded to completion. The live analysis images are snapshots because of technical difficulties experienced with the confocal laser microscope and time-lapse movie was not possible.

Interestingly, the speed variation between the LE cells was also observed in striped expression of maternal and zygotic Ed embryos (Lin *et al.*, 2007). Echinoid (Ed), an immunoglobulin domain-containing cell adhesion molecule is known to interact genetically with Jar (Lin *et al.*, 2007). Moreover, homozygous jar^{322} expressed in wild-type background of null ed^{1F20} mutant allele resulted to 100% embryonic lethality and most embryos displaying dorsal defects. However in my attempt to reproduce the same result, I got 11% embryonic lethality as opposed to the 100%. I observed no evidence of dorsal defects with cuticle preparations (2.2.8) of the dead embryos. The discrepancy of the results is likely because of the different allele mutant employed in this study to that in the literature.

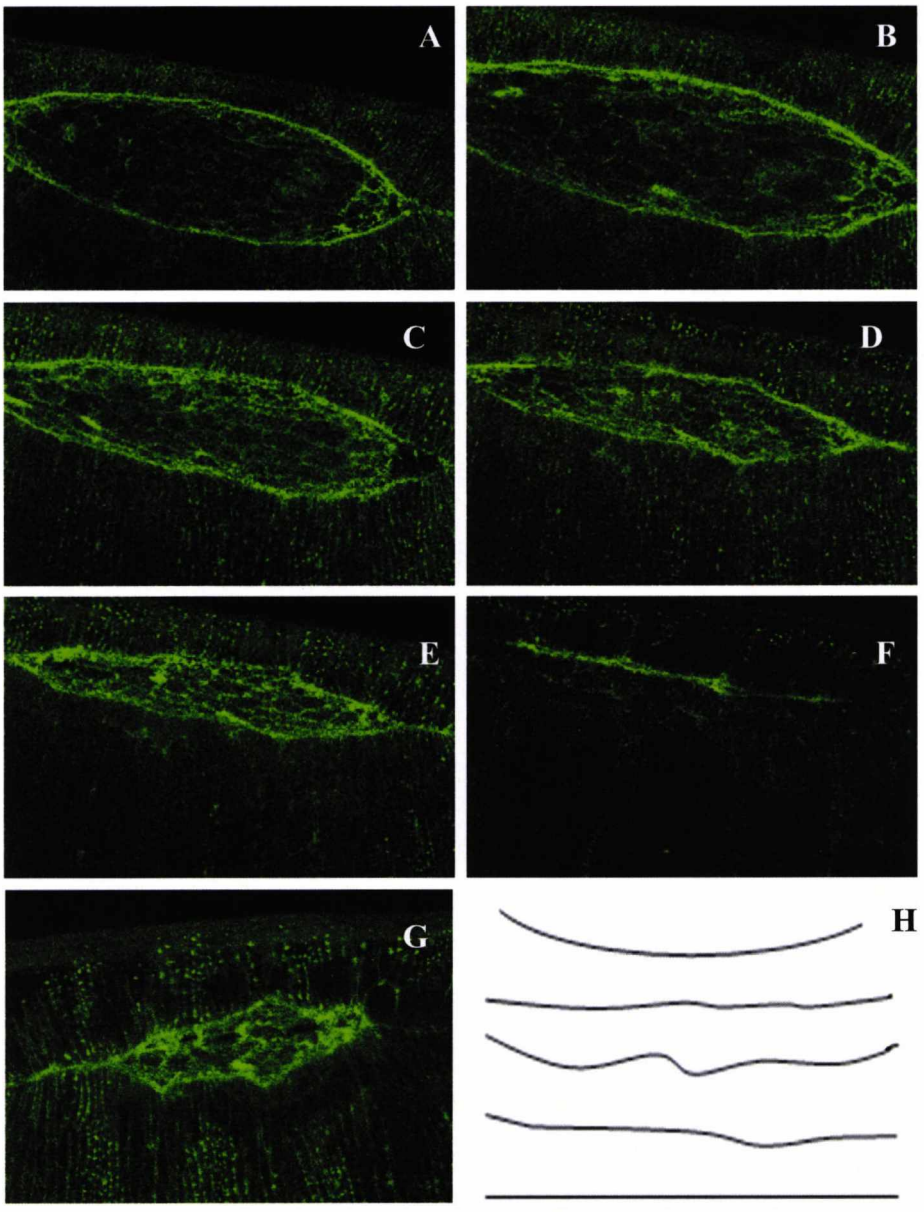

Figure 5.3. The effect of knockdown Jar protein expression levels during dorsal closure. (A) Shown are snapshots images of live dorso-lateral view of *en*GAL4;*SGMCA/jar-RNAi* driven embryo. Following through from (A) the dorsal opening is of the correct shape described roughly as the shape of a human eye. However, in (B) irregular LE is observed which becomes more obvious as dorsal process progresses. Furthermore, as the epidermal fronts near the midline, the once disorganised front row cells appear corrected. And lastly (F) the opposing epidermal sheets fuse along the midline giving a seamless appearance. (G) A close-up of another embryo showing the severity of the dorsal defect (H) Schematic diagram with each line depicting one half of the LE illustrating the progression of the LE in Jar knock-down embryo. Lines not drawn to scale.

In a different confocal live analysis, I co-expressed the Jar-RNAi construct with the GMA actin marker using enGal4, GFP is visualised in segmental stripes. In the earlier live analysis, the GMA marker is expressed ubiquitously under the direct control of a ubiquitous promoter. Dorsal closure commenced as normal but on nearing the zippering phase where normally the extending filopodia/lamelliopodia from the bands of actin at the LE would sense the opposing matching segmental stripes and fuse, the process is delayed (Figure 5.4). In some instances a severe delay in dorsal closure is seen. Dorsal closure is seen to proceed well over 9 hours (3 times the normal). However result was not consistent and therefore difficult to draw any conclusions from. Nonetheless, embryonic lethality of the progeny from the cross, Jar-RNAi enGal4GFP-driven was 2.5% (n = 792). Thus, the embryos proceeded to completion of dorsal closure.

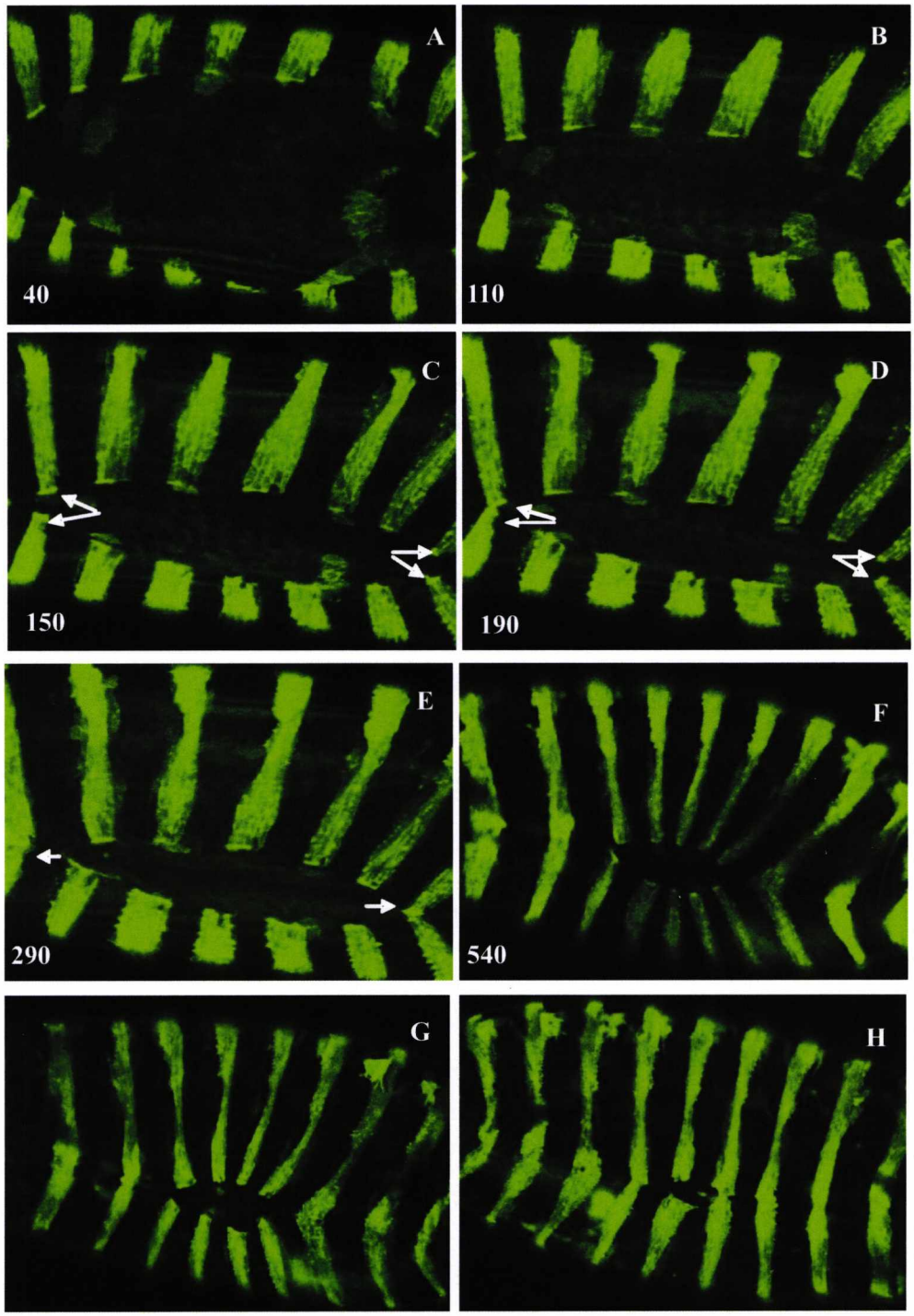

Figure 5.4. Epidermal expression of *UAS-jar-RNAi* controlled by *enGal4;UAS-GMA*. Above are still images with dorsal view from time-lapse movie (63xobj) with time (mins) numbered at the bottom left corners. (A-B) The decrease in amnioserosa surface area clearly indicates that the epidermal stripes have advanced forward to eventually meet in the midline. Beside the contractile actomyosin and AS, filopodia spikes extend dorsally to bring matching stripes into close proximity as illustrated in stripes at the extreme left and right of the images (arrows in stills C-E). However, after 5 hours into the movie we found no more adhesion between the remaining stripes but extending filopodia can still be seen (apparent in movie). (F) Same embryo but shown in 40xobj after 9 hours into closure. (G-H) Images (40xobj) of different embryos laid on the same slide taken after 9 hours.

5.2.3. Embryonic knock down of Jar affects orientation of microtubule arrays but not the actin cytoskeleton

Jar is supposedly involved in actin organisation during dorsal closure and spermatid individualisation (Millo *et al.*, 2004; Rogat and Miller, 2002). Therefore, I investigated the effect that Jar knock down will have on actin and microtubule (MT) cytoskeleton and the consequent effect in the LE cells and the AS cells.

In Jar knock down embryos, I examined actin organisation at the LE in embryos of genotype *GFPactin/jar-RNAi;69BGal4/+* (2.4.5, movie 5.1). I found no observable defect in the contractile apparatus of the LE actomyosin cable during the live imaging (Figure 5.5). In support of this, dorsal closure staged Jar knock-down embryos were fixed for actin staining with phalloidin. Just as before, I found no abnormality in the organisation of the actin cytoskeleton (Figure 5.7). However, there are differences in the ingression between the non-labelled GFP-AS cells and GFP-AS cells expressing Jar RNAi. The GFP-negative AS cells is seen to fade quicker than the neighboring GFP-positive AS cells (Figure 5.5). This implies that knockdown of Jar protects AS cells from apoptosis. However, for a better understanding of the result the rates of the apical constriction of AS cells need quantifying and further, track a single AS cell from the onset of the apoptotic process of AS to completion. Notably, the assembly and disassembly of actomyosin network in the cells occur in asynchrony waves which coincide with the apical constriction and relaxation of AS cells, respectively (David *et al.*, 2010). Repeated apical constrictions of a single AS cell over time result in reduced apical surface area (Solon *et al.*, 2009).

Jar is expressed in the amnioserosa (Milo *et al.*, 2004). I examined the behavioural pattern of the AS cells in embryos expressing Jar RNAi construct driven with an AS-Gal4 driver line. I found no abnormality of the AS cells. However, there is the possibility of a defect, much subtle in the behavioural constriction pattern of the AS cells. Possibly, the lack of functional Jar could be compensated by zip/MyoII as it is demonstrated to provide the majority of the force for actin contraction at the LE and of the AS apical constriction (Blanchard *et al.*, 2010; Franke *et al.*, 2005). Consistent with this, expression pattern of myosin II is unaffected in Jar knock down

embryos and this is in accordance with report that there is no interaction between myosin VI and myosin II during embryogenesis (Figure 5.8) (Petritsch *et al.*, 2003).

I also investigated the possibility of Jar protein function in regulating MT cytoskeletal architecture. MT is reportedly required for the zippering phase of closure (Jankovics and Brunner, 2006) and it is towards the zippering phase that Jar knock down embryos is seen to display abnormality during dorsal closure. Jar RNAi and tubulin were co-expressed using 69BGal4GFP. During the dorsal closure process, MT bundles are seen to align perfectly along the dorsoventral axis of the body plan as normal (Jankovics and Brunner, 2006). However, as dorsal closure draws to completion I noted abnormalities in the organisation of MT (Figure 5.6, movie 5.2). MT bundles are seen to migrate towards a focal point resulting in bunching at point along the midline into 180 minutes of the live analysis. Embryo fails in dorsal closure and was arrested in development.

To explore further, through the RNAi-mediated knock down approach I examined a known myosin VI binding partner, GIPC/synectin in vertebrate and of recent characterised in *Drosophila*, dGIPC, also shown to interact genetically with Jar (Djiane and Mlodzik, 2010). Expressing UAS-synectinRNAi via either enGal4;SGMCA or enGal4;UAS-GMA driver line, I found no observable dorsal defect during live imaging.

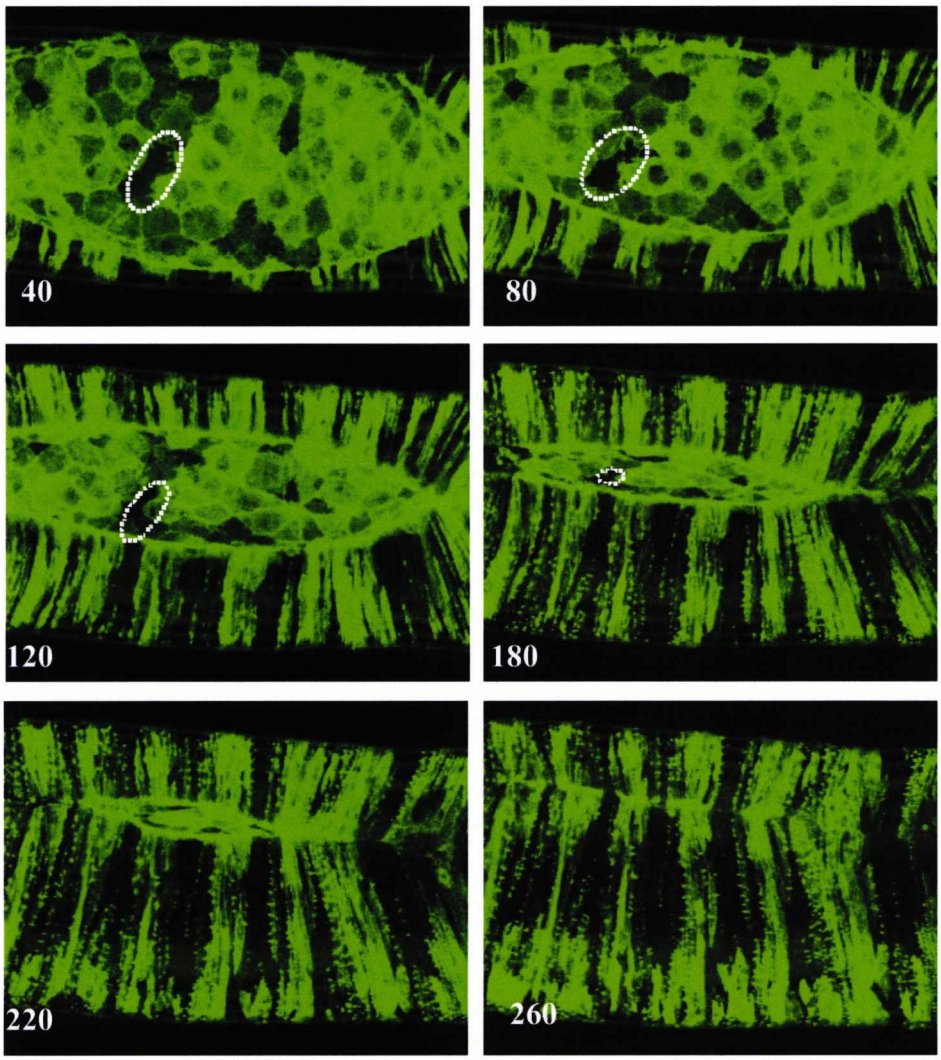

Figure 5.5. Examination of GFP-tagged actin controlled by 69BGal4 driver line in Jar knock-down embryo. Still images taken from live imaging of *GFPactin/jar RNAi;69BGal4/+*-expressing embryo, from the onset of dorsal closure (stage 13, t = 40) to completion (stage 15, t = 260). Time (mins) numbered at the bottom left corners. Following through the white dotted circle (40-180 mins) of a GFP-negative AS cell, it ingresses faster compared to neighboring GFP-positive cells expressing the Jar knock-down construct.

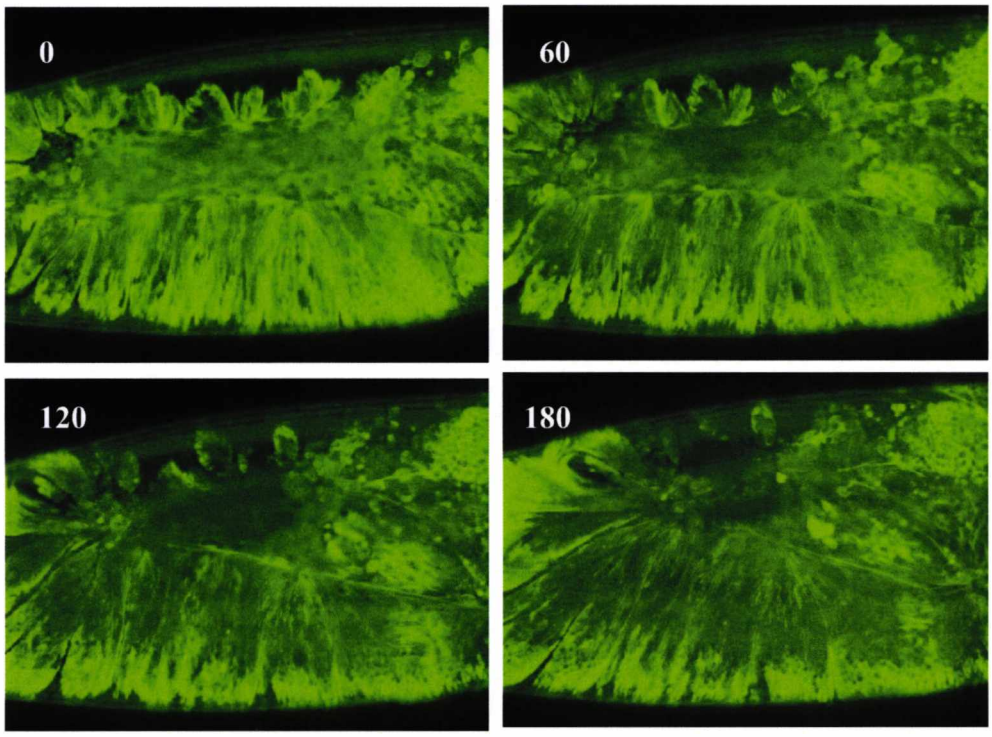

Figure 5.6. MT dynamics in dorsal closure of a dorsoventral view of stage 14 embryo expressing Jar-RNAi coexpressed with GFP-tubulin driven by 69BGal4. A *GFP-α-tubulin/jar-RNAi;69BGal4/+*-expressing embryo showing that MT bundles are aligned perpendicular to the LE but however, as closure nears completion (t = 180 mins) MT arrays orientation is no longer parallel to the D/V cell axis. Note: in the movie 5.2, the embryo is oriented vertically.

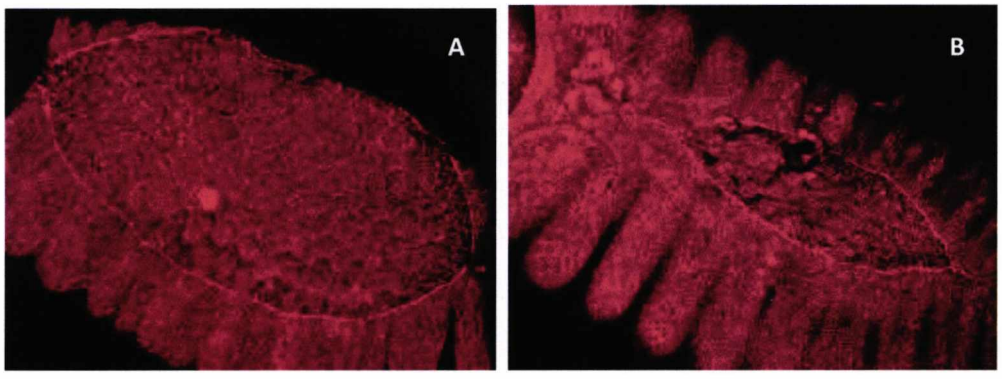

Figure 5.7. Actin organisation in dorsal closure of embryos of genotype *jar RNAi/+;69BGal4/+* stained for rhodamine phallodin. A stage 13 embryo at an early stage of dorsal closure and (B) stage 14 embryo showing the unperturbed outline of assembled actin at the LE.

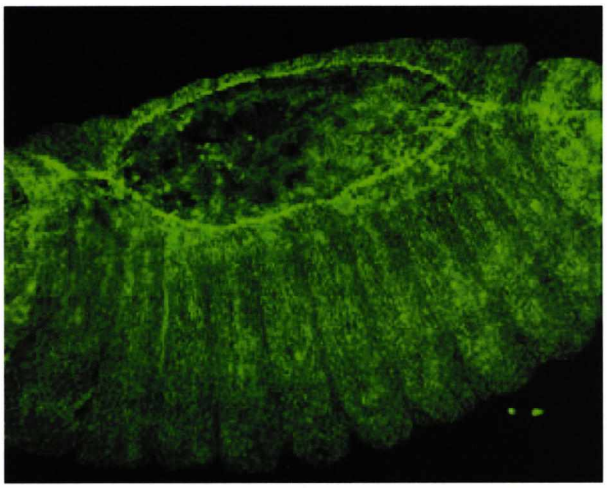

Figure 5.8. Expression of *zip*/MyoII is unaffected in Jar knock-down embryos. Dorsoventral view of a stage 14 embryo expressing Jar-RNAi under the control of 69BGal4 driver line showing clearly punctate distribution of *zip*/MyoII at the LE cells.

5.2.4. Jar is not required for wound repair

Millo *et al.*, (2004) suggested a potential role for myosin VI in wound repair. The expression of ΔATP-jar led to rupture of epithelial cell layers as a result of loss of adhesive properties and so, prevented the recovery of the epidermis. Reportedly, wounds repeatedly induced through mechanical means or laser beams can rapidly heal and more so, closures proceed as normal to completion albeit longer time compare to wild-type (Kiehart *et al.*, 2000).

Coincidentally, I was able to follow through a course of dorsal closure of a wounded embryo expressing Jar-RNAi x enGal4;SGMCA (see movie 5.3). The wound could have been happened in a number of ways: could have been induced in the de-chorionation process or in the transportation process with the use of forceps. At the site of wound is a free flowing yolk from ruptured yolk membrane-bound sack that normally should lie beneath the AS. Despite the wound, contraction of the actomyosin and apical constriction of the AS is normal. With time, regenerated epidermis is seen to advance forward most probably through the contractile actomyosin and of the extending filopodia that is scanning for its matching segment (Figure 5.9C) (Kiehart *et al.*, 2000). Filopodia is reportedly demonstrated to exert significant contractile force to pull forward the epithelial sheet (Millard and Martin, 2008). Notably, long filopodia spikes is seen from the LE cells on the opposite sides

of the wound (Figure 5.9D). Thereafter, filopodia is seen to initiate interaction with the regenerated LE and subsequently, suture together (Figure 5.9E).

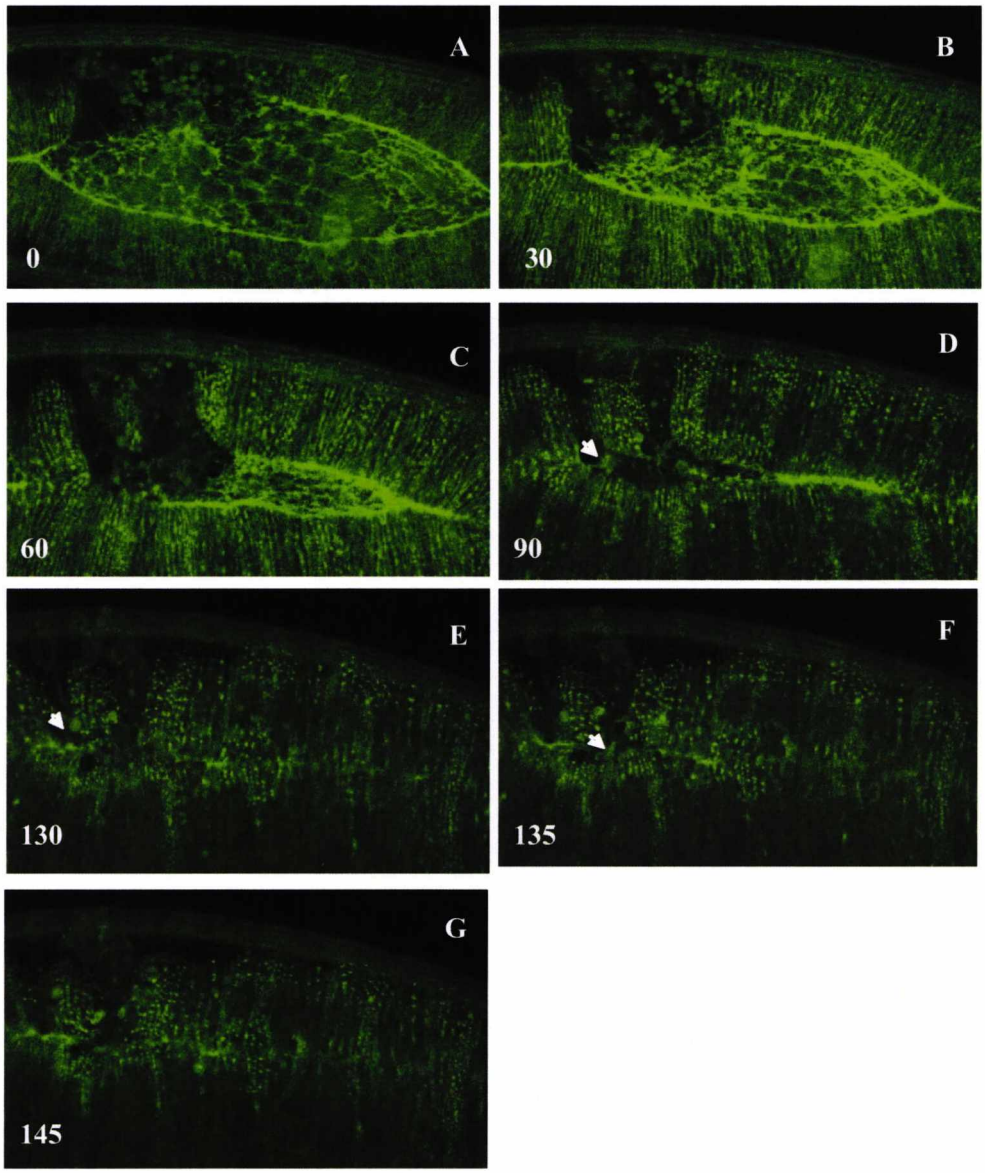

Figure 5.9. Lack of functional Jar does not prevent wound healing. Dorsolateral view of a stage 14 wounded embryo. Time (mins) numbered at the bottom left corners on the still images. In the 0-30 mins extending filopodia from AS cells are noted at entry of wound. As dorsal closure nears to completion as indicate by the fading actin cable (D-E), the healing event is still ongoing because 90 mins into the movie regenerated epidermis stripe has emerged. (D) Filopodia (arrow) is seen to sense the newly formed epidermal front if matched for fusion and subsequently opposing segment adhere and suturing ensues (E, arrow). In 135 mins, another needle-like filopodia (arrow) is also seen.

5.2.5. Embryonic knock down of Jar does not affect cell adhesion

In *Drosophila*, cell-cell adhesion is mediated by E-cadherin (DE-cadherin) through Ca^{2+}-dependent homophilic interactions at the adherens junctions (AJs) (Tepass *et al.*, 1996). Reduced DE-cadherin protein levels and in severe cases, mislocalisation of DE-cadherin to the cell cytoplasm has been reported in expressing dominant negative ΔATP-jar in embryos (Millo *et al.*, 2004). Possibly, Jar could function in the recycling of adhesion molecules of DE-cadherin. Therefore, I examined the adhesive properties of the epidermal cells in Jar knock down dorsal stage embryos.

UAS-Jar-RNAi 69BGal4-driven embryos were staged for dorsal closure and fixed for DE-cadherin antibody staining. For comparison w^{1118} x 69BGal4 embryos were fixed and stained for DE-cadherin antibody. The pattern of DE-cadherin protein expression remained unchanged when compared to control (Figure 5.10).

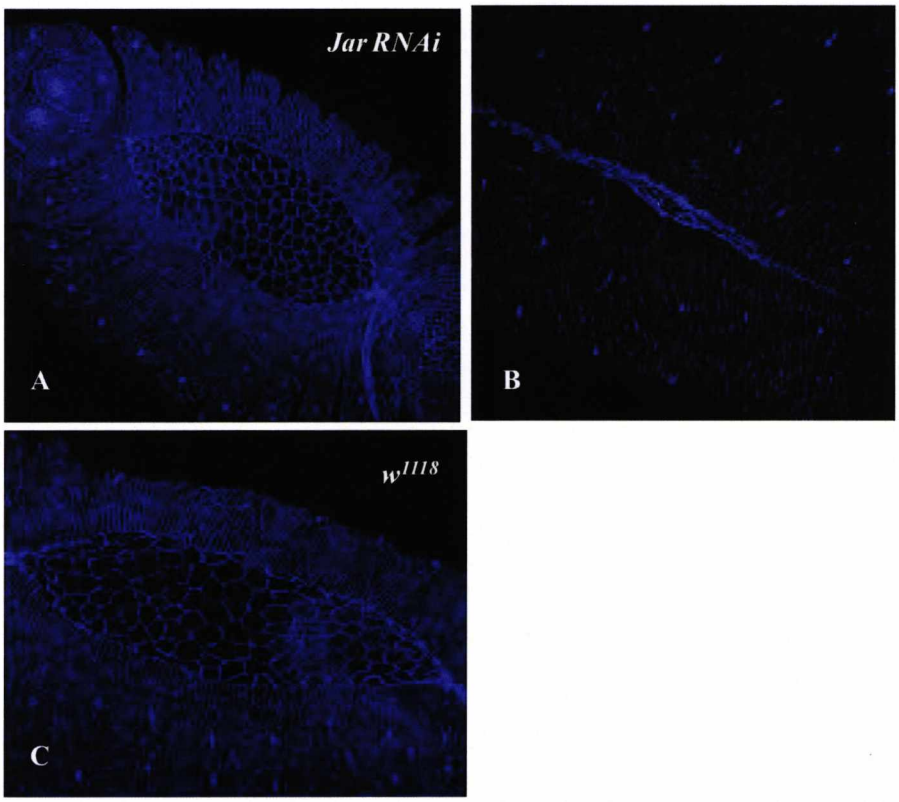

Figure 5.10. DE-cadherin protein expression levels unaffected in Jar knock-down embryos. Both *UAS-jar RNAi* (A-B) and w^{1118} (C) were driven by 69BGal4 in the embryonic epiderm. (A) A dorsolateral view of stage 14 (40xobj) and (B) stage 15 (63xobj) embryos indicating that DE-cadherin protein expression is unperturbed. (B) Dorsal view of stage 14 of w^{1118} embryo (63xobj) showing normal pattern of DE-cadherin protein expression.

5.3. Discussion

Jar is expressed in the dorsal epidermis and in the amnioserosa during dorsal closure (Millo and Bownes, 2007; Millo *et al.*, 2004). Depending on the experimental approach in inhibiting the function of Jar, in expressing dominant negative ΔATP-jar or depleting Jar protein expression through P-element mutagenesis, dorsal phenotypic reports contradict each other. Here, I report contrary to expectations that function of Jar is required for dorsal closure though not essential. Moreover, the data here suggest that Jar may be involved in microtubule organisation during the zippering phase in dorsal closure.

RNAi-based approach has an inherent risk of off-targeting effects. Therefore, I performed a blast query of the nucleotide sequence of *UAS-jar RNAi* transgenic line against the *Drosophila* genome but report came up with only Jar as a hit. The relevance of Jar during dorsal closure is questionable. Despite the dramatic knock down of Jar protein levels, I found that Jar protein is not of importance for embryogenesis which is consistent with reports of the $jar^{322}/Df(3R)S87\text{-}5$ null embryos (Morrison and Miller, 2008 and this study). $jar^{322}/Df(3R)S87\text{-}5$ fly has complete lack of Jar protein expression. The result presented here is in contrary to expressing antisense-RNA Jar expression which resulted in embryonic lethality but no reported dorsal defect (Deng *et al.*, 1999). The discrepancy of the result is most likely due to the different activating nature of the Gal4 drivers. Antisense-RNA Jar was driven with $e22_C$-*Gal4*, a ubiquitous driver in embryos. However, expressing *UAS-jar RNAi* through the ubiquitous epidermal driver, *69BGal4*, Jar expression in other tissues will not be affected. Moreover, cellular localisation study has demonstrated that the expression pattern of Jar is widespread in *Drosophila* (Millo and Bownes, 2007).

Jar knock down in embryos resulted in abnormality of the leading edge during dorsal closure but did not prevent the completion of the process. The cause of this irregularity of the leading edge is unknown but it is not due to gross distortion of the actin cytoskeleton, missing DE-cadherin protein or myosin II protein expression. In contrast, expressing dominant negative ΔATP-jar resulted in missing actin cable and myosin II protein expression at the LE, detachment between the LE cells and amnioserosa and loss of cell surface DE-cadherin (Millo *et al.*, 2004). It is worth

nothing that expressing ΔATP-jar will affect any maternally supplied Jar and could also bind and sequester Jar binding partners that have essential functions. Neither of these will be affected by Jar RNAi expression. Therefore the phenotypic defects in expressing ΔATP-jar are most probable a consequence of the loss/mislocalised cell surface DE-Cadherin. Consistent with this, DE-cadherin protein expression in jar^{R39} and jar^{R235} mutants, is unaffected (Millo *et al.*, 2004).

E-cadherin connects to the cytoskeleton with direct binding to armadillo (Arm; *Drosophila* homologue of β-catenin) which in turn, interacts with α-catenin, thence form tight regulated cadherin-catenin complexes. Stable cohesion between cells require dynamic turnover of E-cadherin at the cell surface through endocytosis and exocytosis to allow redistribution of E-cadherin during epithelial morphogenesis in *Drosophila* (Wirtz-Peitz and Zallen, 2009; Cavey *et al.*, 2008). During dorsal closure, zygotic loss of DE-cadherin results in segmental mismatches, loss of ventral epidermis and weakened actin cable (Gorfinkiel and Arias, 2007). Moreover, defects are severe in the complete abolishment of E-cadherin activity: lack of actin cable assembly at the LE and detachment of the epidermis and AS.

Jar was first implicated as a mediator in cohesion between cells in border cell migration during oogenesis (Geisbrecht and Montell, 2002). Jar associates with DE-cadherin and Arm. The loss-of-function of Jar resulted in impaired border cell migration and consequent reduction in the levels of DE-cadherin and Arm. The over-expression of DE-cadherin and Jar significantly restored the migration defect but, it was suggested that the migration defect was due to the reduced levels of DE-cadherin and Arm (Geisbrecht and Montell, 2002). However, Jar does not have physical interaction with DE-cadherin.

Jar has been demonstrated to interact genetically with Ed to regulate cell morphology during dorsal closure (Lin *et al.*, 2007). Ed is a transmembrane immunoglobulin domain-containing cell adhesion molecule known to cooperate with DE-cadherin to mediate cell adhesion at AJs localised at the interface between the LE (Lin *et al.*, 2007; Wei *et al.*, 2005). During dorsal closure Ed is seen to localise to actin-nucleating center (ANC) at the AJs (Lin *et al.*, 2007). E-cadherin also accumulates at the ANC (Gorfinkiel and Arias, 2007). Null *ed* embryos showed segmental mismatching, lack of actomyosin cable assembly at the LE and few actin-based

protrusions: filopodia/lamellipodia (Lin *et al.*, 2007). These phenotypes overlap with those observed in null DE-cadherin embryos (Gorfinkiel and Arias, 2007). An intracellular domain of Ed, Ed^{intra} was demonstrated to be of importance in regulating the cell morphology. More importantly, Ed^{intra} was shown to interact with Jar (Lin *et al.*, 2007).

Bearing in mind that Jar directly interacts with Ed, the lack of Jar protein expression could result in weakened adhesion between cells and thus, gives a plausible explanation for the irregular LE seen in Jar knock down embryos. Maternal and zygotic mutant *ed* embryos are shown to have irregular migration defects of the LE cells (Lin *et al.*, 2007). In maternal and zygotic mutant *ed* embryos, Jar protein expression is mislocalised and diffused. Furthermore, few of the enGal4-driven ΔATP-jar embryos showed incomplete germ band retraction which is consistent with reports of strong genetic interaction between Ed and Jar during germ band retraction (Lin *et al.*, 2007). The detachment of the germ band tissue from the AS portrayed in enGal4-driven ΔATP-jar during germ band retraction is not surprising because, epidermal leading edge of AS and germ band are notably tightly adherent to one another through adherens junctions and moreover, known to move coherently as one sheet (Schöck and Perrimon, 2002).

Alternatively, the intracellular puncta localisation of DE-cadherin found when expressing ΔATP-jar is suggestive of a block in endocytosis. Recycling of E-cadherin is through the clathrin-mediated endocytic route in epithelial morphogenesis in *Drosophila* (Levayer *et al.*, 2011). Moreover, DE-cadherin is shown to be actively trafficked in the *Drosophila* embryonic ectoderm (Roeth *et al.*, 2009). Vertebrate myosin VI is well shown involved in clathrin-mediated endocytosis (reviewed in Chapter 1). Possibly, expressing Jar RNAi can induce an alternative endocytosis route for DE-cadherin as vertebrate E-cadherin can be endocytosed through clathrin-dependent pathway as well as clathrin-independent pathway (Akhtar and Hotchin, 2001).

Furthermore, I report here that the Jar RNAi co-expressed with tubulin caused misdirection of the MT bundles during the zippering phase in dorsal closure. Microtubule is essential for the zippering phase (Jankovics and Brunner, 2006). Inhibiting MT function through injection of MT depolymerising drugs or by

expressing an MT-severing protein Spastin in embryos inhibited exclusively the zippering process that completes dorsal closure. The embryos arrested and failed to complete dorsal closure (Jankovics and Brunner, 2006). Notably, in axons of the *Drosophila* CNS embryos Jar is in puncta pattern with *Drosophila* cytoplasmic linker (D-CLIP-190), a protein which links vesicles to microtubules (Lantz and Miller, 1998). Affinity chromatography showed that Jar has a direct binding with microtubule-associated protein Cornetto in *Drosophila* embryonic cells (Finan *et al.*, 2011). Cornetto protein is required in neuroblasts for mitotic spindle during the late stages of mitosis and possibly to stabilise the orientation of the mitotic spindle (Bulgheresi *et al.*, 2001).

The data here indicate that Jar may play functional role but not an essential one during embryogenesis. Jar is required but not essential for dorsal closure. The result reinforces the proposed model that Jar plays a homeostatic apoptotic role but in a cell-type manner.

Chapter 6. Complete loss of Jar leads to developmental arrest at distinct time points

6.1. Introduction

Jar gene lies on the right arm of the third chromosome at cytological map position 95F6-95F8. The deficiency *Df(3R)S87-5* removes the region 95F7-96A18, thus uncovers most of the Jar gene but leaves the adjacent CG5706 gene intact (Figure 6.1). The jar^{322}/*Df(3R)S87-5* flies are thus only mutant for Jar. They are viable but male sterile a fact consistent with the phenotype of jar^{1} mutants (Hicks *et al.*, 1999). Using PCR amplification of genomic DNA with primers that span the Jar coding region, it was demonstrated that jar^{322} in trans with *Df(3R)S87-5* only contains exons 14-17 of *jar*, corresponding to the globular tail. Furthermore, the globular tail in isolation was proven non-functional. In summary, Morrison and Miller (2008) characterised the jar^{322}/*Df(3R)S87-5* mutant allele and conclusively demonstrated that the complete loss-of-function of Jar is not lethal. The zygotic and maternal null jar^{322}/*Df(3R)S87-5* showed 60% lethality and no developmental defects in the 40% null mutant adults. 10% arrested during metamorphosis stage. 50% arrested between embryogenesis and larval developmental stages. The arrest points of the 50% were unaccounted for because, jar^{322} homozygotes could not be distinguish from jar^{322}/*Df(3R)S87-5* trans-heterozygotes.

Here, I employed a PCR-based strategy using identical primers to Morrison and Miller (2008), in conjunction with fluorescence protein tags, to distinguish between jar^{322} homozygotes and jar^{322}/*Df(3R)S87-5* trans-heterozygotes. In the light of these we pinpoint the developmental stages at which the 50% *jar* zygotically and maternally null mutants arrested.

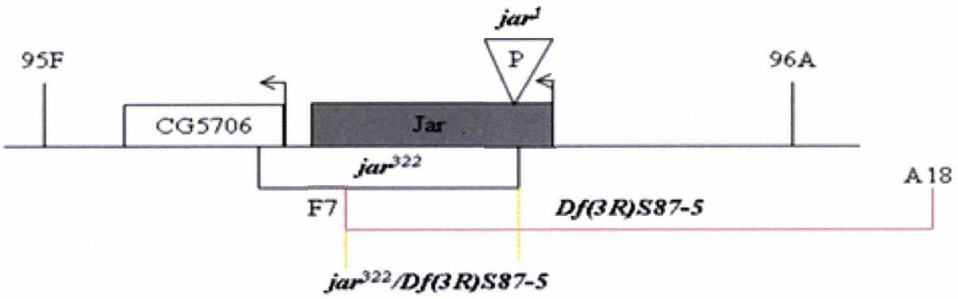

Figure 6.1. Schematic marks a portion of the right arm of the third chromosome showing positions of mutated *jar*^{322} and deletion deficiency *Df(3R)S87-5*. The arrows indicating the transcription start site and direction. Mutated *jar*^{322} has uncovering of the Jar coding gene (exons 3-17) and at least the first exon of CG5706. The deletion deficiency *Df(3R)S87-5* chromosome uncovers the region 95F7-96A18. Thus, *jar*^{322}*/Df(3R)S87-5* contains the region exons 14-17 (Morrison and Miller, 2008). Image modified from Morrison and Miller (2008).

6.2. Results

6.2.1. Genetic schemes to differentiate *jar* homo- from transhetero-zygotes

Here, a genetic cross scheme similar to that done by Morrison and Miller (2008) was designed but with different fluorescent protein tags that allows one to distinguish between the *jar*^{322} homozygotes and *jar*^{322}*/Df(3R)S87-5* trans-heterozygotes. *jar*^{322} was tagged with GFP whereas *Df(3R)S87-5* was tagged with RFP (red fluorescent protein) and this approach allowed resolution between the genotypes generated from the cross scheme (Table 6.1). However, maternal contribution of the fluorescent tags prevented clear determination of the different genotypes. The RFP is fused with a functional histone 2A (His2) variant (Schuh *et al.*, 2007). All cell nuclei are marked with the His2-RFP reporter.

Table 6.1. Fluorescent proteins differentiate between classes of progeny

Classes of progeny	**Marker for indentification**
jar^{322}/TM3, KrGFP	GFP expression only
Df(3R)crb87-5, His2RFP/TM3, KrGFP	GFP + RFP expression
jar^{322}/jar^{322}	Lack of GFP or RFP
jar^{322}/Df(3R)crb87-5, His2-RFP*	RFP expression only

*This genotype will thereafter be selected for further analysis.

To circumvent the issue of the maternal derived fluorescent expression, I reverted to using GFP-expressing balancer as previously done by Morrison and Miller (2008) (Figure 6.2). The GFP tag can be followed through from late embryo to adult (Casso *et al.*, 2000). Moreover, maternal derived expression is not detected from stage 4 of embryogenesis. However I found that the genotypes were much easier to differentiate during the larval stage because larva has no yolk which fluoresces green close to, but yellower than GFP during the embryonic stage.

A cross was undertaken between *jar^{322}/Df(3R)crb87-5* female virgins and *jar^{322}/TM3, KrGFP* males generating two groups, the fluorescent (GFP-positive) and the non-fluorescent group (GFP-negative) (Figure 6.2). The GFP-negative group would either be *jar^{322}* homozygotes or *jar^{322}/Df(3R)S87-5* maternal and zygotic null. The GFP-negative first instar larvae were selected, cultured and followed through to eclosion. The culture was checked every 12-14 hours for dead individuals that were then genotyped using a PCR strategy derived from Morrison and Miller (2008).

The primers (2.6.2.1) used for the PCR amplification were complementary to the sequence of the exons 15-17 which is left of the Jar gene in the maternal and zygotic null *jar^{322}/Df(3R)S87-5* mutant. Because, *jar^{322}* homozygotes contains no Jar gene a visible DNA band on a gel photo would indicate that the dead individual is that of the *jar^{322}/Df(3R)S87-5* null mutant. Genomic PCR was also performed on the standard fly, *w^{1118}* and products were resolved on a 0.8% agarose gel to indicate a

product size of 513 bp. For comparison, a negative control had template DNA replaced with deionised water and this was to check for contamination.

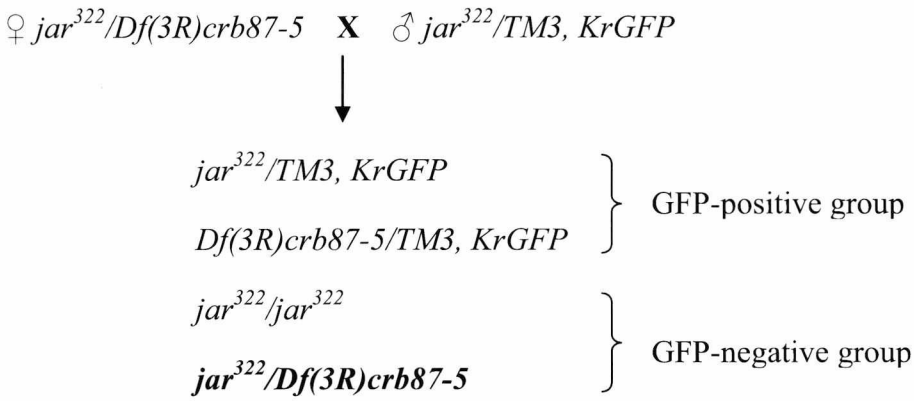

Figure 6.2. A genetic crossing between females of genotype *jar*^{322}*/Df(3R)S87-5* and males of genotype *jar*^{322}*/TM3, KrGFP.* Two groups, GFP-negative and GFP-positive are created in the offspring. GFP-negative group is further assessed for the characterisation of the *jar*^{322} mutant. Note: 25% of the offspring are expected to be heterozygous for *jar*^{322}*/Df(3R)crb87-5* mutant.

6.2.2. *jar* maternal and zygotic nulls survive embryogenesis with no dorsal closure defects

Here, I determine to evaluate the percentage of lethality of *jar* nulls during embryogenesis.

1000 embryos from the cross (Figure 6.2) were randomly selected and transferred to fresh apple plate. I noted that *Df(3R)crb87-5/TM3, KrGFP* heterozygotes were unhealthy and hatched at a slow rate, also noted in the report (Morrison and Miller, 2008). To circumvent the issue of slow growth, the selected embryos were staged for more than 48 hours and then examined for embryonic lethality. Of the 1000 embryos picked, I observed 21 dead embryos. Of the 21 dead embryos analysed by PCR, 2.8% (as opposed to 25% of the expected genotype) were *jar*^{322}*/Df(3R)S87-5* mutants (Figure 6.3). Additionally, I performed cuticle preparation of the dead embryos from a different egg lay of the cross scheme and I found no dorsal defects. In summary Jar is not essential for embryogenesis.

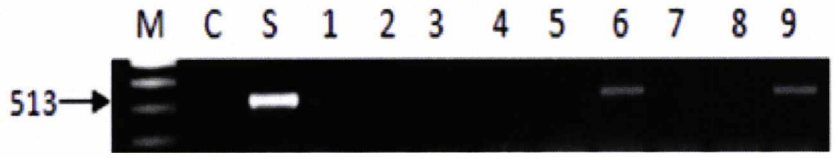

Figure 6.3. Gel electrophoresis genotypes *jar*^{322}*/Df(3R)S87-5* embryos. A representative gel photo showing 3 visible bands (lanes 1, 6 and 9) that belong to *jar*^{322}*/Df(3R)S87-5* mutant and 6 empty lanes that are *jar*^{322} homozygotes. Overall, 3% of *jar*^{322}*/Df(3R)S87-5* mutant embryos are embryonic lethal and contributed to 33% (n =21) of the total dead embryos. M-1 kb size markers starting from 250 bp at the bottom with an increment of 250 bp, C- control, S- standard fly, w^{1118}.

6.2.3. Live imaging of *jar* null reveals irregular LE during dorsal closure

In the previous chapter, cuticle preparation of the RNAi-mediated knock down Jar embryos showed no dorsal defects. However, defect was only apparent during the live analysis of the Jar knock down embryos. Thus, prompting live analysis of *jar*^{322}*/Df(3R)S87-5* dorsal stage embryos.

During the live analysis, total of 22 GFP-tagged embryos were monitored every 20mins under the Confocal laser microscope. It is worth noting that the GFP-expressing embryos were either *SGMCA/+* or *SGMCA;Df(3R)S87-5/jar*^{322} embryos. Of the examined embryos, only 5% (Figure 6.4) was seen to display obvious dorsal defect similar to that exhibited by enGal4;SGMCA/jar-RNAi-driven embryos (Figure 5.3).

At the onset of dorsal closure, the initial migration of epithelial sheets appears normal. However, towards the last step of dorsal closure abnormality is observed at the LE (Figure 6.4B). At the zippering process, the once taut front rows cells show signs of disorganised coordination between cells. Epithelial cells are not synchronised in steps with one another, cells are moving in concert but at different speed. Nearing the end of the zippering process the once slackened front row cells are less pronounced, the irregular LE cells appear corrected and form seamless zipping at the dorsal midline (Figure 6.4D). Because *jar*^{322}*/Df(3R)S87-5* embryos cannot be identified it is practically difficult to analyse the actin cytoskeleton with rhodamine phalloidin immunofluorescence stain.

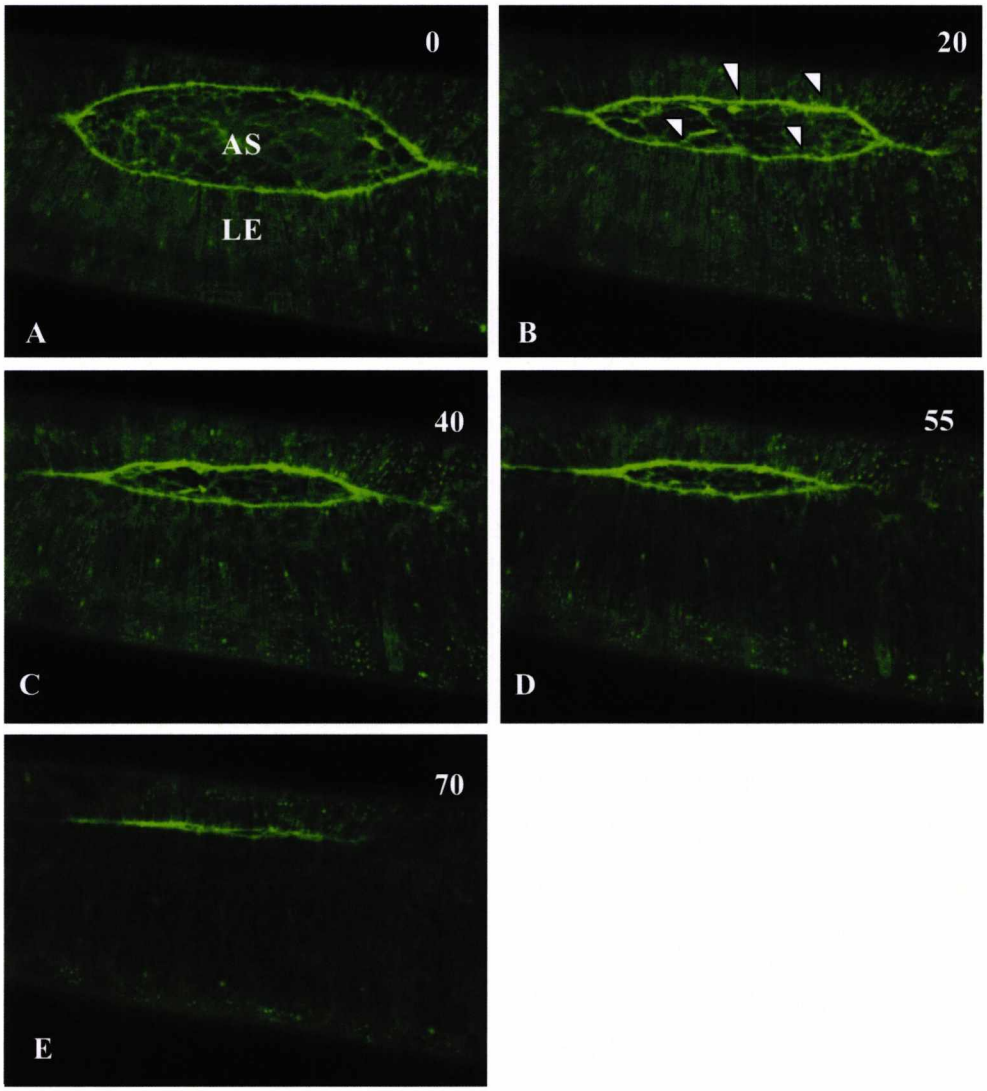

Figure 6.4. *jar*^{322}*/Df(3R)S87-5* embryo exhibits a mild dorsal defect. (A-E) Dorsoventral view of still images from live movie with times (mins) numbered at the top right of each image. At stage 14/15 of the embryo (A) LE cells moves in synchronised fashion but as time progresses (B) the LE is less coordinated, parts of the LE edges are pinched in (arrows in B). The disorganised LE cells are less pronounced after 55 mins (D) as they near the last phase of dorsal closure and in E, dorsal closure completes. AS = amnioserosa. LE = leading edge.

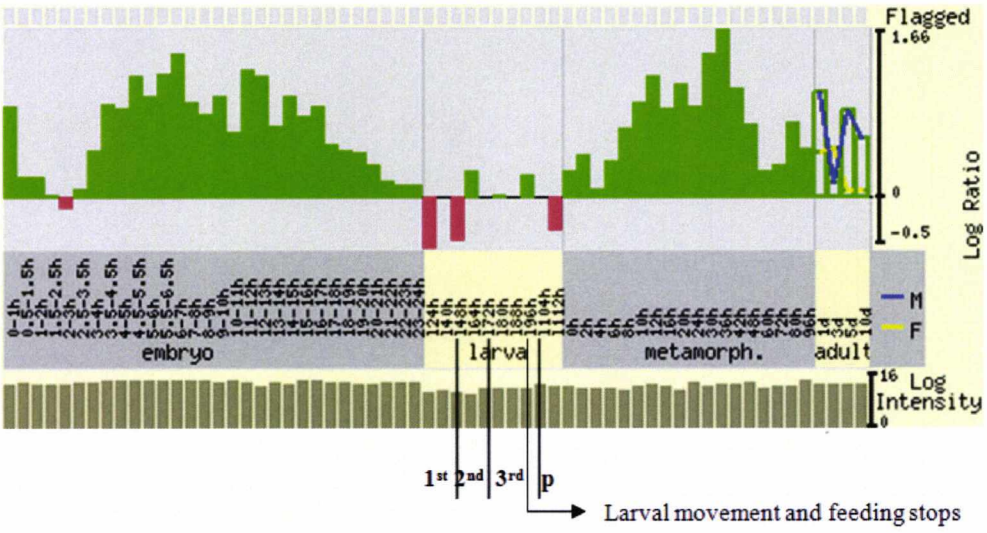

Figure 6.5. Microarray data from the Flybase website (flybase.org) detailing expression profile of Jar throughout the life span of *Drosophila*. During embryogenesis and metamorphosis Jar expression is at its highest but little is expressed during larval stage. Larval section is modified to illustrate the three stages of larvae. During 1st instar Jar is down regulated. Expression down-regulation continues prior to the start of the 2nd instar but then presents little peak of expression. The expression pattern is variable during the 3rd instar development beginning with a weak peak (not so obvious) shown prior to the start of development. The expression level peaks up again in the midst of development but falls right at the very end. Five days after egg laying (AEL) under standard conditions in non-crowding environment, larvae pupariates (P) Jar is downregulated at this point. Worth noting in the adult life males have higher levels of Jar compared to females.

Note: Up-regulated Down-regulated

6.2.4. *jar* maternal and zygotic nulls show increased larval death

At 25 hours, 170 GFP-negative first instar larvae of genotype either jar^{322}/jar^{322} or $jar^{322}/Df(3R)S87\text{-}5$ were selected at random from the plates containing the 1000 embryos (6.2.2) and were transferred to fresh apple plates. The plates were checked daily for dead individuals. Plates were regularly changed but also meant that larvae were also lost in the transferring process.

From the 170 larval populations 71 larvae were unaccounted for. The missing 71 larvae were either dead or lost; larvae may have imbedded themselves in the apple plate or escaped during the transferred process. Therefore, of the 99 larvae that were

accounted for, 36% (36 out of the 99 remaining larvae) died during larval stage but otherwise 63 larvae escapers went on to metamorphosis development stage. 6% larval lethality (6 of 99) were that of the *jar*^{322}*/Df(3R)S87-5* mutants whereas that of the *jar*^{322} homozygotes larvae was 5X the lethality at 30% (30 of 99). Of the 6% *jar*^{322}*/Df(3R)S87-5* larval death, I found that no larvae arrested during the first instar but 4% arrested during the second instar and 2% in the third instar. Identification of larval stages was performed according to technique described in section 2.4.3. The result here is somewhat in agreement with Jar protein expression profile (Figure 6.5) and more so, goes in accordance with the RNAi-jar knockdown larval lethality. Larval deaths were observed from second instar larvae (Figure 6.6).

Larval deaths of the selected non-fluorescent larvae were observed by day 2 from the initial larval selection. By day 3 more than half of the larval population had proceeded to third instar. However first and second instar larvae were still lurking but with very little movement especially that of the first instar. Even more so, first instar larvae were still seen after 5 days and few of the second instar larvae were still viable after two weeks from the initial selection. The slow developers during the second instar stage when dead and analysed on gel were genotyped as *jar*^{322}*/Df(3R)S87-5* mutant and it accounted for 2% of the total second instar lethality. Overall, lethality associated with *jar*^{322}*/Df(3R)S87-5* is largely seen during second and third instar stage but otherwise none in the first instar. In addition, the result of *jar*^{322}*/Df(3R)S87-5* first instar larvae null goes with the fact that I observed no Jar protein expression during the western blot analysis performed on w^{1118} in the previous result chapter (Figure 5.2). Possibly, Jar protein is expressed but very little.

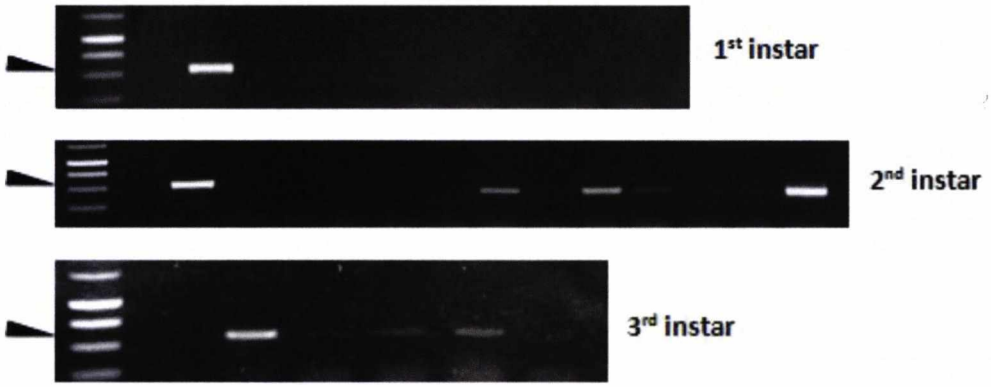

Figure 6.6. Larval lethality is in accordance with expression profile of Jar shown on the microarray data. In summary, total of 19 larvae arrested during the 1st instar but none as a result of *jar*^{322}*/Df(3R)S87-5* null mutant. Total of 13 larvae deaths arrested in 2nd instar and 31% of the deaths were *jar*^{322}*/Df(3R)S87-5* null mutant. In the third instar, there were a total of 4 larvae deaths and 50% of the deaths were *jar*^{322}*/Df(3R)S87-5* null mutant. The black arrows on the left side of each gel photos indicate the expected 513 bp. In each gel photos, the first lane is the size markers-1 kb DNA ladder, the second lane is the control and the third lane is the standardised sample, w^{1118}. Note that a band corresponds to *jar*^{322}*/Df(3R)S87-5* and no band correspond to *jar*^{322}*/jar*^{322}.

6.2.5. *jar* maternal and zygotic nulls show pupal lethality

From the cultured selected non-fluorescent larvae, 63 larvae (out of the 99 larvae) transitioned to metamorphosis stage. During the metamorphosis stage, 22% (14 out of the 63) were pupal lethal and the remainder of the 78% (49 out of the 63) pupae eclosed. At close examination of the dead pupae, few did not seem to complete metamorphosis and some appeared normal looking (pharate adults) in their pupal cases. Interestingly, I observed that *jar*^{322} homozygotes can survive until metamorphosis stage which is in contrary to report which stated that they survive until first to early second instar stage (Petritsch *et al.*, 2003). Of the 22% dead pupae, 8% were *jar*^{322}*/Df(3R)S87-5* null mutant and 14% were *jar*^{322} homozygotes (Figure 6.7).

Interestingly, in the surviving 78% *jar*^{322}*/Df(3R)S87-5* adults, 18% (9 of 49) exhibited wing defects: 4% (of the 18%) showed blisters in their wings whereas the remainder of the 14% bore a resemblance to Serrate wings and Held-out wing

phenotypes in one wing (Figure 6.8). However, there was no observable defects in the legs to report in contrary to reports of transgenic flies which showed malformed legs caused by the driven expression of antisense-jar (Deng *et al.*, 1999). The *jar*^{322}*/Df(3R)S87-5* null mutant adults also displayed a flight problem; they spent more time at the base of the vials. Furthermore, 14.3% (7 of 49) of the *jar*^{322}*/Df(3R)S87-5* adults adults were dead within two to six days after eclosing. The dead adults when analysed by PCR were all genotyped as *jar*^{322}*/Df(3R)S87-5* trans-heterozygotes (Figure 6.7). In addition, all the male and female escapers were mated to virgin females and males of w^{1118}, respectively. In accordance with previous report by Hicks *et al.,* (1999), males were sterile whereas the females were fertile (Morrison and Miller, 2008). Interestingly, I noted also that at least 25% of both sexes of zygotic null *jar*^{322}*/Df(3R)S87-5* were smaller in size in comparison to other genotypes from the same stock. However, this growth defect was not noted in zygotic and maternal null *jar*^{322}*/Df(3R)S87-5* trans-heterozygotes.

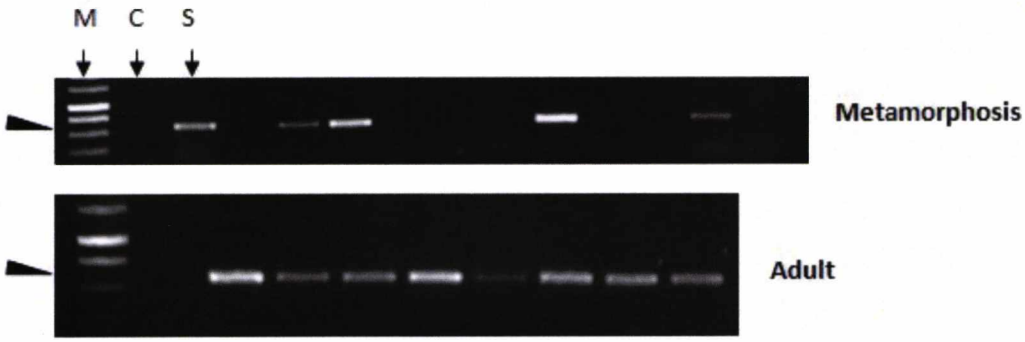

Figure 6.7. Jar is required for metamorphosis and adult development. There were 14 dead pupae in total and 35.7% (5 out of the 14) were *jar*^{322}*/Df(3R)S87-5* null mutant. Whereas, in the adults stage 14.3% of the surviving 49 adults were dead within 2-6 days of eclosing and moreover, were genotype to be *jar*^{322}*/Df(3R)S87-5* null mutant. M- 1 kb DNA ladder, C- control, S- w^{1118} used as standardised sample in both gel photos. Note that a band corresponds to *jar*^{322}*/Df(3R)S87-5* and no band correspond to *jar*^{322}*/jar*^{322}. The black arrows on the left side of each gel photos indicate the expected 513 bp

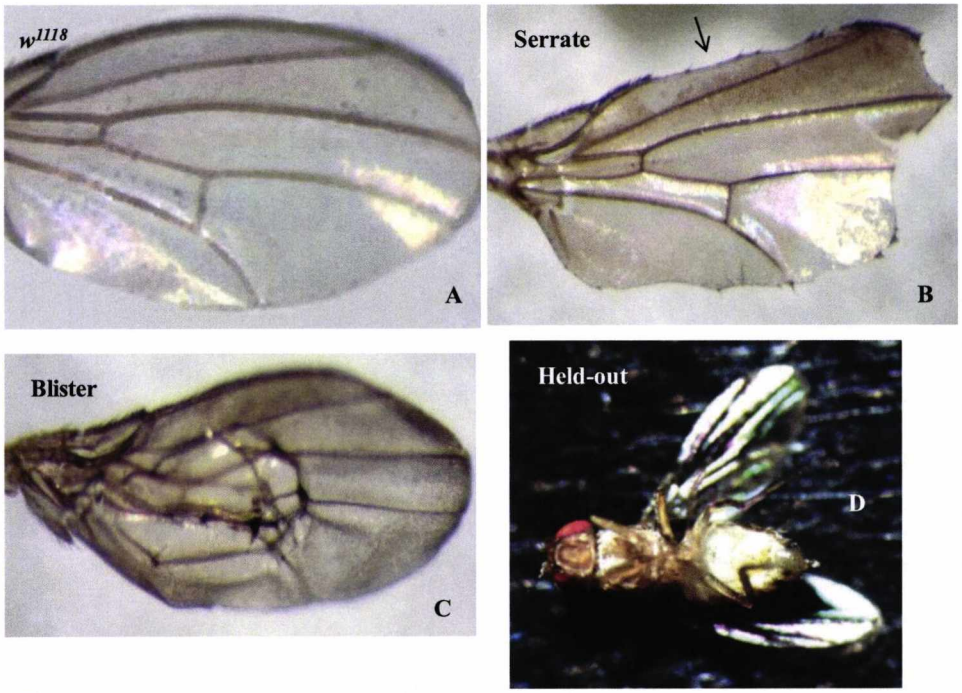

Figure 6.8. Wing defects of *jar*^{322}*/Df(3R)S87-5* null adults. (A) w^{1118} adult wing and (B-D) *jar*^{322}*/Df(3R)S87-5* null wings. (B) Wing defect bear resemblance to Serrate Dominate (gain-of-function mutations): most of the hairs on the anterior margin (arrow) are gone, notches showing around the wing margin. (C) Wing blister phenotype. (D) Female *jar*^{322}*/Df(3R)S87-5* showing held-out wing phenotype in one wing; the wing is held in a dichaete-like fashion.

Table 6.2. Summary of the percentage of lethality across the course of *jar*^{322}*/Df(3R)S87-5* development

Development stages	Number	Lethality (%)
Embryonic	1000	3 (as to 25%)
Larval	99	6
Pupal	63	8
Adult	49	14

6.2.6. The lethal effect of RNAi-mediated Jar knock down is Gal4 line dependent

The RNAi-mediated Jar knock down in *Drosophila* is lethal. More importantly, the phenotypes observed across the course of development brought about by Jar knock down overlap, almost, with that shown by $jar^{322}/Df(3R)S87\text{-}5$ nulls.

Of all the Gal4 drivers (2.1.7) that were available in the lab only two driver lines, *69B* and *en*-Gal4 produced observable phenotypes in the driven expression of *UAS-jar-RNAi*. The two Gal4 drivers produced exact lethality phenotypes across the course of *Drosophila* development and this indicate that the result is reproducible. Expressing *UAS-jar-RNAi* by either *69B* or *en*-Gal4 driver lines gave no significant embryonic lethality: 2% (n = 407) and 2.5% (n = 792), respectively. In addition, I found no observable dorsal defects by cuticle preparation.

Lethality of larvae expressing the Jar RNAi by either 69B or en-Gal4 drivers was observed from second instar larvae but death was prominent during the third and mostly in the metamorphosis stage. During the larval stage, I observed slow molting of second instar into third instar larvae. The third instar larvae were smaller in size as compared to w^{1118} larvae that were set up alongside. The Jar knock down larvae would wander around the side of bottle for days and in some instances, larvae appeared semiparalyzed and can survive in that state for several days without forming puparium and afterwards die. Most larvae survived to pupal stage, few did not complete metamorphosis and some appeared normal looking (pharate adults) but did not eclose.

To demonstrate that the lethal effect of expressing UAS-jar RNAi is Gal4 line dependent, I expressed UAS-jar RNAi enGal4-driven in a jar^{322} heterozygous background (2.4.4). From this cross, 50% lethality is expected (Table 6.3). 150 first/second instar larvae were randomly selected from the cross, 126 got to pupation stage and 77 adult eclosed with wild-type appearance. Therefore 73 (out of the 150) were larval/pupal lethal, 24 during larval stage and 49 during pupal stage. In summary, of the expected 50% lethality I got 47%. This clearly indicates that the lethal effect of RNAi-mediated Jar knock down is Gal4 line dependent.

Table 6.3. The percentage of lethality of Jar RNAi enGal4-driven in *jar*^{322} heterozygous background.

Genotype	Probability (%)	Viability
jar RNAi/enGal4; jar^{322}*/+**	25	lethal
+/enGal4;jar^{322}*/+*	25	viable
*jar-RNAi/enGal4;+/+**	25	lethal
+/enGal4;+/+	25	viable

*The total of the expected lethality in these genotypes is 50% but result gave 47% which is near enough.

6.2.7. Wing imaginal disc reveals a punctate stain of Jar protein

The complete loss of Jar showed varied wing phenotypes. Furthermore, the driven expression of *UAS-antisense-jar* produces adults with malformed legs and unexpanded wings (Deng *et al.*, 1999). However, expression profile of Jar has yet to be established in the wing imaginal disc.

Firstly, I had to establish the expression pattern of Jar in the wing imaginal disc. Wing discs were dissected from third instar larvae of w^{1118} and stained with Jar antibody (Figure 6.9). Next, I took a step further and co-stained the wing disc for actin and Jar protein. Additionally, I also observed expression pattern of Jar in leg, eye and antenna imaginal discs from third instar larvae (Figure 6.10). Interestingly, the expression pattern of Jar in the imaginal discs coincides with cellular localisation pattern of GFP-tagged myosin VI (Millo and Bownes, 2007). Furthermore, I noted that the Jar stain was of a punctate distribution as compared to control that had Jar antibody omitted. Noticeably, the wing discs dissected at different time during the third instar crawling and molting period gave different intensity of Jar stain. This is evident in the microarray data (Figure 6.5) that shows variation in Jar protein expression during the third instar period.

Because, the RNAi-mediated Jar knock down was successful in embryos, the same approach was tested in the wing disc. Moreover, 69B and en-Gal4 also drives expression in the wing disc. Examination of the wing disc expressing enGal4-driven UAS-Jar RNAi showed no difference between the posterior and the anterior compartment of the wing disc (Figure 6.9D).

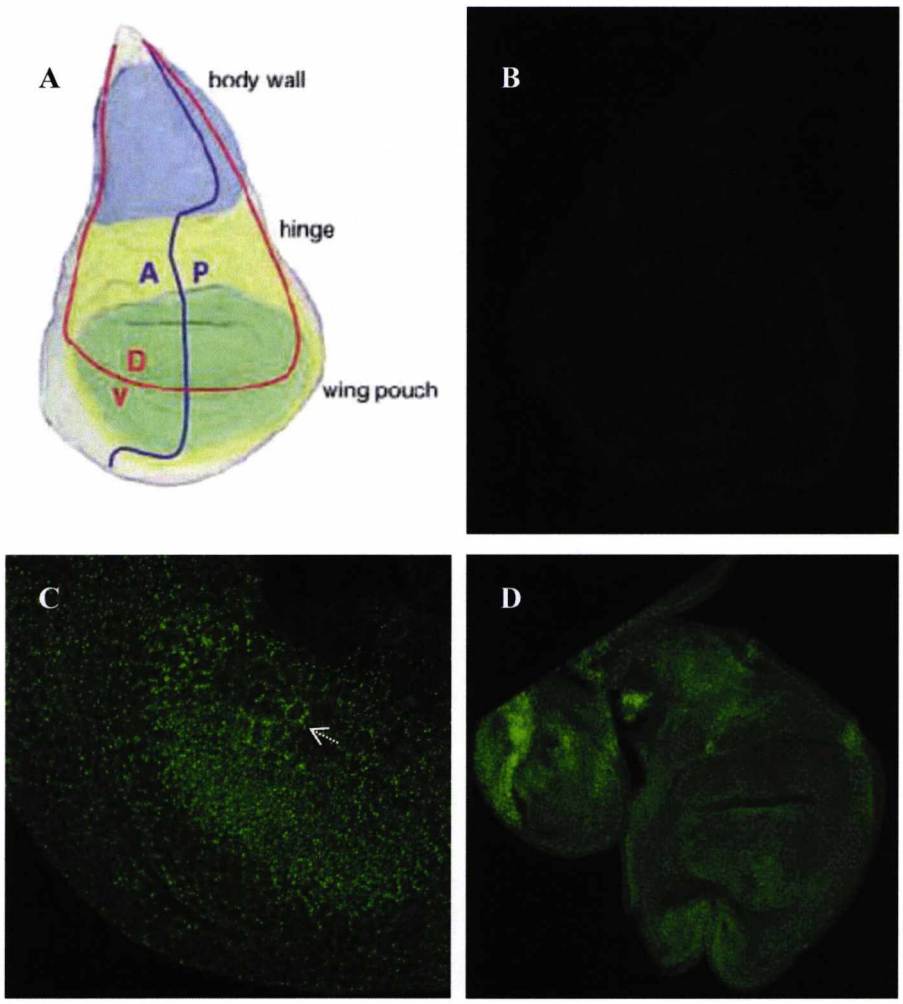

Figure 6.9. Establishing expression profile of Jar in wild-type and Jar knock down in wing disc. Wing disc illustrating the different compartments: Anterior (A), Posterior (P), Dorsal (D) and Ventral (V). The wing pouch gives rise to the adult wing blade. Image adapted from Butler *et al.*, (2003). (B) Control disc with Jar antibody omitted from the immuno-labelling procedure (C) Close examination of wildtype expression of Jar showing punctate distribution around the cell membrane example indicated by arrow in the prospective wing blade. (D*)* Jar expression is relatively low and there is no clear distinction between the A and the P compartments in the UAS-jar-RNAi enGal4-driven disc. However, there is an indication of reduced Jar protein expression in the P compartment compared to A in the attached haltere disc (A/P compartment boundary of a haltere disc is labelled in similar fashion as that of the wing disc). Noteworthy that expression pattern of Jar protein is not ascertain as yet in haltere disc and so cannot draw a conclusion on the haltere disc result.

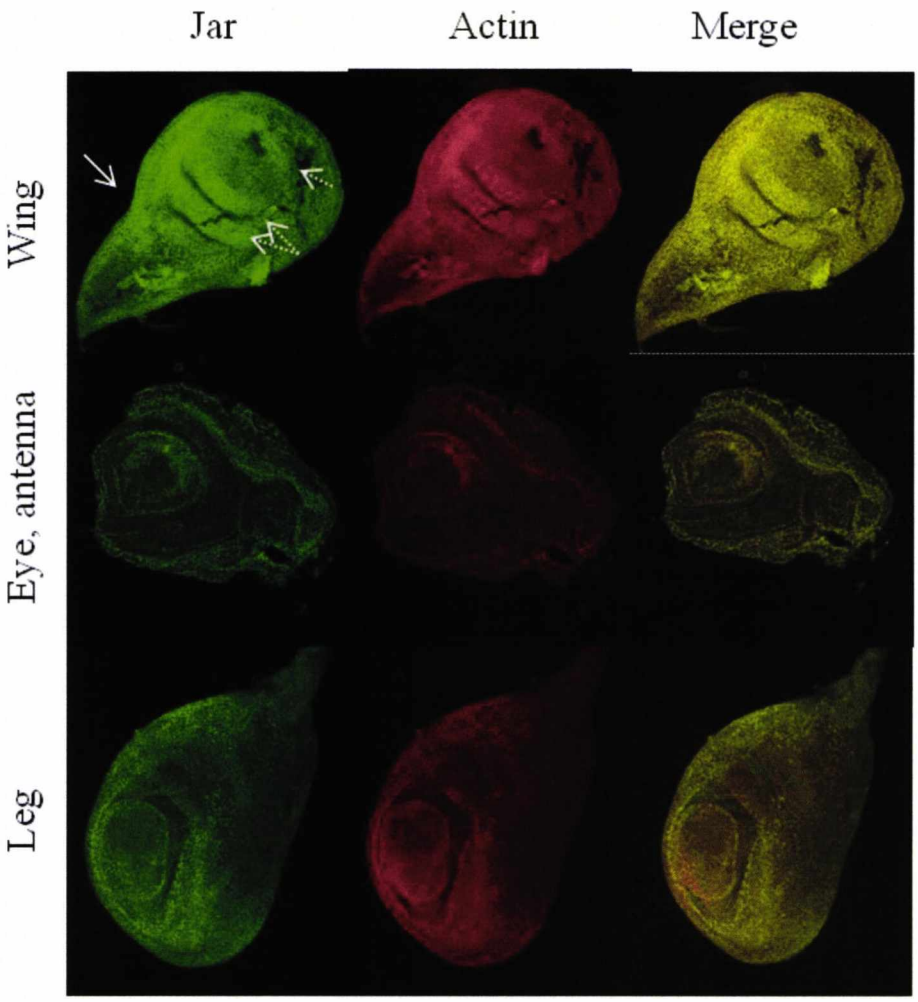

Figure 6.10. Wildtype expression of Jar protein in third instar imaginal discs co-stained for actin. The wing disc is from an early third instar larvae with arrows indicating strong Jar expression in the D/V compartment, hinge and along the body wall.

6.2.8. RNAi-mediated Ed knock down acts as a null in the wing disc

Echinoid (Ed) is a known cell adhesion molecule in the wing disc (Wei *et al.*, 2005). Ed is demonstrated to be of importance for support of adhesion in the wing disc when acting in cooperation with E-cadherin. Ed is reportedly expressed at the D/V boundary in the wing disc (Wei *et al.*, 2005). The loss-of-function Ed produces wing defects. I examined if by expressing RNAi-mediated Ed knock down I get similar wing defects as shown in published reports.

RNAi-mediated knock down approach was able to mimic the exact effect of loss-of-function of Ed in the wing disc. Expressing *UAS-ed-RNAi* by *69BGal4* driver produced viable adults with wing defects. The 69BGal4 driver activates UAS-responsive gene expression throughout the wing blade region of a third-instar wing

imaginal disc (Brand and Perrimon, 1993). The Ed RNAi transgene was able to mimic the exact effect of harbouring null allele ed^{1x5} clones in the wing imaginal disc clone: altered patterns of trichomes, extra vein material, loss of wing vein and ectopic sensillum campaniforme along vein L3 (Figure 6.11) (Wei *et al.*, 2005). The loss of Ed function also produced an enlarged posterior compartment. The overgrowth phenotype is specific to loss-of-function of Ed. A recent report showed that expressing different Ed transgenic lines obtained from the VDRC (including the same Ed RNAi used here) using a specific Gal4 driver for posterior compartment of a wing disc gave the same overgrowth phenotype (Yue *et al.*, 2012). Moreover, I noted that the wing blade was of an arc shape and not flat as in wild-type wing which was the only defect not before reported. Overall, the RNAi-mediated knock down of protein levels proves an alternative approach in which to investigate biological functions of genes.

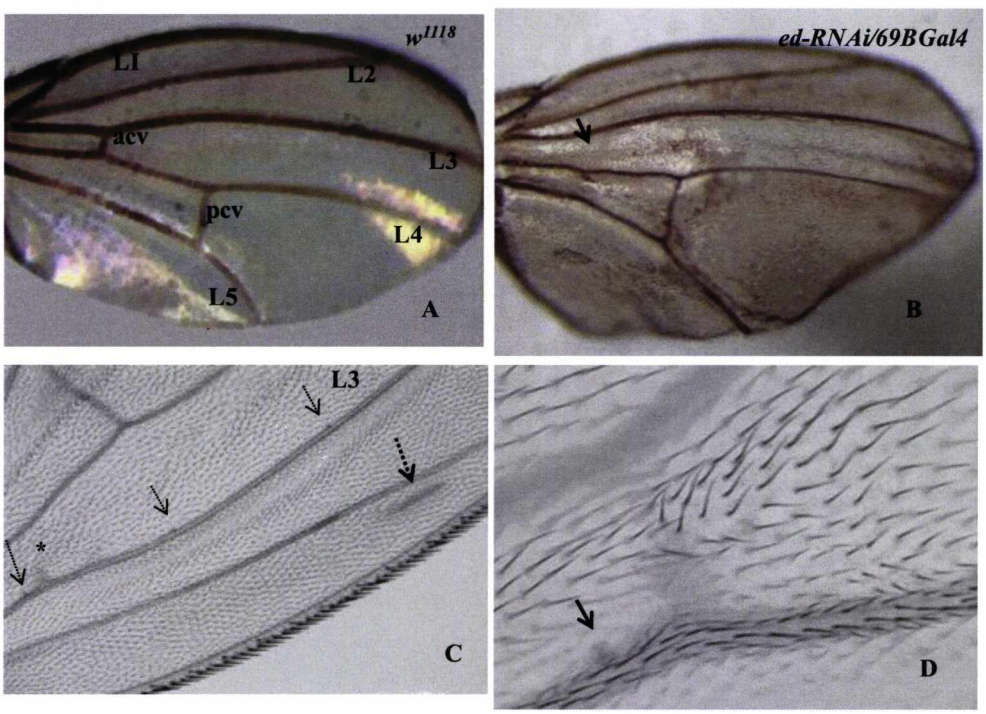

Figure 6.11. Ed RNAi 69BGal4-driven causes wing defects. (A) w^{1118} adult wing blade designated with longitudinal veins (L1-5), anterior crossveins (acv) and posterior crossveins (pcv). (B) Wing blade of the driven expression of *69BGal4/ed-RNAi* showing missing acv and enlarged posterior compartment of the wing disc. (C) Close examination of the posterior region showing extra vein material, three deposits of sensillum campaniforme along L3 (arrows). (D) Magnified portion of asterisk in C showing the altered patterns of trichomes and ectopic sensillum campaniforme (arrow).

6.3. Discussion

Here, I characterised the *jar*^{322}*/Df(3R)S87-5* null mutant and concluded that Jar is important for *Drosophila* development. I was able to produce results consistent with previous published work done on the null *jar*^{322}*/Df(3R)S87-5* mutant (Morrison and Miller, 2008). However, I further expanded on the project and pinpointed arrest points during the course of *Drosophila* development. I noted defects not previously reported for loss-of-function of Jar. Importantly, the defects I report here overlaps, with the effect of expressing RNAi-mediated Jar knock down.

Complete loss-of-function of Jar in *jar*^{322}*/Df(3R)S87-5* null mutant shows low embryonic lethality with a mild dorsal defect, with no deaths during the first instar but few in the second and third instar and lethality largely seen during metamorphosis and adult stages. In contrast, *jar*^{R39} and *jar*^{R235} mutants die during embryogenesis and in few instances exhibit dorsal defect but lethality is largely seen in the first instar larval stage (Millo *et al.*, 2004). *jar*^{R39} and *jar*^{R235} mutants have undetectable Jar protein expression in late embryogenesis confirmed through antibody staining and western blot analysis but mRNA transcripts are reported to persist until the larval stage though at a lower level in comparison to wild-type. The phenotypic defects of *jar*^{R39} and *jar*^{R235} mutants are identical to loss-of-functions of genes located upstream of Jar (detailed in 1.5.2.4).

In contrast, mutant *jar*^{322}is reported to survive embryogenesis but die as first or second instar larvae. The phenotypic defects associated with *jar*^{322}*/Df(3R)S87-5* can be rescued by expression of a myosin VI cDNA transgene driven by hsp8 promoter but fails to rescue *jar*^{322} homozygotes and *jar*^{322}*/Df(3R)S87-4* (a deficiency that uncovers both Jar and the adjacent CG5706 gene) (Morrison and Miller, 2008). Therefore, the lethality reported here can be attributed to loss-of-function of Jar. *jar*^{322}*/Df(3R)S87-5* null showed lethality of 10% during metamorphosis, 50% between embryonic and larval stages but 40% null mutant *jar* are viable with no defects (Morrison and Miller, 2008). Using a PCR strategy I pinpoint lethality stages of *jar*^{322}*/Df(3R)S87-5* null.

Here, the reports show that loss-of-function of Jar attributed only 3% embryonic lethality compared to the expected rate of 25% and no dorsal phenotype. Although, there was the occasional sighting of the irregular LE which was only observed

during the live analysis of the *jar*^{322}*/Df(3R)S87-5* embryo. The irregular LE cells are very apparent in the knock down of Jar protein levels in embryos (Chapter 5). Overall, the results confirm that the complete lack of Jar protein is not essential but argues that to a lesser extent Jar is required for processes in embryogenesis probably, in readiness for the next developmental stage.

Despite the subtle role of Jar during embryogenesis, loss-of-function of Jar has a profound effect in post-embryonic developmental stages. The *jar*^{322}*/Df(3R)S87-5* larvae were sluggish in mobility and few were slow developers in the second instar. These phenotypes mirror that exhibited in RNAi-mediated Jar knock down larvae, as they too display locomotor defect (prominent in third instar larval stage). These abnormalities raise the possibility of Jar implication in *Drosophila* neuromuscular junction (NMJ). Notably, Jar is reportedly present in the CNS of *Drosophila* and peripheral nerve systems in embryos (Millo and Bownes, 2007; Lantz and Miller, 1998). Interestingly, a recent report demonstrated that Jar is important for proper synaptic function and morphology in *Drosophila* NMJ development (Kisiel *et al.*, 2011). Neuronal study done on the *jar*^{322}*/Df(3R)S87-5* null third instar larvae showed reduced locomotor activity identical to the report here. Furthermore, dGIPC, a known binding partner of Jar is demonstrated to function in adult *Drosophila* CNS (Kim *et al.*, 2010). Loss-of-function of dGIPC showed locomotor defect and reduced life span in adults.

More interestingly, the 8% lethality I report here is closely similar to the 10% lethality documented during metamorphosis by Morrison and Miller (2008). The remainder 2% that was not obtained could be attributed to *jar*^{322} homozygotes as I found that they can survive until metamorphosis stage. Furthermore, I report few defects in the surviving *jar*^{322}*/Df(3R)S87-5* adults which is contrary to previous report (Morrison and Miller, 2008). The report found no defects in the 40% of the surviving *jar*^{322}*/Df(3R)S87-5* null adults. Here, I report that the *jar*^{322}*/Df(3R)S87-5* null adult escapers, showed locomotor defect, wing defects and reduced life span. Coincidentally, these abnormalities were also protrayed in transgenic antisense-jar driven flies but the wing defect was an unexpanded wing phenotype (Deng *et al.*, 1999). The unexpanded wing phenotype may well represent loss of a subset of Jar function which would not be surprising as Jar is widespread and is multifunctional.

Jar is important for wing morphogenesis (Deng *et al.*, 1999 and this study). GFP-tagged myosin VI is expressed in larval wing disc (expression apparant in third instar stage), in cells of epithelial sheet and at points of cell contacts of the epithelial during wing disc eversion in metarmorphosis (Millo and Bownes, 2007). Few of the jar^{322}/*Df(3R)S87-5* null adults showed blisters in their wings. Blisters are as a result of failure of bonding between dorsal and ventral wing epithelial cell sheets during wing maturation, as the fly pupariates (Kiger Jr *et al.*, 2007). The wing blister phenotype is also caused by lack of integrin activity (Domínguez-Giménez *et al.*, 2007). Integrin are extracellular matrix (ECM) that establishes cell contacts between dorsal and ventral epithelia (Kiger *et al.*, 2007). Mutant alleles of the *Drosophila* PS integrin subunit genes have been shown to result in wing blisters, held-out wing phenotype and flight impairment (Brabant *et al.*, 1996; Brower *et al.*, 1995; Zusman *et al.*, 1993). All these phenotypes are identical to that displaying in the surviving jar^{322}/*Df(3R)S87-5* null adults.

Interestingly, myosins have been implicated in *Drosophila* wing morphogenesis such as the nonmuscle myosin II (Franke *et al.*, 2010; Major and Irvine, 2006) and the unconventional myosin VIIA encoded by *crinkled* (*ck*) gene in *Drosophila* (Kiehart *et al.*, 2004). However *zipper* (*zip*) which encodes nonmuscle myosin II and *ck*/MyoVIIA are thought to act antagonistically in relative to processes during wing morphogenesis. *zip*/MyoII is preferentially expressed at the dorsal-ventral compartment boundary in the wing imaginal discs (Major and Irvine, 2006). The expression of truncated alleles of *zip*/MyoII result in wing blisters but is more prevalent in the overexpression of *ck*/MyoVIIA (Franke *et al.*, 2010). More interestingly, myosin II accumulation at the dorsal-ventral boundary is regulated downstream of Notch signalling (Major and Irvine, 2006).

Additionally, 14% of the surviving null adults (total of 49 adults) showed Serrated wing defects that bear resemblance to dominant gain-of function mutation of Ser^{D} (Thomas *et al.*, 1991, 1995). The *Serrate* (*Ser*) gene encodes an essential ligand-containing EGF-like repeats for Notch signalling which is demonstrated to be of importance for *Drosophila* development including wing. *Ser* is expressed at the dorsal compartment of the wing imaginal disc but induces its functions through Notch receptor that resides at the dorsal-ventral interface of the wing imaginal disc. A selector gene *apterous* is reportedly responsible for the establishment of dorsal

Notch and PS1 activation (O'Keefe and Thomas, 2001). The result here clearly indicates that Jar is expressed in dorsoventral region of the wing which coincides with cellular localisation report of Jar in the wing disc and in our Jar protein stained third instar wing disc (Millo and Bownes, 2007). The wing defects of the *jar*^{322}*/Df(3R)S87-5* null adults reflect impaired signalling at the dorsoventral region of the wing. Moreover, the punctate stain in the wing disc presented here is suggestive of Jar interaction with membranous and vesicular structures. Interestingly, a transposon-based screen in the developing *Drosophila* eye to identify genes involved in Notch signalling identified Jar as a modifier of Notch signalling (Shalaby *et al.*, 2009).

The report here suggests that the clonal loss of Jar via RNAi-mediated knock down has more profound lethality effect in *Drosophila* development in comparison to global loss in null mutant *jar*^{322}*/Df(3R)S87-5* which has a lesser effect. Expressing UAS-Jar RNAi with ubiquitous driver, sghGal4 produce no phenotype. Thus, prompted the idea that phenotypes are reported in tissues which express high level of Jar protein levels (Deng *et al.*, 1999). Only few of the many Gal4 drivers that were employed to express antisense-Jar generated phenotypes (Deng *et al.*, 1999). Possibly, Jar protein was knocked-down in tissues that are of necessity for *Drosophila* survival. More interestingly, expressing UAS-ed-RNAi by 69BGal4 gave the exact wing phenotype previously reported for null allele *ed*^{1x5} clones (Wei *et al.*, 2005). Thus, indicates that the phenotypes of the RNAi-mediated Jar knock down are a representative of function of Jar.

Here, I have characterised the *jar*^{322}*/Df(3R)S87-5* null mutant and pinpointed arrest points throughout the life cycle of *Drosophila.* The phenotypes in the *jar*^{322}*/Df(3R)S87-5* null are mirrored by the effect of expressing RNAi-mediated Jar knock down. The array of phenotypes I report here reflects the expected diverse roles of Jar and of new roles needing further investigation.

Chapter 7. Discussion

7.1. Summary

In brief, this project started off investigating a working model that Jar function during dorsal closure is regulated by Pak. The theory was based on previous work demonstrating that phosphorylation at a Pak phosphorylation site in the myosin VI head domain has potential to regulate protein function in similar manner as to that which occurs in myosin I. Moreover, striped embryonic expression of either a dominant negative Jar or a dominant negative Pak construct causes if not exact, highly overlapping dorsal closure phenotypes. However, since initiating this study a paper (Morrison and Miller, 2008) was published demonstrating that animals lacking both maternal and zygotic Jar protein can survive to adulthood, albeit at 40% of the expected frequency. Thus, while Jar is required in *Drosophila*, it is not essential for development. This publication clearly has major implications for our working model for Jar regulation during dorsal closure. However, there are number of questions left to address, namely (1) the lethality associated with embryonic expression of the dominant negative *ΔATP-jar* construct (Millo *et al.*, 2004) (2) why a large proportion of Jar maternal and zygotic null larvae and pupae die, and why many adults show a much reduced lifespan (Morrison and Miller, 2008 and this study) and (3) the post-embryonic lethality associated with expression of *UAS-jar-RNAi* (this study).

1. Hypothesis

The aim of this study was to provide in vivo evidence supporting a functional interaction between *jar* and *pak*. The initial experimental approach taken was to test for genetic interactions.

In summary, in two separate models and stages of *Drosophila*: dorsal closure and wing development, my observations indicate clearly that there is no genetic interaction between *jar* and *pak*.

2. To test the position of Jar in the dorsal closure hierarchy

Although no clear evidence was found to support the initial hypothesis, the importance of Jar in dorsal closure remains an unresolved issue. Jar is expressed in the dorsal epidermis and amnioserosa during dorsal closure (Millo and Bownes, 2007; Millo *et al.*, 2004). My data supports a non-essential role for Jar in dorsal closure and I question, if Jar is even in the dorsal closure hierarchy. Therefore, to investigate Jar's potential requirement in dorsal closure, the effect on Jar expression level was assessed in mutations, dominant negative and activated forms of the major signalling pathways implicated for epithelial morphogenesis.

Surprisingly, Jar is directly regulated by JNK signalling pathway and is down-regulated by the RhoGTPase pathway. Additionally, embryonic expression of the dominant negative Pak has no effect on the expression pattern of Jar. This supports the findings of the initial hypothesis. Jar is clearly distributed in punctate manner in dominant negative Pak enGal4-driven embryos at what appears to be cell-cell junctions.

3. Alternative approach to test the function of Jar in dorsal closure

Genetic and dominant-negative Jar approaches in the literature have produced contradictory outcomes in relation to Jar function during dorsal closure. To investigate the functional significance of Jar in dorsal closure, an alternative approach deemed necessary. Therefore, I employed the use of tissue-specific RNAi-mediated knock down using the GAL4/UAS expression system.

The RNAi-mediated knock down of Jar experiment resulted in an irregular LE but it did not prevent the completion of dorsal closure. These phenotypes are not because of distortion of the actin cytoskeleton. However, the co-expression of Jar RNAi and tubulin did cause disorientation of microtubule towards the last step, zippering phase of dorsal closure and embryos arrested in development. Furthermore, cell adhesion mediated by expression of DE-cadherin is not affected in Jar RNAi driven embryos. Moreover, I observed consistent phenotypes with different Gal4 drivers. Thus, with some degree of confidence I report that phenotypes generated by the RNAi-mediated

knock down of Jar is a mirror reflection of function of Jar in *Drosophila* development. I conclude that Jar is required but not essential for dorsal closure.

In the case of Jar-RNAi expression, it could be argued that off-target effects might have incurred, least likely, because the lethal effect of expressing Jar-RNAi overlaps highly with lethality phenotypes of Jar maternal and zygotic nulls.

4. Complete characterisation of *jar*^{322} mutant

Morrison and Miller, (2008) characterised the *jar*^{322} mutant allele and conclusively demonstrated that the complete loss-of-function of Jar is not lethal because 40% of maternal and zygotic mutants survived.

The effect of the RNAi-mediated Jar knock down is larval and pupal lethal. The characterisation of the mutant *jar*^{322} provides another approach to determine function of Jar in post-embryonic stages of *Drosophila*. Using PCR-based approach, I confirm and expand on the previous work. I pinpointed development arrest points of the *jar*^{322}*/Df(3R)S87-5* null mutant. Complete loss of Jar leads to larval death, larvae that were slow developers and with locomotor defect, pupal death and adults with wing defects, flight impairment and short lifespan.

7.2. General Discussion

While I provide no evidence for the initial hypothesis, the collective data in this project implicates Jar involvement in major signalling pathways that are of importance for correct development and are also of major significance in the pathology field. The primary results gained from the study have allowed one to have an overview of potential multifunction of Jar in the life course of *Drosophila* development.

7.2.1 Pak kinase regulation of Jar

As earlier stated, the fundamental basis of my work was to provide in vivo evidence that Jar functionality is dependent on Pak kinase phosphorylation. In vitro assay provided preliminary evidence to indicate that Group I Paks have the potential to phosphorylate and thus, regulate function of myosin VI (Yoshimura *et al.*, 2001; Buss *et al.*, 1998).

Pak homologues are known to phosphorylate the motor domain of myosin 1 in the same homologous site as myosin VI and thus, regulate acto-myosin ATPase and functional activities of myosin I (Attanapola *et al.*, 2009; Fujita-Becker *et al.*, 2005). Furthermore, Pak can directly/indirectly regulate myosin II by direct phosphorylation of myosin II regulatory light chain or direct phosphorylation and inhibition of myosin light chain kinase (reviewed in Bokoch, 2003). Nonetheless, there seems to be contradictory reports in regard to myosin II phosphorylation activity by Pak.

Here, I provide genetic evidence that there is no interaction between *jar* and *pak*. *jar* and *pak* mutants can survive to post-embryonic stage as has been demonstrated in previous work (Morrison and Miller, 2008, Conder *et al.*, 2004; Petritsch *et al.*, 2003; Hing *et al.*, 1999). However, for the purpose of testing the hypothesis, *jarpak* double mutants were generated. The result gave clear indication of no interaction between the two proteins. Jar is expressed as normal in dominant negative dPakAID enGal4-driven embryos. That said, I cannot the rule out the possibility that the phosphorylation status of Jar might be affected. Possibly, Pak3 or Pak-like kinases could functional phosphorylate Jar in *dpak* mutants and in expressing dominant negative *dpak-AID* in embryos, respectively (Bahri *et al.*, 2010; Conder *et al.*, 2004; Morrison *et al.*, 2000).

Furthermore, the wing was used as an alternative approach to investigate the interaction between *jar* and *pak*. Functions of Jar and Pak are required for wing morphogenesis (Deng *et al.*, 1999; Hing *et al.*, 1999 and this study). The loss-of-function of Pak through mutations or RNAi-mediated knock down causes crumpled wing phenotype. Expressing Pak-RNAi in jar^{322} mutant heterozygous background again gave clear indication of no interaction between *jar* and *pak*.

Overall, I demonstrate that in two different models and development stages there is no evidence of interaction between *jar* and *pak*. Possibly, the mechanistic basis that regulates Jar activation is, dependent on the cellular context noted by the differential expression of Jar isoforms (Lantz and Miller, 1998; Kellerman and Miller, 1992). Seemingly, there could be interplay amongst the several potential regulatory mechanisms outlined for vertebrate myosin VI (Buss and Kendrick-Jones, 2008).

7.2.2. Embryonic function of Jar

Expressing RNAi-mediated Jar knock down in embryos shows irregular LE during the confocal live imaging of dorsal closure. The exact irregular LE was also seen during the live analysis of the $jar^{322}/Df(3R)S87\text{-}5$ null mutant embryo but in few percentages of null embryos. Moreover, RNAi-mediated Jar knock down or the complete loss of Jar in $jar^{322}/Df(3R)S87\text{-}5$ null embryo is not embryonic lethal.

Jar could be involved during the zippering phase in dorsal closure and in cooperation with microtubules. Dorsal closure started as normal in Jar knock down embryos and irregularity of the LE was seen towards the last phase of dorsal closure. Consistent with this, microtubule is essential for the zippering phase in dorsal closure (Jankovics and Brunner, 2006). Alternatively, the irregular LE could also be due to unstable anchoring of Ed between adjacent LE cells. In support of this, irregular migration of the LE cells is reported in null *ed* embryos (Lin *et al.*, 2007). Jar is showed to genetically interact with Ed for cell morphology during dorsal closure (Lin *et al.*, 2007). Ed is shown to co-operate with DE-cadherin to mediate cell adhesion (Wei *et al.*, 2005; Lin *et al.*, 2007). Possibly, Jar interacts with Ed that in turn associates with DE-cadherin in strengthening the cell contacts. Thus, lack of function of Jar weakens the cell contacts. Jar could possibly, be required for the recycling of DE-cadherin. Embryonic expression of RNAi-mediated Jar knock down had no effect on DE-cadherin protein expression which is in contrast to expressing dominant negative ΔATP-jar construct (Millo *et al.*, 2004). Expressing dominant negative ΔATP-jar caused intracellular puncta localisation of DE-cadherin which is suggestive of a block in endocytosis. In support of the idea, in mammalian cell culture system the tail domain of myosin VI shown to be essential for targeting

myosin VI to clathrin-coated pits/vesicles when overexpressed acted as dominant negative and reduced internalisation of clathrin-coated vesicles (Aschenbrenner *et al.*, 2003; Buss *et al.*, 2001b).

Chapter 1 reviewed myosin VI involvement in clathrin-dependent pathway. The functional loss of myosin VI leads to defective clathrin-mediated endocytosis and consequent reduction in the internalisation of clathrin-coated vesicles. However in an unusual circumstance an alternative pathway is upregulated (reviewed in, Hansen and Nichols, 2009). A study found reduced uptake of clathrin-coated vesicles in several of myosin VI knock out cell lines (Puri, 2009). In the same cell lines, plasma-membrane receptors such as transferrin and epidermal growth factor receptors, clathrin adaptor protein, AP-2 were found to relocalise to caveolin. Therefore, I reason a similar scenario that in the expression of Jar-RNAi, an alternative endocytosis route could be upregulated. Redistribution of E-cadherin through endocytosis and exocytosis is required for E-cadherin function to maintain stable cohesion between epithelial cells in *Drosophila* (reviewed in, Wirtz-Peitz and Zallen, 2009). Dynamic turnover of DE-cadherin is through clathrin-mediated endocytosis (Levayer *et al.*, 2011). In vertebrate cells, E-cadherin may be endocytosed by caveolae-dependent pathway when clathrin-dependent pathway is down-regulated (Akhtar and Hotchin, 2001).

There is no direct interaction between Jar and DE-cadherin as yet to support the theory that Jar is involved in DE-cadherin recycling. In *Drosophila* eye, Ed is shown to regulate Flamingo endocytosis and most probably, all of the receptors/CAMs at the adherens junctions because of its interaction with AP-2 (Ho *et al.*, 2010). However, it is unlikely in the case of DE-cadherin as Ed is not required for localisation of E-cadherin. E-cadherin is reportedly shown to control Ed recruitment to adherens junctions in *Drosophila* wing disc (Wei *et al.*, 2005). Nonetheless, dorsal phenotypes in null *ed* embryos overlap, highly with the effect of functional loss of dorsal DE-cadherin (Gorfinkiel and Arias, 2007). Furthermore, the phenotypes resulted from expressing dominant negative ΔATP-jar in embryos overlap with the effect of functional loss of DE-cadherin protein (Gorfinkiel and Arias, 2007). Thus, indicates that Jar is part of the larger adhesion complexes.

Possibly, Jar is required for Ed to stably cooperate with E-cadherin to strengthen and stabilise the cell-cell junctions. The loss of E-cadherin is a major factor in promoting cancer metastases (reviewed in, Makrilia *et al.*, 2009; Wijnhoven *et al.*, 2000). E-cadherin is required for maintenance of epithelial polarity in *Drosophila* (Mirkovic and Mlodzik, 2006). E-cadherin provides a molecular link between loss of cell polarity and tumour malignancy (Igaki *et al.*, 2006). The loss of polarity is shown to prompt activation of the JNK signalling pathway (Igaki *et al.*, 2006). Furthermore, the loss of E-cadherin prompts activation of proapoptotic role of JNK signalling in *Drosophila* (Igaki *et al.*, 2006).

Notably, I report that the dorsal expression of Jar is upregulated in direct response to constitutive active JNK signalling. In addition, Jar localises within apoptotic cells generated in expressing dominant negative Rho. Jar homologue is found over-expressed in cancer cells and is shown to function in a p53-dependent prosurvival pathway (Dunn *et al.*, 2006; Jung *et al.*, 2006; Yoshida *et al.*, 2004). More importantly, *Drosophila* p53 activation requires the activity of the JNK pathway (Martin *et al.*, 2009). Moreover, the expression of the dominant negative $RhoA^{N19}$ construct activates the JNK transcriptional activation pathway (Bloor and Kiehart, 2002). JNK signalling is of importance for cell growth and cell survival. Conversely, JNK can promote tumour growth and invasion and apoptosis in *Drosophila* as well cancer progression in vertebrates (reviewed in, Igaki, 2009). In summary, I postulate that somehow, Jar promotes E-cadherin function by mediating stable cohesion between cells.

7.2.3. Neuronal/larval development

Null mutant $jar^{322}/Df(3R)S87\text{-}5$ larvae were lethal, slow developers and with locomotor defects. RNAi-mediated Jar knock down larvae exhibited the exact phenotype seen for null $jar^{322}/Df(3R)S87\text{-}5$ larvae. These abormalities are suggestive of defect in neuronal systems. Jar is shown present in the CNS of *Drosophila* and peripheral nerve systems (Millo and Bownes, 2007; Lantz and Miller, 1998). In the axons of the *Drosophila* CNS embryos, Jar is seen in puncta distribution pattern and in colocalisation with *Drosophila* CLIP-190 (D- CLIP-190), a microtubule binding

protein involved in the attachment of vesicles to microtubules (Lantz and Miller, 1998). Thus, suggestive of vesicle trafficking.

A study on the *jar*^{322}*/Df(3R)S87-5* null larvae found that they showed reduced locomotor activity (Kisiel *et al.*, 2011). The null third instar larval NMJ showed a reduction in NMJ length, reduced synaptic bouton number and disruption in synaptic vesicle localisation. Consistent with this, vertebrate myosin VI is shown to be present in the nervous system of chicken, mouse and rat and loss-of-function of myosin VI causes neuronal defects (Osterweil *et al.*, 2005; Wu *et al.*, 2002; Suter *et al.*, 2000). For instance, in a brain of a mouse myosin VI localises to synapses and is predominantly at postsynaptic density (PSD) where it exist in a complex with α-amino-3-hydroxy-5-methyl-4-isoxazole propionic acid (AMPA)–type glutamate receptor (AMPAR), SAP97 (synapse-associated protein important for AMPAR trafficking protein) and AP-2 (clathrin adaptor protein) (Nash *et al.*, 2010; Osterweil *et al.*, 2005). SAP97 interacts directly with myosin VI via its first PDZ domain. At the PSD wherein continual recycling of AMPAR occurs via clathrin-mediated endocytosis, myosin VI is proposed to participate in the trafficking of SAP97-containing AMPAR. In the inhibition of function of myosin VI, the hippocampus exhibit reduced number of synapses, surface expression of AMPARs at synapses, short dendritic spines and consequent astrogliosis (Nash *et al.*, 2010; Osterweil *et al.*, 2005).

Notably, myosin V mutants are reported to have increase late larval lethality and development delay during larval phase and phenotypes which are exact for our report of *jar*^{322}*/Df(3R)S87-5* null larvae (Mermall *et al.*, 2005). However, there were no defects in neuronal cell fate determinant reported for myosin V mutants although expression profile and cellular localisation showed high expression levels of myosin V in *Drosophila* CNS (Mermall *et al.*, 2005). Myosin V and myosin VI in vertebrates are postulated to have related but distinct roles in the neuronal system (Suter *et al.*, 1999). Myosin V and myosin VI are expressed in similar puncta pattern, partially colocalise but have distinct subcellular pattern in both chicken brain and cultured dorsal root ganglion neurons (Suter *et al.*, 2000). Myosin V is shown to function in vesicle trafficking in both neuronal and non-neuronal cells as has been demonstrated for myosin VI (Correia *et al.*, 2008; Desnos *et al.*, 2007). A proteomics-based approach in *Drosophila* embryonic cells showed that myosin VI

and myosin V localise to most of the same subcellular compartments and possibly share the same cargoes between them (Finan *et al.*, 2011). Furthermore, myosin V and myosin VI partially overlap during spermatid individualisation (Mermall *et al.*, 2005). Myosin V mutant is male sterile as has been demonstrated for jar^{1} mutants (Mermall *et al.*, 2005; Hicks *et al.*, 1999).

Myosin II is important for trafficking of synaptic vesicle within *Drosophila* larval neuromuscular boutons (Seabrooke *et al.*, 2010). Myosin II is predominantly in the presynaptic terminal and at a lower extent in the PSD where it colocalises with Disc large (Dlg), *Drosophila* homologue of synapse-associated protein SAP97. The effect of myosin II on vesicle traffic is dose-dependent; the over-expression or the reduction of myosin II impairs the mobility of synaptic vesicles. However, the precise role of myosin II in *Drosophila* NMJ is yet to be explored. Notably, general myosin inhibitor ML-9 also resulted in reduced vesicle mobility in a dose-dependent manner prompting the possibilities that other myosins are involve in *Drosophila* NMJ (Seabrooke *et al.*, 2010). Possibly, myosin V could partially compensate for loss of Jar function.

The loss-of-function of dGIPC, a known binding partner of Jar resulted in locomotor defect and reduced life span (Finan *et al.*, 2011; Kim *et al.*, 2010). The locomotor defect was associated with programmed cell death (Kim *et al.*, 2010). Therefore, brings back the idea of Jar as a homeostatic apoptotic protein.

7.2.4. Wing morphogenesis/metarmorphosis

Null $jar^{322}/Df(3R)S87\text{-}5$ and RNAi-mediated Jar knock down have increase pupal lethality with the pupae displaying different development abnormalities. In addition null $jar^{322}/Df(3R)S87\text{-}5$ escapers have varied wing defects. Here, I discuss in respect to the wing defects because they are the only visible morphological defects that can be explained. My observation of the different wing defects clearly pointed to imbalance of signalling pathways located at the dorsal-ventral (D/V) interface of the wing disc which coincidentally corresponds exactly with the expression pattern of Jar during wing disc eversion (Milo and Bownes, 2007). It is worth noting that these

signalling pathways implicated at the D/V boundary are also involved in wide variety of developmental processes in *Drosophila*. More importantly, the wing disc eversion during metarmorphosis is mediated through direct and indirect actions of JNK activity (Pastor-Pareja *et al.*, 2004).

Fringe (Fng), a dorsal secreted molecule and Apterous, a selector and a transcription factor gene are both important in maintaining the D/V boundary (Figure 7.1) (Milán and Cohen, 2003; O' Keefe and Thomas, 2001). Fng, restricted to the dorsal compartment binds and subsequently, modulates the Notch's response to its ligands. Serrate (Ser) and Delta (Dl) are both Notch ligands. The Fng inhibits Ser activation of Notch but augments the activity of Dl to activate Notch signalling and as a consequent signalling is restricted to the D/V boundary. Additionally, the PS1 cooperates with ventrally expressed PS2 to establish cell contacts between dorsal and ventral of the wing epithelial during pupation.

While I provide no evidence as to the exact function of Jar during wing morphogenesis, based on previous implications I favour a model whereby Jar is involved in receptor internalisation at the D/V boundary and this helps to maintain homeostatic balance. Endocytosis is reportedly essential for signalling ligands at the D/V axis and is preferentially through the clathrin-dependent pathway. In *Drosophila*, Notch endocytosis is preferentially through the clathrin-dependent route but it can also occur through clathrin-independent endocytosis (Windler and Bilder, 2010; Yamamoto *et al.*, 2010). Jar has been identified as a modifier of Notch signalling in the developing *Drosophila* eye (Shalaby *et al.*, 2009).

Interestingly, Ed is reportedly present at the D/V boundary in the wing disc and is shown to colocalise with Notch and Dl (Wei *et al.*, 2005; Rawlins *et al.*, 2003). Ed interacts with the Notch signalling pathway during embryonic neurogenesis, genetically during adult PNS development and possibly acts synergistically with genes of the Notch signalling pathway in the wing disc (Ahmed *et al.*, 2003; Rawlins *et al.*, 2003). However, loss of functional Ed did not affect endocytosis of N and Dl. (Rawlins *et al.*, 2003).

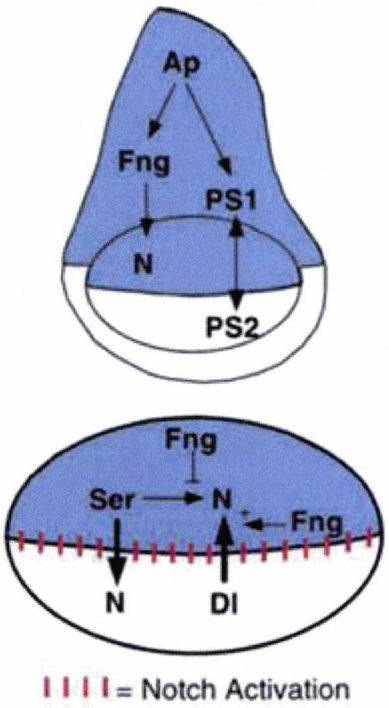

Figure 7.1. Function of Apterous in defining the D/V compartmentalisation in late third instar wing disc. Notice the expression of the affected function and signalling molecules in few of Jar maternal and zygotic null escapers. Image adapted from O' Keefe and Thomas (2001).

Consistent with my proposal, the loss of endocytic function of Jar could prompt cell death. In support of this, inappropriate Notch signalling in the wing disc prompts activation of apoptosis but in concert with other survival cues (Milán *et al.*, 2002). Notch mutants are shown to exhibit high levels of JNK signalling in the dorsal epidermis of embryos (Zecchini *et al.*, 1999). JNK signalling pathway has been demonstrated active during apoptosis in the wing disc and also in response to reduced Wingless (Wg) signalling which is synergistically linked with Notch signalling (Adachi-Yamada and O'Connor, 2002). Notch signalling induces Wg expression at the D/V boundary and in turn, wing margin and pattern are defined along the D/V boundary.

Furthermore, integrin trafficking is required for its function and moreover, can go through clathrin-dependent pathway in *Drosophila* (Caswell *et al.*, 2009). In vertebrate, Dab2, a myosin VI binding partner in the trafficking machinery is shown involved in β1 integrin endocytosis (Caswell *et al.*, 2009; Morris *et al.*, 2002).

However, Jar does not have the conserved binding domain necessary for Dab, the *Drosophila* homologue of Dab2 (Finan *et al.*, 2011). GIPC is known to associate with different integrins (Valdembri *et al.*, 2009). GIPC is shown required for myosin VI-dependent regulation of integrin traffic and function in human endothelial cells (Valdembri *et al.*, 2009). The complete loss-of-function of dGIPC causes no observable defect in the viable adults but the over-expression of dGIPC results in PCP defect (Djiane and Mlodzik, 2010). Moreover the removal of one copy of Jar was shown to suppress the PCP defect. Possibly, Jar has distinct functions in PCP and in integrin function and signalling.

Bearing the above information in mind, if the prosurvival function of myosin VI is conserved in *Drosophila*, the loss-of-function of Jar in cellular homeostasis could prompt activation of cell death in several developmental processes given the wide pattern of Jar expression but in a cell-type manner.

7.2.5. Jar as a homeostatic apoptotic protein?

Vertebrate myosin VI is transcriptionally regulated by p53 and stress signals (Tamaki *et al.*, 2007; Jung *et al.*, 2006). In *Drosophila*, I observe that Jar is directly regulated by JNK Kinase signalling, also a stress-activated protein kinase. The function of *DmP53* is mediated by the activity of the JNK pathway (Martin *et al.*, 2009). Thus, I reason that the defects reported in this project can be attributed directly or indirectly to active JNK signal. Furthermore, function of Jar is potentially regulated by JNK signalling under normal physiological conditions.

Myosin VI translocates from endocytic vesicles, membrane ruffles and the cytosol to the Golgi complex, perinuclear membrane and the nucleus in response to p53 (Jung *et al.*, 2006). p53 also follows similar relocalisation route upon DNA damage or certain cellular conditions as has been demonstrated for myosin VI (O'Brate and Giannakakou, 2003). For instance, in the nucleus of mammalian cells myosin VI was reportedly found highly expressed and was shown to modulate RNAPII-dependent transcription (Vreugde *et al.*, 2006). Myosin VI is recruited to the promoter and intergenic regions of active genes, encoding urokinase plasminogen activator (uPA)

among other active genes noted in the report. Of interest, uPA promotes mestastic spreading of cancer cells. This correlates well with reports that depletion of myosin VI was found to impede migration of both ovarian and prostate cancer cells *in vitro* and ovarian tumour dissemination *in vivo* as well as border cell migration in *Drosophila*, a model reminiscent of cancer cell invasion (Dunn *et al.*, 2006; Yoshida *et al.*, 2004; Geisbrecht and Montell, 2002). Strinkingly, uPA is a target gene of c-Fos (Eferl and Wagner, 2003). Importantly, c-Fos is a downstream effector of the JNK transcriptional activation pathway. Furthermore, another cellular localisation study identified myosin VI expressed in nucleus of PC12 cells, a model of adrenal medulla chromaffin cells which are homologous to sympathetic neurons (Majewski *et al.*, 2010). It was suggested that the presence of myosin VI in the nucleus is an indication of vesicle transport to the nucleus and/or trafficking within the nucleus. In support of the idea, nuclear myosin I cooperates with actin to modulate RNA polymerases I and II transcription and has functional role in intranuclear transport (Hofmann *et al.*, 2006). Thus, I can envision a similar scenario for myosin VI to function in intranuclear transport.

Furthermore, both functional and cellular localisation studies have reported myosin VI at the trans-side of the Golgi network (TGN) and with secretory vesicles at the plasma membrane (Bond *et al.*, 2011; Warner *et al.*, 2003; Buss *et al.*, 1998). In addition, myosin VI is implicated in basolaterally-targeted secretory cargoes in polarized cells and the early endosome (Au *et al.*, 2007). The primary function of the TGN is cargo sorting (reviewed in, Glick and Nakano, 2009). TGN serves to produce clathrin-coated vesicles and which are afterwards delivered to endosomes en route to the plasma membrane or lysosome. In addition, secretory cargoes are delivered directly from the TGN to the plasma membrane but via different routes. Various clathrin adaptors are shown to mediate membrane traffic between the TGN and endosomes. During apoptosis the Golgi complex undergoes irreversible disassembly and consequently, secretory pathway is inhibited (Hicks and Machamer, 2005; Machamer, 2003).

The loss-of-function of myosin VI has been shown to cause an increase of a cell's sensitivity to apoptosis (Jung *et al.*, 2006). p53 stability is compromised due to reduced activation of ATM, a protein kinase responsible for phosphorylation and consequent activation of p53 (Jung *et al.*, 2006). Moreover, Golgi complex is

fragmented and consequently, both exocytosis and secretion are reduced (Warner *et al.*, 2003).

Strikingly, *Drosophila* ATM, *dATM* mutants die as pupae or eclose with eye and wing malformations (Song *et al.*, 2004). The loss of function of dATM results in p53-mediated apoptosis during development. More interestingly, the wings display notches at the margin and occasional blisters as has been reported here for maternal and zygotic *jar* null escapers. This further strengthens the idea of Jar being a homeostatic apoptotic protein. The loss of functions of several proapoptotic genes such as POSH (a JNK scaffolding protein), Eiger (*Drosophila* homologue of Tumor necrosis factor) and Tak1 (a JNKKK) are viable but cause visible morphological defects only when they are overexpressed (Lennox and Stronach, 2010; Igaki *et al.*, 2002; Vidal *et al.*, 2001). In addition, p53 mutants or expressing dominant negative p53 causes no effect on development (Martin *et al.*, 2009). These proapoptotic proteins are also expressed normally in non-apoptotic cells (Lennox and Stronach, 2010; Igaki *et al.*, 2002). However, their functions are not established as yet in normal development. Seemingly, Jar shares function with its vertebrate counterparts. A proteomics-based approach in *Drosophila* embryonic cells identified several proteins that directly bind to Jar such as proteins involved in Notch signalling, dGIPC, Golgi proteins, clathrin accessory proteins and many more (Finan *et al.*, 2011). Collectively, the reports go nicely with our proposal that Jar is a homeostatic apoptotic gene and is important for normal development.

7.3. Future work

This study has undoubtedly, paved the way for numerous researches and would be reinforced by number of experimental designs such as the few outlined below.

7.3.1. Re-examine Jar function in dorsal closure

GFP-tagged Jar was shown to rescue male sterility, a feature characteristic of loss of Jar function during spermatogenesis (Millo *et al.*, 2004). Therefore a live imaging of GFP-tagged Jar in dorsal closure would give a clear demonstration of function.

Generate also a GFP-tag Jar-RNAi construct and this would give a clear explanation of the irregular LE during live imaging of dorsal closure. There are several UAS-Jar RNAi constructs available from the VDRC collections. Therefore, examine if expressing these different transgenic Jar RNAi lines would produce similar phenotypes. In addition, investigate the effect on the expression pattern of Ed in Jar knock down dorsal stage embryos. This is to reinforce the idea that Jar is required for the stability of the cell-cell junctions.

7.3.2. Determining phosphorylation status of Jar

Western blot assay has shown that Jar is differentially spliced. Western blot assay can also determine if either the threonines located in the head or tail domain of Jar (Figure 3.1) is phosphorylated by generating anti-phosphothreonine-specific antibodies against these sites. This will provide us with information that Jar can be phosphorylated *in vivo* as has been demonstrated for vertebrate myosin VI *in vitro*.

7.3.3. Build upon primary data of the Jar-DN construct

Dominant negative Jar-DN construct generated intracellular puncta of DE-cadherin. Is this result artificial? DE-cadherin is shown to be actively trafficked in the *Drosophila* embryonic ectoderm (Roeth *et al.*, 2009). Therefore investigate if Jar is involved in DE-cadherin endocytosis using the model epithelium. This will help explain the result of the reduced/mislocalised DE-cadherin found in expressing dominant negative Jar-DN construct in embryo (Millo *et al.*, 2004). Possibly, an alternative route of endocytosis is up-regulated in RNAi-mediated Jar knock down in embryos.

7.3.4. Examine Jar position in the apoptotic program

The wing disc is shown a popular model system in which to study apoptosis because aside that it is a 2-dimensional system, very little apoptosis is prompted during normal development. Apoptotic cells can artificially be generated in the wing disc. The wing disc can respond with apoptotic stimuli when subjected to external stress and cells are kept alive (termed undead cells) in the presence of baculovirus caspase inhibitor p53 (Morata *et al.*, 2011; Martin *et al.*, 2009). In brief, apoptotic pathway is continuously active in the wing disc.

Importantly, the induction of apoptosis in the wing disc generates normal apoptotic pathway. Development signalling pathways such as JNK, Dpp, and Wg are ectopically expressed as well as the upregulation of proapoptotic genes (Morata *et al.*, 2011). In addition, the induced apoptosis is mediated by the JNK pathway in a p53-dependent manner (Igaki, 2009).

This experimental approach could be used to determine position of Jar in the apoptotic program. This also will establish if Jar is transcriptionally regulated in a p53-dependent manner as has been demonstrated for vertebrate myosin VI. However, the downside of this experiment is that persistent activation of the JNK signal causes hyperplastic overgrowth in the wing disc (Pérez-Garijo *et al.*, 2009).

7.3.5. Genetic interactions

The wing defects implicated Jar in Notch signalling and integrin function and signalling. Therefore test for genetic interactions between the proteins (shown below) to have a better understanding of the primary data. This help tackle the question whether notch signalling and integrin function and signalling are dependent on Jar function?

a. Between *jar* and ***mys*** (integrin)

b. Between *jar* and ***Notch***

7.4. Final conclusion

During the course of my study I have stumbled upon new revelations that most probably, would change the direction of research in understanding the molecular mechanistic function of Jar and thus, its homologues. My investigating the functionality of Jar has opened up a whole field of inquiry into the biological significance of Jar protein.

This project provides evidence to establish that Jar is directly regulated by JNK transcriptional activation pathway and down-regulated by the RhoGTPase pathway. Taking into account the number of phenotypes reported in this project, Jar is implicated in array of cellular and developmental processes. Therefore, it seems plausible that the function of Jar is in response to cues emanating directly or indirectly from the JNK signalling. Understandably, JNK signalling is a key factor in development processes, conserved between vertebrate and invertebrate systems. Subsequently, other key development signalling pathways are also activated. Thus, implies that Jar is a multifaceted protein, not surprising giving the wide-ranging expression pattern of Jar. The basic knowledge gained from studies in *Drosophila* would undoubtedly help understand the function of its vertebrate homologues and more importantly, Jar and human myosin VI share 52% sequence identity and 70% similarity. And seemingly, Jar shares similar binding partners as vertebrate myosin VI.

References

Abo, A., Qu, J., Cammarano, M. S., Dan, C., Fritsch, A., Baud, V., et al. (1998). PAK4, a novel effector for CDC42Hs, is implicated in the reorganization of the actin cytoskeleton and in the formation of filopodia. *The EMBO journal*, *17*(22):6527-6540.

Adachi-Yamada, T., & O'Connor, M. B. (2002). Morphogenetic apoptosis: a mechanism for correcting discontinuities in morphogen gradients. *Dev Biol*, *251*(1):74-90.

Affolter, M., Nellen, D., Nussbaumer, U., & Basler, K. (1994). Multiple requirements for the receptor serine/threonine kinase thick veins reveal novel functions of TGF beta homologs during *Drosophila* embryogenesis. *Development*, *120*(11):3105-3117.

Ahmed, A., Chandra, S., Magarinos, M., & Vaessin, H. (2003). Echinoid mutants exhibit neurogenic phenotypes and show synergistic interactions with the Notch signaling pathway. *Development*, *130*(25):6295-6304.

Ahmed, Z. M., Morell, R. J., Riazuddin, S., Gropman, A., Shaukat, S., Ahmad, M. M., et al. (2003). Mutations of myo6 are associated with recessive deafness, DFNB37. *Am J Hum Genet*, *72*(5):1315-1322.

Akhtar, N., & Hotchin, N. A. (2001). Rac1 regulates adherens junctions through endocytosis of E-cadherin. *Mol Biol Cell*, *12*(4):847-862.

Altman, D., Sweeney, H. L., & Spudich, J. A. (2004). The mechanism of myosin VI translocation and its load-induced anchoring. *Cell*, *116*(5):737-749.

Ameen, N., & Apodaca, G. (2007). Defective CTFR apical endocytosis and enterocyte brush border in myosin VI deficient mice. *Traffic*, *8*(8):998-1006.

Arden, S. D., Puri, C., Au, J. S. Y., Kendrick-Jones, J., & Buss, F. (2007). Myosin VI is required for targeted membrane transport during cytokinesis. *Mol Biol Cell*, *18*(12):4750-4761.

Arias-Romero, L., & Chernoff, J. (2008). A tale of two Paks. *Biol Cell*, *100*:97-108.

Aschenbrenner, L., Lee, T. T., & Hasson, T. (2003). Myo6 facilitates the translocation of endocytic vesicles from cell peripheries. *Mol Biol Cell*, *14*(7):2728-2743.

Attanapola, S. L., Alexander, C. J., & Mulvihill, D. P. (2009). Ste20-kinase-dependent TEDS-site phosphorylation modulates the dynamic localisation and endocytic function of the fission yeast class I myosin, Myo1. *J Cell Sci*, *122*(21):3856- 3861.

Au, J. S. Y., Puri, C., Ihrke, G., Kendrick-Jones, J., & Buss, F. (2007). Myosin VI is required for sorting of AP-1B–dependent cargo to the basolateral domain in polarized MDCK cells. *J Cell Biol*, *177*(1):103-114.

Avraham, K. B., Hasson, T., Sobe, T., Balsara, B., Testa, J. R., Skvorak, A. B., et al. (1997). Characterization of unconventional MYO6, the human homologue of the gene responsible for deafness in Snell's waltzer mice. *Hum Mol Genet*, *6*(8):1225-1231.

Bahloul, A., Chevreux, G., Wells, A. L., Martin, D., Nolt, J., Yang, Z., et al. (2004). The unique insert in myosin VI is a structural calcium–calmodulin binding site. *Proc Natl Acad Sci U S A*, *101*(14):4787-4792.

Bahri, S. M., Choy, J. M., Manser, E., Lim, L., & Yang, X. (2009). The *Drosophila* homologue of Arf-GAP GIT1, dGIT, is required for proper muscle morphogenesis and guidance during embryogenesis. *Dev Biol*, *325*(1):15-23.

Bahri, S., Wang, S., Conder, R., Choy, J., Vlachos, S., Dong, K., et al. (2010). The leading edge during dorsal closure as a model for epithelial plasticity: Pak is required for recruitment of the Scribble complex and septate junction formation. *Development*, *137*(12):2023-2032.

Baker, J. E., Krementsova, E. B., Kennedy, G. G., Armstrong, A., Trybus, K. M., & Warshaw, D. M. (2004). Myosin V processivity: multiple kinetic pathways for head-to-head coordination. *Proc Natl Acad Sci U S A*, *101*(15):5542-5546.

Baker, J. P., & Titus, M. A. (1997). A family of unconventional myosins from the nematode *Caenorhabditis elegans*. *J Mol Biol*, *272*(4):523-535.

Baker, J. P., & Titus, M. A. (1998). Myosins: matching functions with motors. *Curr Opin Cell Biol*, *10*(1):80-86.

Bement, W. M., & Mooseker, M. S. (1995). TEDS rule: a molecular rationale for differential regulation of myosins by phosphorylation of the heavy chain head. *Cell Motil Cytoskeleton*, *31*(2):87-92.

Berg, J. S., Powell, B. C., & Cheney, R. E. (2001). A millennial myosin census. *Mol Biol Cell*, *12*(4):780.

Biemesderfer, D., Mentone, S. A., Mooseker, M., & Hasson, T. (2002). Expression of myosin VI within the early endocytic pathway in adult and developing proximal tubules. *Am J Physiol Renal Physiol*, *282*(5):F785-794.

Blanchard, G. B., Murugesu, S., Adams, R. J., Martinez-Arias, A., & Gorfinkiel, N. (2010). Cytoskeletal dynamics and supracellular organisation of cell shape fluctuations during dorsal closure. *Development*, *137*(16):2743-2752.

Bloor, J. W., & Kiehart, D. P. (2002). *Drosophila* RhoA regulates the cytoskeleton and cell-cell adhesion in the developing epidermis. *Development*, *129*(13):3173-3183.

Bokoch, G. M. (2003). Biology of the p21-activated kinases. *Annu Rev Biochem*, *72*(1):743-781.

Bond, L. M., Peden, A. A., Kendrick-Jones, J., Sellers, J. R., & Buss, F. (2011). Myosin VI and its binding partner optineurin are involved in secretory vesicle fusion at the plasma membrane. *Mol Biol Cell*, *22*(1):54-65.

Brabant, M. C., Fristrom, D., Bunch, T. A., & Brower, D. L. (1996). Distinct spatial and temporal functions for PS integrins during *Drosophila* wing morphogenesis. *Development*, *122*(10):3307-3317.

Brand, A. H., & Perrimon, N. (1993). Targeted gene expression as a means of altering cell fates and generating dominant phenotypes. *Development*, *118*(2):401-415.

BRECKLER, J., AU, K., CHENG, J., HASSON, T., & BURNSIDE, B. (2000). Novel myosin VI isoform is abundantly expressed in retina. *Exp Eye Res*, *70*(1):121-134.

Brower, D. L., Bunch, T. A., Mukai, L., Adamson, T. E., Wehrli, M., Lam, S., et al. (1995). Nonequivalent requirements for PS1 and PS2 integrin at cell attachments in *Drosophila*: genetic analysis of the alpha PS1 integrin subunit. *Development*, *121*(5):1311-1320.

Bryant, Z., Altman, D., & Spudich, J. A. (2007). The power stroke of myosin VI and the basis of reverse directionality. *Proc Natl Acad Sci U S A*, *104*(3):772-777.

Brzeska, H., & Korn, E. D. (1996). Regulation of class I and class II myosins by heavy chain phosphorylation. *J Biol Chem*, *271*(29):16983-16986.

Brzeska, H., Knaus, U. G., Wang, Z. Y., Bokoch, G. M., & Korn, E. D. (1997). P21-activated kinase has substrate specificity similar to Acanthamoeba myosin I heavy chain kinase and activates Acanthamoeba myosin I. *Proc Natl Acad Sci*, *94*(4):1092-1095.

Bulgheresi, S., Kleiner, E., & Knoblich, J. A. (2001). Inscuteable-dependent apical localization of the microtubule-binding protein cornetto suggests a role in asymmetric cell division. *J Cell Sci*, *114*(20):3655-3662.

Buss, F., & Kendrick-Jones, J. (2008). How are the cellular functions of myosin VI regulated within the cell? *Biochem Biophys Res Communications*, *369*(1):165-175.

Buss, F., Arden, S. D., Lindsay, M., Luzio, J. P., & Kendrick-Jones, J. (2001b). Myosin VI isoform localized to clathrin-coated vesicles with a role in clathrin-mediated endocytosis. *The EMBO Journal*, *20*(14):3676-3684.

Buss, F., Kendrick-Jones, J., Lionne, C., Knight, A. E., Côté, G. P., & Paul Luzio, J. (1998). The localization of myosin VI at the golgi complex and leading edge of fibroblasts and its phosphorylation and recruitment into membrane ruffles of A431 cells after growth factor stimulation. *J Cell Biol*, *143*(6):1535-1545.

Buss, F., Luzio, J. P., & Kendrick-Jones, J. (2001a). Myosin VI, a new force in clathrin mediated endocytosis. *FEBS letters*, *508*(3):295-299.

Buss, F., Spudich, G., & Kendrick-Jones, J. (2004). Myosin VI: cellular functions and motor properties. *Annu. Rev. Cell Dev. Biol*, *20*:649-676.

Butler, M. J., Jacobsen, T. L., Cain, D. M., Jarman, M. G., Hubank, M., Whittle, J. R. S., et al. (2003). Discovery of genes with highly restricted expression patterns in the *Drosophila* wing disc using DNA oligonucleotide microarrays. *Development*, *130*(4):659-670.

Casso, D., Ramírez-Weber, F. A., & Kornberg, T. B. (2000). GFP-tagged balancer chromosomes for *Drosophila melanogaster*. *Mechan Dev*, *91*(1-2):451-454.

Caswell, P. T., Vadrevu, S., & Norman, J. C. (2009). Integrins: masters and slaves of endocytic transport. *Nat Rev Mol Cell Biol*, *10*(12):843-853.

Cavey, M., Rauzi, M., Lenne, P. F., & Lecuit, T. (2008). A two-tiered mechanism for stabilization and immobilization of E-cadherin. *Nature*, *453*(7196):751-756.

Chibalina, M. V., Seaman, M. N. J., Miller, C. C., Kendrick-Jones, J., & Buss, F. (2007). Myosin VI and its interacting protein LMTK2 regulate tubule formation and transport to the endocytic recycling compartment. *J Cell Sci*, *120*(24):4278-4288.

Cho, S. J., & Chen, X. (2010). Myosin VI is differentially regulated by DNA damage in p53-and cell type-dependent manners. *J Biol Chem*, *285*(35):27159-27166.

Le Clainche, C., & Carlier, M. F. (2008). Regulation of actin assembly associated with protrusion and adhesion in cell migration. *Physiol Rev*, *88*(2):489-513.

Collaco, A., Jakab, R., Hegan, P., Mooseker, M., & Ameen, N. (2010). AP-2 directs myosin VI-dependent Endocytosis of Cystic fibrosis Transmembrane Conductance Regulator Chloride Channels in the intestine. *J Biol Chem*, *285*(22):17177-17187.

Conder, R., Yu, H., Ricos, M., Hing, H., Chia, W., Lim, L., et al. (2004). dPak is required for integrity of the leading edge cytoskeleton during *Drosophila* dorsal closure but does not signal through the JNK cascade. *Dev Biol*, *276*(2):378-390.

Conder, R., Yu, H., Zahedi, B., & Harden, N. (2007). The serine/threonine kinase dPak is required for polarized assembly of f-actin bundles and apical-basal polarity in the *Drosophila* follicular epithelium. *Dev Biol*, *305*(2):470-482.

Correia, S. S., Bassani, S., Brown, T. C., Lisé, M. F., Backos, D. S., El-Husseini, A., et al. (2008). Motor protein-dependent transport of AMPA receptors into spines during long-term potentiation. *Nat NeuroSci*, *11*(4):457-466

Cramer, L. P. (2000). Myosin VI: roles for a minus end-directed actin motor in cells. *J Cell Biol*, *150*(6):F121-126.

Dance, A. L., Miller, M., Seragaki, S., Aryal, P., White, B., Aschenbrenner, L., et al. (2004). Regulation of myosin VI targeting to endocytic compartments. *Traffic*, *5*(10):98-813.

David, D. J. V., Tishkina, A., & Harris, T. J. C. (2010). The PAR complex regulates pulsed actomyosin contractions during amnioserosa apical constriction in *Drosophila*. *Development*, *137*(10):1645-1655.

Davis, R. J. (2000). Signal transduction by the JNK group of MAP kinases. *Cell*, *103*(2):239-252.

DeMali, K. A., & Burridge, K. (2003). Coupling membrane protrusion and cell adhesion. *J Cell Sci*, *116*(12):2389-2397.

Deng, W., Leaper, K., & Bownes, M. (1999). A targeted gene silencing technique shows that *Drosophila* myosin VI is required for egg chamber and imaginal disc morphogenesis. *J Cell Sci*, *112*(21):3677-3690.

Desnos, C., Huet, S., & Darchen, F. (2007). "Should i stay or should i go?": myosin V function in organelle trafficking. *Biol Cell*, *99*:411-423.

De La Cruz, E. M., Ostap, E. M., & Sweeney, H. L. (2001). Kinetic mechanism and regulation of myosin VI. *J Biol Chem*, *276*(34):32373-32381.

Dietzl, G., Chen, D., Schnorrer, F., Su, K. C., Barinova, Y., Fellner, M., et al. (2007). A genome-wide transgenic RNAi library for conditional gene inactivation in *Drosophila*. *Nature*, *448*(7150):151-156.

Djiane, A., & Mlodzik, M. (2010). The *Drosophila* GIPC homologue can modulate myosin based processes and planar cell polarity but is not essential for development. *PLoS One*, *5*(6), p. e11228.

Doherty, G. J., & McMahon, H. T. (2009). Mechanisms of endocytosis. *Annu Rev Biochem*, *78*:857-902.

Domínguez-Giménez, P., Brown, N. H., & Martín-Bermudo, M. D. (2007). Integrin-ECM interactions regulate the changes in cell shape driving the morphogenesis of the *Drosophila* wing epithelium. *J Cell Sci*, *120*(6):1061-1071.

Dunn, T. A., Chen, S., Faith, D. A., Hicks, J. L., Platz, E. A., Chen, Y., et al. (2006). A novel role of myosin VI in human prostate cancer. *Am J Pathol*, *169*(5):1843-1854.

Eferl, R., & Wagner, E. F. (2003). AP-1: a double-edged sword in tumorigenesis. *Nat Rev Cancer*, *3*(11):859-868.

Finan, D., Hartman, M. A., & Spudich, J. A. (2011). Proteomics approach to study the functions of *Drosophila* myosin VI through identification of multiple cargo-binding proteins. *Proc Natl Acad Sci*, *108*(14):5566-5571.

Franke, J. D., Montague, R. A., & Kiehart, D. P. (2005). Nonmuscle myosin II generates forces that transmit tension and drive contraction in multiple tissues during dorsal closure. *Curr Biol*, *15*(24):2208-2221.

Franke, J. D., Montague, R. A., & Kiehart, D. P. (2010). Nonmuscle myosin II is required for cell proliferation, cell sheet adhesion and wing hair morphology during wing morphogenesis. *Dev Biol*, *345*(2):117-132.

Fuchs, S. Y., Adler, V., Pincus, M. R., & Ronai, Z. (1998). MEKK1/JNK signaling stabilizes and activates p53. *Proc Natl Acad Sci*, *95*(18):10541-10546.

Fujita-Becker, S., Dürrwang, U., Erent, M., Clark, R. J., Geeves, M. A., & Manstein, D. J. (2005). Changes in Mg2+ ion concentration and heavy chain phosphorylation regulate the motor activity of a class I myosin. *J Biol Chem*, *280*(7):6064-6071.

Geisbrecht, E. R., & Montell, D. J. (2002). Myosin VI is required for E-cadherin-mediated border cell migration. *Nat Cell Biol*, *4*(8):616-620.

Glick, B. S., & Nakano, A. (2009). Membrane traffic within the Golgi apparatus. *Annu Rev Cell Dev Biol*, *25*:113-132.

Glise, B., & Noselli, S. (1997). Coupling of Jun amino-terminal kinase and Decapentaplegic signaling pathways in *Drosophila* morphogenesis. *Genes Dev*, *11*(13):1738-1747.

Gloor, G. B., C. R. Preston, D. M. Johnson-Schlitz, N. A. Nassif, R. W. Phillis, W. K. Benz, H. M. Robertson and W. R. Engels. (1993). Type I repressors of P element mobility. *Genetics,* 135:81-95.

Gorfinkiel, N., & Arias, A. M. (2007). Requirements for adherens junction components in the interaction between epithelial tissues during dorsal closure in *Drosophila*. *J Cell Sci*, *120*(18):3289-3298.

Gorfinkiel, N., Blanchard, G. B., Adams, R. J., & Martinez Arias, A. (2009). Mechanical control of global cell behaviour during dorsal closure in *Drosophila*. *Development*, *136*(11):1889-1898.

Gotoh, N., Yan, Q., Du, Z., Biemesderfer, D., Kashgarian, M., Mooseker, M. S., et al. (2010). Altered renal proximal tubular endocytosis and histology in mice lacking myosin VI. *Cytoskeleton*, *67*(3):178-192.

Hansen, C. G., & Nichols, B. J. (2009). Molecular mechanisms of clathrin-independent endocytosis. *J Cell Sci*, *122*(11):1713-1721.

Harden, N., Lee, J., Loh, H. Y., Ong, Y. M., Tan, I., Leung, T., et al. (1996). A *Drosophila* homolog of the Rac-and Cdc42-activated serine/threonine kinase PAK is a potential focal adhesion and focal complex protein that colocalizes with dynamic actin structures. *Mol Cell Biol*, *16*(5):1896-1908.

Harden, N., Ricos, M., Ong, Y. M., Chia, W., & Lim, L. (1999). Participation of small GTPases in dorsal closure of the *Drosophila* embryo: distinct roles for Rho subfamily proteins in epithelial morphogenesis. *J Cell Sci*, *112*(3):273-284.

Hasson, T. (2003). Myosin VI: two distinct roles in endocytosis. *J Cell Sci*, *116*(17): 3453-3461.

Hasson, T., & Mooseker, M. S. (1994). Porcine myosin-VI: characterization of a new mammalian unconventional myosin. *J Cell Biol*, *127*(2):425-440.

Hasson, T., Gillespie, P. G., Garcia, J. A., MacDonald, R. B., Zhao, Y., Yee, A. G., et al. (1997). Unconventional myosins in inner-ear sensory epithelia. *J Cell Biol*, *137*(6):1287-1307.

Heintzelman, M. B., Hasson, T., & Mooseker, M. S. (1994). Multiple unconventional myosin domains of the intestinal brush border cytoskeleton. *J Cell Sci*, *107*(12), p. 3535.

Herranz, H., & Morata, G. (2001). The functions of pannier during *Drosophila* embryogenesis. *Development*, *128*(23):4837-4846.

Herranz, H., Morata, G., & Milán, M. (2006). Calderón encodes an organic cation transporter of the major facilitator superfamily required for cell growth and proliferation of *Drosophila* tissues. *Development*, *133*(14):2617-2625.

Hicks, J. L., Deng, W. M., Rogat, A. D., Miller, K. G., & Bownes, M. (1999). Class VI unconventional myosin is required for spermatogenesis in *Drosophila*. *Mol Biol Cell*, *10*(12):4341-4353.

Hicks, S. W., & Machamer, C. E. (2005). Golgi structure in stress sensing and apoptosis. *Biochim Biophys Acta*, *1744*(3):406-414.

Ho, Y. H., Lien, M. T., Lin, C. M., Wei, S. Y., Chang, L. H., & Hsu, J. C. (2010). Echinoid regulates flamingo endocytosis to control ommatidial rotation in the *Drosophila* eye. *Development*, *137*(5):745-754.

Hodge, T., Jamie, M., & Cope, T. (2000). A myosin family tree. *J Cell Sci*, *113*(19): 3353-3354.

Hofmann, W. A. H. W. A., Johnson, T. J. T., Klapczynski, M. K. M., Fan, J. L. F. J., & Primal de Lanerolle, P. (2006). From transcription to transport: emerging roles for nuclear myosin I. *Biochem Cell Biol*, *84*(4):418-426.

Homma, K., Yoshimura, M., Saito, J., Ikebe, R., & Ikebe, M. (2001). The core of the motor domain determines the direction of myosin movement. *Nature*, *412*(6849):831-834.

Igaki, T. (2009). Correcting developmental errors by apoptosis: lessons from *Drosophila* JNK signaling. *Apoptosis*, *14*(8):1021-1028.

Igaki, T., Kanda, H., Yamamoto-Goto, Y., Kanuka, H., Kuranaga, E., Aigaki, T., et al. (2002). Eiger, a TNF superfamily ligand that triggers the *Drosophila* JNK pathway. *The EMBO Journal*, *21*(12):3009-3018.

Igaki, T., Pagliarini, R. A., & Xu, T. (2006). Loss of cell polarity drives tumor growth and invasion through JNK activation in *Drosophila*. *Curr Biol*, *16*(11):1139-1146.

Inoue, A., Sato, O., Homma, K., & Ikebe, M. (2002). Doc-2/Dab2 is the binding partner of myosin VI. *Biochem Biophys Research Commun*, *292*(2):300-307.

Jacinto, A., Wood, W., Balayo, T., Turmaine, M., Martinez-Arias, A., & Martin, P. (2000). Dynamic actin-based epithelial adhesion and cell matching during *Drosophila* dorsal closure. *Curr Biol*, *10*(22):1420-1426.

Jacinto, A., Wood, W., Woolner, S., Hiley, C., Turner, L., Wilson, C., et al. (2002b). Dynamic analysis of actin cable function during *Drosophila* dorsal closure. *Curr Biol*, *12*(14):1245-1250.

Jacinto, A., Woolner, S., & Martin, P. (2002a). Dynamic analysis of dorsal closure in *Drosophila*: from genetics to cell biology. *Dev Cell*, *3*(1):9-19.

Jaffer, Z. M., & Chernoff, J. (2002). P21-activated kinases: three more join the Pak. I*nt J Biochem Cell Biol*, *34*(7):713-717.

Jankovics, F., & Brunner, D. (2006). Transiently reorganized microtubules are essential for zippering during dorsal closure in *Drosophila melanogaster*. *Dev Cell*, *11*(3):375-385.

Jochum, W., Passegue, E., & Wagner, E. F. (2001). Ap-1 in mouse development and tumorigenesis. *Oncogene*, *20*(19):2401-2412.

Johnson, N. L., Gardner, A. M., Diener, K. M., Lange-Carter, C. A., Gleavy, J., Jarpe, M. B., et al. (1996). Signal transduction pathways regulated by mitogen-activated/extracellular response kinase kinase kinase induce cell death. *J Biol Chem*, *271*(6):3229-3237.

Jung, E. J., Liu, G., Zhou, W., & Chen, X. (2006). Myosin VI is a mediator of the p53-dependent cell survival pathway. *Mol Cell Biol*, *26*(6):2175-2186.

Kellerman, K. A., & Miller, K. G. (1992). An unconventional myosin heavy chain gene from *Drosophila melanogaster*. *J Cell Biol*, *119*(4):823-834.

Kiehart, D. P., Franke, J. D., Chee, M. K., Montague, R., Chen, T., Roote, J., et al. (2004). *Drosophila* crinkled, mutations of which disrupt morphogenesis and cause lethality, encodes fly myosin VIIa. *Genetics*, *168*(3):1337-1352.

Kiehart, D. P., Galbraith, C. G., Edwards, K. A., Rickoll, W. L., & Montague, R. A. (2000). Multiple forces contribute to cell sheet morphogenesis for dorsal closure in *Drosophila*. *J Cell Biol*, *149*(2):471-490.

Kiger Jr, J. A., Natzle, J. E., Kimbrell, D. A., Paddy, M. R., Kleinhesselink, K., & Green, M. (2007). Tissue remodeling during maturation of the *Drosophila* wing. *Dev Biol*, *301*(1):178-191.

Kim, J., Lee, S., Ko, S., & Kim-Ha, J. (2010). dGIPC is required for the locomotive activity and longevity in *Drosophila*. *Biochem Biophys Res Commun*. *402*(3)565-570

Kim, S., & Flavell, R. (2008). Myosin I: from yeast to human. *Cell Mol Life Sci*, *65*(14):2128-2137.

Kisiel, M., Majumdar, D., Campbell, S., & Stewart, B. (2011). Myosin VI contributes to synaptic transmission and development at the *Drosophila* neuromuscular junction. *BMC Neurosci*, *12*(1):65.

Knight, P. J., Thirumurugan, K., Xu, Y., Wang, F., Kalverda, A. P., Stafford, W. F., et al. (2005). The predicted coiled-coil domain of myosin 10 forms a novel elongated domain that lengthens the head. *J Biol Chem*, *280*(41):34702-34708.

Krilleke, D., Ucur, E., Pulte, D., Schulze Osthoff, K., Debatin, K. M., & Herr, I. (2003). Inhibition of jnk signaling diminishes early but not late cellular stress induced apoptosis. *Int J Cancer*, *107*(4):520-527.

Lantz, V. A., & Miller, K. G. (1998). A class VI unconventional myosin is associated with a homologue of a microtubule-binding protein, cytoplasmic linker protein–170, in neurons and at the posterior pole of *Drosophila* embryos. *J Cell Biol*, *140*(4):897-910.

Laviolette, M. J., Nunes, P., Peyre, J. B., Aigaki, T., & Stewart, B. A. (2005). A genetic screen for suppressors of *Drosophila* NSF2 neuromuscular junction overgrowth. *Genetics*, *170*(2):779-792.

Layton, A. T., Toyama, Y., Yang, G. Q., Edwards, G. S., Kiehart, D. P., & Venakides, S. (2009). *Drosophila* morphogenesis: tissue force laws and the modeling of dorsal closure. *HFSP J*, *3*(6):441-460.

Lennox, A. L., & Stronach, B. (2010). POSH misexpression induces caspase dependent cell death in *Drosophila*. *Dev Dyn, 239*(2):651-664.

Levayer, R., Pelissier-Monier, A., & Lecuit, T. (2011). Spatial regulation of Dia and myosin-II by RhoGEF2 controls initiation of E-cadherin endocytosis during epithelial morphogenesis. *Nat Cell Biol*, *13*(5):529-540.

Liao, J. C., Elting, M. W., Delp, S. L., Spudich, J. A., & Bryant, Z. (2009). Engineered myosin VI motors reveal minimal structural determinants of directionality and processivity. *J Mol Biol*, *392*(4):862-867.

Lin, H. P., Chen, H. M., Wei, S. Y., Chen, L. Y., Chang, L. H., Sun, Y. J., et al. (2007). Cell adhesion molecule echinoid associates with unconventional myosin VI/Jaguar motor to regulate cell morphology during dorsal closure in *Drosophila*. *Dev Biol*, *311*(2):423-433.

Lister, I., Schmitz, S., Walker, M., Trinick, J., Buss, F., Veigel, C., et al. (2004). A monomeric myosin VI with a large working stroke. *EMBO J*, *23*(8):1729-1738.

Liu, R., Woolner, S., Johndrow, J. E., Metzger, D., Flores, A., & Parkhurst, S. M. (2008). Sisyphus, the *Drosophila* myosin XV homolog, traffics within filopodia transporting key sensory and adhesion cargos. *Development*, *135*(1):53-63.

Machamer, C. E. (2003). Golgi disassembly in apoptosis: cause or effect? *Trends Cell Biol*, *13*(6):279-281.

Majewski, L., Sobczak, M., & R dowicz, M. J. (2010). Myosin VI is associated with secretory granules and is present in the nucleus in adrenal medulla chromaffin cells. *Acta biochim Pol*, *57*(1):109-114.

Major, R. J., & Irvine, K. D. (2006). Localization and requirement for myosin II at the dorsal ventral compartment boundary of the *Drosophila* wing. *Dev Dyn, 235*(11):3051-3058.

Makrilia, N., Kollias, A., Manolopoulos, L., & Syrigos, K. (2009). Cell adhesion molecules: role and clinical significance in cancer. *Cancer Invest, 27*(10):1023-1037.

Markus Affolter, T. M. (2001). Nuclear interpretation of Dpp signaling in *Drosophila*. *EMBO J, 20*(13):3298-3305.

Martín, F. A., Peréz-Garijo, A., & Morata, G. (2009). Apoptosis in *Drosophila*: compensatory proliferation and undead cells. *Int J Dev Biol, 53*(8-10):1341-1347.

Martin, P., & Parkhurst, S. M. (2004). Parallels between tissue repair and embryo morphogenesis. *Development, 131*(13):3021-3034.

Martin, P., & Wood, W. (2002). Epithelial fusions in the embryo. *Curr Opin Cell Biol, 14*(5):569-574.

Melchionda, S., Ahituv, N., Bisceglia, L., Sobe, T., Glaser, F., Rabionet, R., et al. (2001). MYO6, the human homologue of the gene responsible for deafness in Snell's waltzer mice, is mutated in autosomal dominant nonsyndromic hearing loss. *Am J Hum Genet, 69*(3):635-640.

Ménétrey, J., Llinas, P., Mukherjea, M., Sweeney, H. L., & Houdusse, A. (2007). The structural basis for the large powerstroke of myosin VI. *Cell, 131*(2):300-308.

Mentzel, B., & Raabe, T. (2005). Phylogenetic and structural analysis of the *Drosophila melanogaster* p21-activated kinase dmpak3. *Gene, 349*:25-33.

Menzel, N., Melzer, J., Waschke, J., Lenz, C., Wecklein, H., Lochnit, G., et al. (2008). The *Drosophila* p21-activated kinase mbt modulates DE-cadherin-mediated cell adhesion by phosphorylation of Armadillo. *Biochem. J, 416*:231-241.

Menzel, N., Schneeberger, D., & Raabe, T. (2007). The *Drosophila* p21 activated kinase mbt regulates the actin cytoskeleton and adherens junctions to control photoreceptor cell morphogenesis. *Mechan Dev, 124*(1):78-90.

Mermall, V., & Miller, K. G. (1995). The 95f unconventional myosin is required for proper organization of the *Drosophila* syncytial blastoderm. *J Cell Biol*, *129*(6): 1575-1588.

Mermall, V., Bonafé, N., Jones, L., Sellers, J. R., Cooley, L., & Mooseker, M. S. (2005). *Drosophila* myosin V is required for larval development and spermatid individualization. *Dev Biol*, *286*(1):238-255.

Mermall, V., Post, P. L., & Mooseker, M. S. (1998). Unconventional myosins in cell movement, membrane traffic, and signal transduction. *Science*, *279*(5350):527-533.

Milán, M., & Cohen, S. M. (2003). A re-evaluation of the contributions of Apterous and Notch to the dorsoventral lineage restriction boundary in the *Drosophila* wing. *Development*, *130*(3):553-562.

Milán, M., Pérez, L., & Cohen, S. M. (2002). Short-range cell interactions and cell survival in the *Drosophila* wing. *Dev Cell*, *2*(6):797-805.

Millard, T. H., & Martin, P. (2008). Dynamic analysis of filopodial interactions during the zippering phase of *Drosophila* dorsal closure. *Development*, *135*(4):621-626.

Millo, H., & Bownes, M. (2007). The expression pattern and cellular localisation of myosin VI during the *Drosophila melanogaster* life cycle. *Gene expression patterns*, *7*(4):501-510.

Millo, H., Leaper, K., Lazou, V., & Bownes, M. (2004). Myosin VI plays a role in cell-cell adhesion during epithelial morphogenesis. *Mechan Dev*, *121*(11):1335-1351.

Mirkovic, I., & Mlodzik, M. (2006). Cooperative activities of *Drosophila* DE-cadherin and DN-cadherin regulate the cell motility process of ommatidial rotation. *Development*, *133*(17):3283-3293.

Molli, P. R., Li, D. Q., Murray, B., Rayala, S. K., & Kumar, R. (2009). Pak signaling in oncogenesis. *Oncogene*, *28*(28):2545-2555.

Morata, G., Shlevkov, E., & Pérez Garijo, A. (2011). Mitogenic signaling from apoptotic cells in *Drosophila*. *Dev Growth Differ*, *53*(2):168-176.

Morris, S. M., Arden, S. D., Roberts, R. C., Kendrick Jones, J., Cooper, J. A., Luzio, J. P., et al. (2002). Myosin VI binds to and localises with Dab2, potentially linking receptor mediated endocytosis and the actin cytoskeleton. *Traffic*, *3*(5):331-341.

Morrison, D. K., Murakami, M. S., & Cleghon, V. (2000). Protein kinases and phosphatases in the *Drosophila* genome. *J Cell Biol*, *150*(2):F57-62.

Morrison, J. K., & Miller, K. G. (2008). Genetic characterization of the *Drosophila* Jaguar322 mutant reveals that complete myosin VI loss of function is not lethal. *Genetics*, *179*(1):711-716.

Morriswood, B., Ryzhakov, G., Puri, C., Arden, S. D., Roberts, R., Dendrou, C., et al. (2007). T6BP and NDP52 are myosin VI binding partners with potential roles in cytokine signalling and cell adhesion. *J Cell Sci*, *120*(15):2574-2585.

Naccache, S. N., & Hasson, T. (2006). Myosin VI altered at threonine 406 stabilizes actin filaments in vivo. *Cell Motil Cytoskeleton*, *63*(10):633-645.

Naccache, S. N., Hasson, T., & Horowitz, A. (2006). Binding of internalized receptors to the PDZ domain of GIPC/synectin recruits myosin VI to endocytic vesicles. *Proc Natl Acad Sci U S A*, *103*(34):12735-12740.

Nakano, A., & Luini, A. (2010). Passage through the Golgi. *Curr Opin Cell Biol, 22*(4):471-478.

Nash, J. E., Appleby, V. J., Corrêa, S. A. L., Wu, H., Fitzjohn, S. M., Garner, C. C., et al. (2010). Disruption of the interaction between myosin VI and SAP97 is associated with a reduction in the number of AMPARs at hippocampal synapses. *J Neurochem*, *112*(3):677-690.

Neisch, A. L., Speck, O., Stronach, B., & Fehon, R. G. (2010). Rho1 regulates apoptosis via activation of the JNK signaling pathway at the plasma membrane. *J Cell Biol*, *189*(2):311-323.

Niewiadomska, P., Godt, D., & Tepass, U. (1999). DE-cadherin is required for intercellular motility during *Drosophila* oogenesis. *J Cell Biol*, *144*(3):533-547.

Nishikawa, S., Homma, K., Komori, Y., Iwaki, M., Wazawa, T., Hikikoshi Iwone, A., et al. (2002). Class VI myosin moves processively along actin filaments backward with large steps. *Biochem Biophys Res Commun*, *290*(1):311-317.

Noguchi, T., Frank, D. J., Isaji, M., & Miller, K. G. (2009). Coiled-coil-mediated dimerization is not required for myosin VI to stabilize actin during spermatid individualization in *Drosophila melanogaster*. *Mol Biol Cell*, *20*(1):358-367.

Noguchi, T., Lenartowska, M., & Miller, K. G. (2006). Myosin VI stabilizes an actin network during *Drosophila* spermatid individualization. *Mol Biol Cell*, *17*(6):2559-2571.

Novak, K. D., & Titus, M. A. (1998). The myosin I SH3 domain and TEDS rule phosphorylation site are required for in vivo function. *Mol Biol Cell*, *9*(1):75-88.

O'Brate, A., & Giannakakou, P. (2003). The importance of p53 location: nuclear or cytoplasmic zip code? *Drug Resist Updat*, *6*(6):313-322.

O'Connor, M. B., Umulis, D., Othmer, H. G., & Blair, S. S. (2006). Shaping BMP morphogen gradients in the *Drosophila* embryo and pupal wing. *Development*, *133*(2):183-193.

O'Keefe, D. D., & Thomas, J. B. (2001). *Drosophila* wing development in the absence of dorsal identity. *Development*, *128*(5):703-710.

Odronitz, F., & Kollmar, M. (2007). Drawing the tree of eukaryotic life based on the analysis of 2,269 manually annotated myosins from 328 species. *Genome Biol*, *8*(9):R196.

Okten, Z., Churchman, L. S., Rock, R. S., & Spudich, J. A. (2004). Myosin VI walks hand-over-hand along actin. *Nat Struc Mol Bio*, *11*(9):884-887.

Ostap, E. M., Lin, T., Rosenfeld, S. S., & Tang, N. (2002). Mechanism of regulation of acanthamoeba myosin-Ic by heavy-chain phosphorylation. *Biochemistry*, *41*(41): 12450-12456.

Osterweil, E., Wells, D. G., & Mooseker, M. S. (2005). A role for myosin VI in postsynaptic structure and glutamate receptor endocytosis. *J Cell Biol*, *168*(2):329-338.

Pandey, A., Dan, I., Kristiansen, T. Z., Watanabe, N. M., Voldby, J., Kajikawa, E., et al. (2002). Cloning and characterization of PAK5, a novel member of mammalian p21-activated kinase-II subfamily that is predominantly expressed in brain. *Oncogene*, *21*(24):3939-3948.

Park, H., Li, A., Chen, L. Q., Houdusse, A., Selvin, P. R., & Sweeney, H. L. (2007). The unique insert at the end of the myosin VI motor is the sole determinant of directionality. *Proc Natl Acad Sci*, *104*(3):778-783.

Park, H., Ramamurthy, B., Travaglia, M., Safer, D., Chen, L. Q., Franzini-Armstrong, C., et al. (2006). Full-length myosin VI dimerizes and moves processively along actin filaments upon monomer clustering. *Mol Cell*, *21*(3):331-336.

Pastor-Pareja, J. C., Grawe, F., Marti'n-Blanco, E., & Garci'a-Bellido, A. (2004). Invasive cell behavior during *Drosophila* imaginal disc eversion is mediated by the jnk signaling cascade. *Dev Cell*, *7*(3):387-399.

Pérez-Garijo, A., Shlevkov, E., & Morata, G. (2009). The role of Dpp and Wg in compensatory proliferation and in the formation of hyperplastic overgrowths caused by apoptotic cells in the *Drosophila* wing disc. *Development*, *136*(7):1169-1177.

Petritsch, C., Tavosanis, G., Turck, C. W., Jan, L. Y., & Jan, Y. N. (2003). The *Drosophila* myosin VI Jaguar is required for basal protein targeting and correct spindle orientation in mitotic neuroblasts. *Dev Cell*, *4*(2):273-281.

Phichith, D., Travaglia, M., Yang, Z., Liu, X., Zong, A. B., Safer, D., et al. (2009). Cargo binding induces dimerization of myosin VI. *Proc Natl Acad Sci U S A*, *106*(41):17320-17324.

Pollard, T. D. (2010). Mechanics of cytokinesis in eukaryotes. *Curr Opin Cell Biol*, *22*(1):50-56.

Puri, C. (2009). Loss of myosin VI no insert isoform (NoI) induces a defect in clathrin-mediated endocytosis and leads to caveolar endocytosis of transferrin receptor. *J Biol Chem*, *284*(50):34998-35014.

Puri, C. (2010). Effects of loss of myosin VI no-insert isoform on clathrin-mediated endocytosis of plasma-membrane receptors. *Commun Integr Biol*, *3*(3):234-237.

Rawlins, E. L., Lovegrove, B., & Jarman, A. P. (2003). Echinoid facilitates notch pathway signalling during *Drosophila* neurogenesis through functional interaction with delta. *Development*, *130*(26):6475-6484.

Redowicz, M. J. (2002). Myosins and pathology: genetics and biology. *ACTA Biochim Pol*, *49*(4):789-804.

Reed, B. C., Cefalu, C., Bellaire, B. H., Cardelli, J. A., Louis, T., Salamon, J., et al. (2005). Glut1CBP (TIP2/GIPC1) interactions with glut1 and myosin VI: evidence supporting an adapter function for glut1cbp. *Mol Biol Cell*, *16*(9):4183-4201.

Reed, B. H., Wilk, R., & Lipshitz, H. D. (2001). Downregulation of Jun kinase signaling in the amnioserosa is essential for dorsal closure of the *Drosophila* embryo. *Curr Biol*, *11*(14):1098-1108.

Ricos, M. G., Harden, N., Sem, K. P., Lim, L., & Chia, W. (1999). Dcdc42 acts in TGF-beta signaling during *Drosophila* morphogenesis: distinct roles for the Drac1/JNK and Dcdc42/TGF-beta cascades in cytoskeletal regulation. *J Cell Sci*, *112*(8):1225-1235.

Riesgo-Escovar, J. R., Jenni, M., Fritz, A., & Hafen, E. (1996). The *Drosophila* Jun-N-terminal kinase is required for cell morphogenesis but not for djun-dependent cell fate specification in the eye. *Genes Dev*, *10*(21):2759-2768.

Roberts, R., Lister, I., Schmitz, S., Walker, M., Veigel, C., Trinick, J., et al. (2004). Myosin VI: cellular functions and motor properties. *Philos TransR Soc Lond B: Biol Sci*, *359*(1452):1931-1944.

Rock, R. S., Rice, S. E., Wells, A. L., Purcell, T. J., Spudich, J. A., & Sweeney, H. L. (2001). Myosin VI is a processive motor with a large step size. *Proc Natl Acad Sci U S A*, *98*(24):13655-13659.

Rodriguez-Diaz, A., Toyama, Y., Abravanel, D. L., Wiemann, J. M., Wells, A. R., Tulu, U. S., et al. (2008). Actomyosin purse strings: renewable resources that make morphogenesis robust and resilient. *HFSP J*, *2*(4):220-237

Roeth, J. F., Sawyer, J. K., Wilner, D. A., & Peifer, M. (2009). Rab11 helps maintain apical crumbs and adherens junctions in the *Drosophila* embryonic ectoderm. *PLoS One*, *4*(10), p. e7634.

Rogat, A. D., & Miller, K. G. (2002). A role for myosin VI in actin dynamics at sites of membrane remodeling during *Drosophila* spermatogenesis. *J Cell Sci*, *115*(24): 4855-4865.

Ryder, E., & Russell, S. (2003). Transposable elements as tools for genomics and genetics in *Drosophila*. *Brief Funct Genomic Proteomic, 2*(1):57-71.

Sahlender, D. A., Roberts, R. C., Arden, S. D., Spudich, G., Taylor, M. J., Luzio, J. P., et al. (2005). Optineurin links myosin vi to the golgi complex and is involved in Golgi organization and exocytosis. *J Cell Biol*, *169*(2):285-295.

Sakata, S., Watanabe, Y., Usukura, J., & Mabuchi, I. (2007). Characterization of native myosin VI isolated from sea urchin eggs. *J Biochem*, *142*(4):481-490.

Schöck, F., & Perrimon, N. (2002). Cellular processes associated with germ band retraction in *Drosophila*. *Dev Biol*, *248*(1):29-39.

Schürmann, A., & Bokoch, G. M. (2001). Role of p 21 activated kinases in cell survival and apoptotic pathways. *Drug Dev Res*, *52*(4):542-548.

Schuh, M., Lehner, C. F., & Heidmann, S. (2007). Incorporation of *Drosophila* CID/CENP-A and CENP-C into centromeres during early embryonic anaphase. *Curr Biol*, *17*(3):237-243.

Seabrooke, S., Qiu, X., & Stewart, B. (2010). Nonmuscle myosin II helps regulate synaptic vesicle mobility at the drosophila neuromuscular junction. *J Neurosci*, *11*(1):37.

Self, T., Sobe, T., Copeland, N. G., Jenkins, N. A., Avraham, K. B., & Steel, K. P. (1999). Role of myosin VI in the differentiation of cochlear hair cells. *Deve Biol*, *214*(2): 331-341.

Sellers, J. R. (2000). Myosins: a diverse superfamily. *Biochim Biophys Acta Mol Cell Res*, *1496*(1):3-22.

Shalaby, N. A., Parks, A. L., Morreale, E. J., Osswalt, M. C., Pfau, K. M., Pierce, E. L., et al. (2009). A screen for modifiers of notch signaling uncovers amun, a protein with a critical role in sensory organ development. *Genetics*, *182*(4):1061-1076.

Shawn, S. C. L. (2005). Specificity and versatility of SH3 and other proline-recognition domains: structural basis and implications for cellular signal transduction. *Biochem J*, *390*(Pt 3):641.

Simonova, O. B., & Burdina, N. V. (2009). Morphogenetic movement of cells in embryogenesis of *Drosophila melanogaster*: mechanism and genetic control. *Ontogenez, 40*(5):355-372.

Solon, J., Kaya-Çopur, A., Colombelli, J., & Brunner, D. (2009). Pulsed forces timed by a ratchet-like mechanism drive directed tissue movement during dorsal closure. *Cell*, *137*(7):1331-1342.

Song, Y. H., Mirey, G., Betson, M., Haber, D. A., & Settleman, J. (2004). The *Drosophila* atm ortholog, datm, mediates the response to ionizing radiation and to spontaneous DNA damage during development. *Curr Biol*, *14*(15):1354-1359.

Spink, B. J., Sivaramakrishnan, S., Lipfert, J., Doniach, S., & Spudich, J. A. (2008). Long single -helical tail domains bridge the gap between structure and function of myosin VI. *Nat Struc Mol Biol*, *15*(6):591-597.

Spudich, G., Chibalina, M. V., Au, J. S. Y., Arden, S. D., Buss, F., & Kendrick-Jones, J. (2007). Myosin VI targeting to clathrin-coated structures and dimerisation is mediated by binding to Disabled-2 and PtdIns (4, 5) P2. *Nat Cell Biol*, *9*(2):176-183.

Stronach, B. (2005). Dissecting JNK signalling, one KKKinase at a time. *Dev Dyn*, *232*(3):575-584.

Stronach, B. E., & Perrimon, N. (2001). Investigation of leading edge formation at the interface of amnioserosa and dorsal ectoderm in the *Drosophila* embryo. *Development*, *128*(15):2905-2913.

Stronach, B., & Perrimon, N. (2002). Activation of the JNK pathway during dorsal closure in *Drosophila* requires the mixed lineage kinase, slipper. *Genes Dev*, *16*(3):377-387.

Suter, D. M., Espindola, F. S., Lin, C. H., Forscher, P., & Mooseker, M. S. (2000). Localization of unconventional myosins V and VI in neuronal growth cones. *J Neurobiol*, *42*(3):370-382.

Sweeney, H. L., Park, H., Zong, A. B., Yang, Z., Selvin, P. R., & Rosenfeld, S. S. (2007). How myosin VI coordinates its heads during processive movement. *EMBO J*, *26*(11):2682-2692.

Szczepanowska, J. (2009). Involvement of Rac/Cdc42/PAK pathway in cytoskeletal rearrangements. *Acta Biochim Pol*, *56*(2):225-234.

Tamaki, K., Kamakura, M., Nakamichi, N., Taniura, H., & Yoneda, Y. (2008). Upregulation of MYO6 expression after traumatic stress in mouse hippocampus. *Neurosci Letts*, *433*(3):183-187.

Tepass, U., Gruszynski-DeFeo, E., Haag, T. A., Omatyar, L., Török, T., & Hartenstein, V. (1996). Shotgun encodes *Drosophila* E-cadherin and is preferentially required during cell rearrangement in the neurectoderm and other morphogenetically active epithelia. *Genes Dev*, *10*(6):672-685.

Thomas, U., Jonsson, F., Speicher, S. A., & Knust, E. (1995). Phenotypic and molecular characterization of Ser (d), a dominant allele of the *Drosophila* gene Serrate. *Genetics*, *139*(1):203-213.

Thomas, U., Speicher, S. A., & Knust, E. (1991). The *Drosophila* gene Serrate encodes an EGF-like transmembrane protein with a complex expression pattern in embryos and wing discs. *Development*, *111*(3):749-761.

Valdembri, D., Caswell, P. T., Anderson, K. I., Schwarz, J. P., König, I., Astanina, E., et al. (2009). Neuropilin-1/GIPC1 signaling regulates alpha5beta1 integrin traffic and function in endothelial cells. *PLoS Biol*, *7*(1):e25.

Vicente-Manzanares, M., Webb, D. J., & Horwitz, A. R. (2005). Cell migration at a glance. *J Cell Sci*, *118*(21):4917-4919.

Vidal, M., Larson, D. E., & Cagan, R. L. (2006). Csk-deficient boundary cells are eliminated from normal *Drosophila* epithelia by exclusion, migration, and apoptosis. *Dev Cell*, *10*(1):33-44.

Vidal, S., Khush, R. S., Leulier, F., Tzou, P., Nakamura, M., & Lemaitre, B. (2001). Mutations in the *Drosophila* dTAK1 gene reveal a conserved function for MAPKKKs in the control of rel/NF-B-dependent innate immune responses. *Genes Dev*, *15*(15):1900-1912.

Vreugde, S., Ferrai, C., Miluzio, A., Hauben, E., Marchisio, P. C., Crippa, M. P., et al. (2006). Nuclear myosin VI enhances RNA polymerase II-dependent transcription. *Mol Cell*, *23*(5):749-755.

Warner, C. L., Stewart, A., Luzio, J. P., Steel, K. P., Libby, R. T., Kendrick-Jones, J., et al. (2003). Loss of myosin VI reduces secretion and the size of the Golgi in fibroblasts from Snell's waltzer mice. *EMBO J*, *22*(3):569-579.

Wei, S. Y., Escudero, L. M., Yu, F., Chang, L. H., Chen, L. Y., Ho, Y. H., et al. (2005). Echinoid is a component of adherens junctions that cooperates with DE-cadherin to mediate cell adhesion. *Dev Cell*, *8*(4):493-504.

Wells, A. L., Lin, A. W., Chen, L. Q., Safer, D., Cain, S. M., Hasson, T., et al. (1999). Myosin VI is an actin-based motor that moves backwards. *Nature*, *401*(6752):505-508.

Wells, C., & Jones, G. (2010). The emerging importance of Group II Paks. *Biochem. J*, *425*:465-473.

Wijnhoven, B., Dinjens, W., & Pignatelli, M. (2000). E-cadherin-catenin cell-cell adhesion complex and human cancer. *Br J Surg*, *87*(8):992-1005.

Windler, S. L., & Bilder, D. (2010). Endocytic internalization routes required for Delta/Notch signaling. *Curr Biol*, *20*(6):538-543.

Wirtz-Peitz, F., & Zallen, J. A. (2009). Junctional trafficking and epithelial morphogenesis. *Curr Opin Genet Dev*, *19*(4):350-356.

Wood, W., Jacinto, A., Grose, R., Woolner, S., Gale, J., Wilson, C., et al. (2002). Wound healing recapitulates morphogenesis in *Drosophila* embryos. *Nat Cell Biol*, *4*(11):907-912.

Woolner, S., Jacinto, A., & Martin, P. (2005). The small GTPase rac plays multiple roles in epithelial sheet fusion--dynamic studies of *Drosophila* dorsal closure. *Dev Biol*, *282*(1):163-173.

Wu, H., Nash, J. E., Zamorano, P., & Garner, C. C. (2002). Interaction of SAP97 with minus-end-directed actin motor myosin VI. Implications for AMPA receptor tracfficking. *J Biol Chem*, *277*(34):30928-30934.

Xia, Y., & Karin, M. (2004). The control of cell motility and epithelial morphogenesis by Jun kinases. *Trends Cell Biol*, *14*(2):94-101.

Yamamoto, S., Charng, W. L., & Bellen, H. J. (2010). Endocytosis and intracellular trafficking of Notch and its ligands. *Curr Top Dev Biol*, *92*:165-200.

Yamashita, R. A., & May, G. S. (1998). Constitutive activation of endocytosis by mutation of myoA, the myosin I gene of *Aspergillus nidulans*. *J Biol Chem*, *273*(23):14644-14648.

Yang, Y., Kovács, M., Sakamoto, T., Zhang, F., Kiehart, D. P., & Sellers, J. R. (2006). Dimerized *Drosophila* myosin VIIa: A processive motor. *Natl Acad Sci U S A*, 103(15):5746-5751

Yildiz, A., Park, H., Safer, D., Yang, Z., Chen, L. Q., Selvin, P. R., et al. (2004). Myosin VI steps via a hand-over-hand mechanism with its lever arm undergoing fluctuations when attached to actin. *J Biol Chem*, *279*(36):37223-37226.

Yoshida, H., Cheng, W., Hung, J., Montell, D., Geisbrecht, E., Rosen, D., et al. (2004). Lessons from border cell migration in the *Drosophila* ovary: a role for myosin VI in dissemination of human ovarian cancer. *Proc Natl Acad Sci USA*, *101*(21):8144-8149.

Yoshimura, M., Homma, K., Saito, J., Inoue, A., Ikebe, R., & Ikebe, M. (2001). Dual regulation of mammalian myosin VI motor function. *J Biol Chem*, *276*(43):39600-39607.

Young, P., Richman, A., Ketchum, A., & Kiehart, D. (1993). Morphogenesis in *Drosophila* requires nonmuscle myosin heavy chain function. *Genes Dev*, *7*(1): 29-41.

Yu, C., Feng, W., Wei, Z., Miyanoiri, Y., Wen, W., Zhao, Y., et al. (2009). Myosin VI undergoes cargo-mediated dimerization. *Cell, 138*(3):537-548.

Yue, T., Tian, A., & Jiang, J. (2012). The cell adhesion molecule echinoid functions as a tumor suppressor and upstream regulator of the Hippo signaling pathway. *Dev Cell, 22*(2):255-267.

Zecchini, V., Brennan, K., & Martinez-Arias, A. (1999). An activity of notch regulates JNK signalling and affects dorsal closure in *Drosophila*. *Curr Biol, 9*(9):460-469.

Zhang, Q., Zheng, Q., & Lu, X. (1999). A genetic screen for modifiers of *Drosophila* Src42A identifies mutations in Egfr, rolled and a novel signaling gene. *Genetics, 151*(2):697-711.

Zhao, Z., & Manser, E. (2005). Pak and other Rho-associated kinases–effectors with surprisingly diverse mechanisms of regulation. *Biochem J, 386*(Pt 2):201-214.

Zusman, S., Grinblat, Y., Yee, G., Kafatos, F. C., & Hynes, R. O. (1993). Analyses of PS integrin functions during *Drosophila* development. *Development, 118*(3):737-750.